23rd Annual
Trabecular Meshwork Study Club

December 12 – 14, 2024

Dana Hotel Mission Bay, San Diego, CA

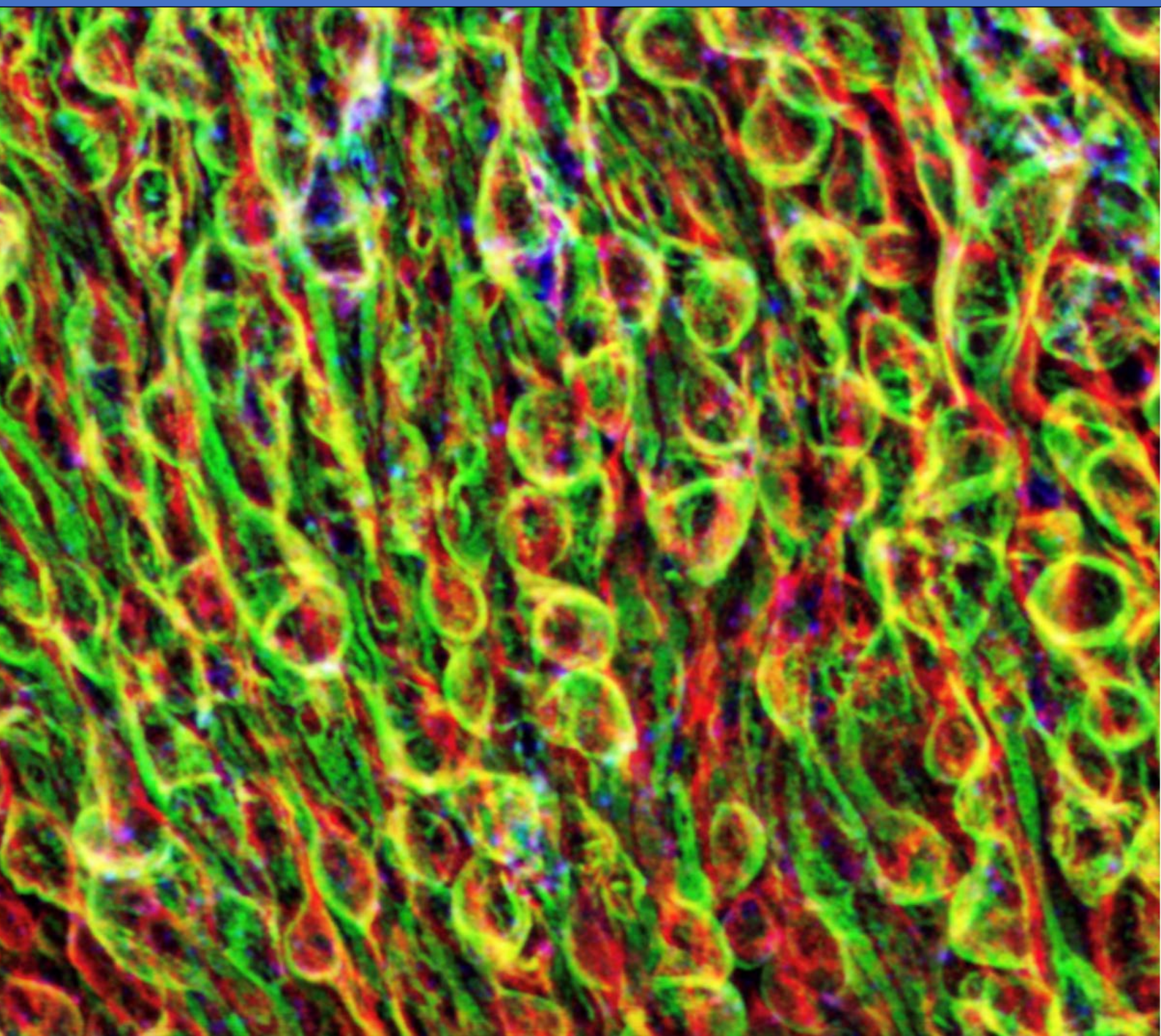

Produced by Kugler Publications, P.O. Box 20538, 1001 NM Amsterdam, The Netherlands, on behalf of the Trabecular Meshwork Study Club.

Cover image: Courtesy of Darryl Overby

Table of Contents

Sponsors

We thank our sponsors for their confidence in the work we do, and their generous support which makes this forum of information sharing, dialogue, debate and collaboration possible.

abbvie

Anonymous

BrightFocus™ Foundation

GLAUCOMA RESEARCH FOUNDATION

Rick and Phyllis Halprin in Memory of Louise Halprin

Jeanette Houston

To further glaucoma research and the search for a cure

The Western Glaucoma Foundation

WELCOME MESHWORKERS TO THE 2024 TRABECULAR MESHWORK STUDY CLUB

The trabecular meshwork study club meeting was started 24 years ago by Shan Lin and myself as a means of emphasizing outflow research. We wanted a basic science meeting that would foster conversations and collaborations among basic and clinician scientists, feeling that there were already plenty of clinical glaucoma meetings. The creation of collaboration remains one of our main criteria for success. Over time, our knowledge of the cell biology of outflow has evolved. In addition to this invite-only, in person meeting we have launched the Trabecular Meshwork Society Virtual, an online, free, forum for all interested in the TM during the academic year. Many of you have participated in this endeavor (thank you) and we encourage you to continue and spread the word to your colleagues, as one means of being asked to participate in Meshwork Study Club. Other aspects of this meeting include the creation of white papers on TM relevant topics, fund raising to perpetuate the meeting and maintaining a cordial informality while facilitating networking. Serving attendees good wine helps too.

We have integrated a book series, with four volumes now published which is useful for both fund raising and enhancing collaboration. Many of the articles in these books created by Simon Bakker at Kugler Publications are useful in fund raising for this meeting. Although some may argue that any use of paper is antiquated, these books have been well received and have succeeded in helping to solidify information.

Our on-site meeting has been typically scheduled to coordinate with the meetings of the American Society for Cell Biology. We still attempt to maintain this coordination. In the past, we actually sponsored attendance of meshworkers at the ASCB meeting. The science there is more advanced than what one finds within most ophthalmology meetings. However, we have always made an exception when cell biology is in the cold Northeast as these locations are not popular with our attendees. Thus we will be looking for a location in southwest in 2026. We are flexible; Hawaii is not out of the question particularly because Thelma is expert at getting good hotel rates in Hawaii.

Our study club meeting uses a Gordon conference model so it funds as much airfare as the budget will tolerate plus hotel and meals. However, to receive your stipend, and to be asked back, you must stay until the end of the meeting. Thelma will be available to hand out checks for evaluations just as Griff did in the past. Griff's contributions to this meeting were many especially with the paperwork and it is worth noting that she was working on evaluations of the 2023 meeting when she fell in baggage claim at SFO bgand subsequently passed in January of 2024. We miss the energy that Griff brought to our meeting.

We have limited attendance in order to stay small enough to have very cordial interactions by people with active RO1s on outflow who have first authored outflow papers. We realize that many more people want to come than we can accommodate and this is the reason that we have the white papers and the on line meeting as well as the Kugler books.

We are always trying to improve. Please share your comments with Colleen, Dan, Thelma and myself. Please consider writing in one of the Kugler books which are especially a good place to publish risky new concepts to get them out in front of the glaucoma community. Keep in mind that this is at its core not a clinical meeting. There is no CME. The purpose is to advance our understanding of outflow to lead to better therapies specifically in the anterior segment of the eye.

Thank you for attending and participating in the 2024 meeting.

John

John R. Samples, MD
glaucoma@gmail.com

Professor, Washington State University College of Medicine

Agenda

Thursday, December 12, 2024		
6:00PM – 7:30PM		**Opening Reception**
Friday, December 13, 2024		
7:45	John Samples	Introduction
Session 1: Mechanobiology of the TM *Darryl Overby, moderator*		
8:00	Ernst Tamm	**1.** Piezo2-Positive Mechanoreceptors of Trigeminal Origin Form a Distinct Neuronal Network Throughout the Trabecular Meshwork and Scleral Spur of the Human Eye
8:15	Michael Elliott	**2.** Molecular and Functional Characterization of Caveolae Mechanosensors in Trabecular Meshwork
8:30	Alireza Karimi	**3.** Modulation of Traction Forces and ECM Reorganization in Glaucomatous TM/JCT Tissues Using ROCK and YAP/TAZ Inhibition
8:45	Samuel Herberg	**4.** The Emerging Case for Altered Mechanoepigenetics in Glaucomatous TM Cell Pathobiology
9:00	Amir Vahabikashi	**5.** Altered Distribution of Vimentin Intermediate Filaments in Glaucomatous Schlemm's Canal Endothelial Cells
9:15	David Krizaj	**6.** TREK-1 Channels Regulate Conventional Outflow and Intraocular Pressure
9:30	Ross Ethier	**7.** Schlemm's Canal Cell Mechanobiology and Pore Formation
9:45 – 10:30 Break		
Session 2: Transcriptomics, Gene Expression Profiling & Genetics *Donna Peters, moderator*		
10:30	Kate Keller	**8.** Fibrosis-Related Gene Expression Profile in Primary Cells Cultured From Normal and Glaucomatous Trabecular Meshwork
10:45	Diana Lozano	**9.** Profiling IOP-Responsive Genes in Anterior and Posterior Ocular Tissues Following a Controlled Elevation of IOP

11:00	Abe Clark	**10.** TM Transcriptomes From Mice That Develop Dexamethasone-Induced Ocular Hypertension (Responders) Compared to Strains Resistant to Developing DEX-OHT (Nonresponders)
11:15	Revathi Balasubramanian	**11.** Transcriptomics, Models, and Mechanisms of Congenital Glaucoma
11:30	Sai Nair	**12.** Genetic Interaction Between Transcription Factors in the Maintenance of Ocular Drainage Tissue
11:45	Inas Aboobakar	**13.** From Genetic Association to Functional Mechanisms: The Protective Role of ANGPTL7 Coding Variants in Ocular Hypertension and Glaucoma
12:00	Yiqin Du	**14.** Differential Expression of MMPs in TM Cells and TM Stem Cells and the Effects
12:15 – 1:45 Lunch		
1:45	Carol Toris	Update on Tonography Consensus Recommendation
Session 3: New Models and Tools to Study the TM and SC *Colleen McDowell, moderator*		
2:00	Gulab Zode	**15.** A Novel Cre-Inducible Mouse Model of Myocilin Glaucoma for Studying Trabecular Meshwork Outflow and Neurodegeneration in Glaucoma
2:15	Ben Thomson	**16.** New Tools for Genetic Targeting of the Schlemm's Canal Endothelium
2:30	Markus Kuehn	**17.** Magnetic Steering of Adipose Tissue-Derived Mesenchymal Stem Cells in Human Ocular Perfusion Culture
2:45	Ester Reina-Torres	**18.** Segmental Outflow Patterns Coincide with Local Hypoxia and VEGF Expression in the TM
3:00 – 3:45 Break		
Session 4: Schlemm's Canal and Distal Outflow *Dan Stamer, moderator*		
3:45	Colleen McDowell	**19.** Effect of CGRP on SC and TM Cell Function
4:00	David Swain	**20.** Investigation of Two Pore Types in Schlemm's Canal Inner Wall Endothelium in Different Flow-Type Areas Using Serial Block-Face Scanning Electron Microscopy

4:15	Haiyan Gong	**21.** Investigation of the Effect of Netarsudil on the Inner Wall Endothelial Cells of Schlemm's Canal of Human Eye Using Serial Block-Face Scanning Electron Microscopy
4:30	Darryl Overby	**22.** Microenvironmental Factors Influencing Barrier Function in Cultured Human Schlemm's Canal Endothelial Cells
4:45	Murray Johnstone	**23.** Valve-Like Structures Distal to SC in the Human Eye: An SEM Study
6:00	**Group Dinner**	

Saturday, December 14, 2024

Keynote Lecture		
8:00	Carol Toris	**24.** Past, Present, and Future of Aqueous Humor Dynamics Research: It's About More Than Just the TM
Session 5: ECM, Extracellular Vesicles, and Macrophages in the TM *Paloma Liton, moderator*		
8:45	Fiona McDonnell	**25.** Reversing Dex-Induced ECM Changes in TM Cells With Extracellular Vesicles
9:00	Padhu Pattabiraman	**26.** Clusterin as a Signal Attenuator and a Bonafide ECM Sensor: A Mechanistic Study
9:15	Katy Liu	**27.** Macrophages in the Conventional Outflow Tract
9:30 – 10:15 Break		
Session 6: TM Cell Biology *Ross Ethier, moderator*		
10:15	Yutao Liu	**28.** The miRNA-mRNA Interactive Networks in Regulating Estrogen and TGFβ Signaling in HTM Cells Under Cyclic Mechanical Stretch
10:30	Weiming Mao	**29.** The Association Between Cross-Linked Actin Networks (CLANs) and Trabecular Meshwork Cell Proliferation and Senescence
10:45	Donna Peters	**30.** Age-Related Dysregulation of α5β1 and αvβ3 Integrin Activity Promotes Profibrotic Phenotype in Trabecular Meshwork (TM) Cells
11:00	Paloma Liton	**31.** Tubulin Acetylation Enhances Microtubule Stability in Trabecular Meshwork Cells Under Mechanical Stress
11:15	Yang Sun	**32.** Matrine Reduces Intraocular Pressure in Corticosteroid-Induced Ocular Hypertensive Mouse Eyes
11:30	Vasantha Rao	**33.** Understudied Aspects of Cell-Cell Junctions in the Trabecular Meshwork: Implications for Aqueous Humor Outflow and Intraocular Pressure
11:45	Hannah Youngblood	**34.** Myocilin^{A427T} and the Balance Between Proteostasis and Proteotoxicity
12:00 – 1:30 Lunch		

Session 7: Secondary and Angle Closure Glaucomas *Kate Keller, moderator*		
1:30	Sanjoy Battacharya	**35.** A Comparison of Primary and Secondary Glaucomatous Aqueous Humor Deposits
1:45	Gillian McLellan	**36.** Identification of a Novel Genetic Variant Associated With Primary Acute Angle Closure (PACG) and Goniodysgenesis in Dogs
Session 8: Clinical "trabeculo" studies *Kate Keller and John Samples, moderators*		
2:00	Joel Schuman	**37.** A New Approach to Glaucoma: Regenerating the Trabecular Meshwork With Stem Cells
2:15	Gavin Roddy	**38.** Selective Laser Trabeculoplasty in Patients on Systemic Immunosuppressive Therapy
2:30	Shan Lin	**39.** Suprachoroidal Stents: Accessing the Other Outflow Pathway
2:45	Mike Fautsch	**40.** CKLP1 to QLS-111: The Long Winding Road From Innovation to Patient Care
3:00	John Danias	**41.** Interesting Clinical Cases Involving the TM
3:15	John Samples	Closing Comments, Evaluation & Stipends

TM Society 2024 Keynote Speaker: Carol Toris

Carol Toris has been conducting research for 34 years at the University of Nebraska Medical Center (UNMC) where she is now a Professor Emeritus, at Case Western Reserve University (CWRU) where she is now an Adjunct Professor and at the Ohio State University Medical Center (OSUMC) where she continues to work as a Research Professor. Throughout her career she has worked with a large group of collaborators and staff to investigate aqueous humor dynamics (AHD) and intraocular pressure (IOP) regulation. Her work has focused on factors regulating IOP changes under various situations and in different live animal models including mice, cats, rabbits, dogs, nonhuman primates, and humans. Her clinical work includes the study of ocular pathologies affecting IOP and normal changes that take place during aging and over a 24-hour period. She has investigated novel IOP lowering drugs when dosed alone or together, during the day and at night, and under different pathological conditions. She currently studies effects on outflow facility of novel glaucoma drainage devices or Schlemm's canal procedures. At OSUMC she is working with a team developing a large database in humans of IOP, ocular and systemic biometrics, aqueous humor production, outflow facility, episcleral venous pressure, uveoscleral outflow, and UBM imaging of the anterior segment. This team has collected data from healthy control volunteers and patients with ocular hypertension with or without glaucoma on no or various glaucoma drugs. With this database, that will be shared with the research community, she and her team are writing numerous papers on causes of the IOP elevation in glaucoma and ways to treat it. Her studies have been funded by industry in the form of collaborations or Investigator Initiated Trials, by receiving Foundation grants and by collaborations with PIs funded by NIH or DoD. This work has generated well over 250 publications, book chapters, review articles and abstracts. She currently is working with new technologies to improve techniques to measure each parameter of aqueous humor dynamics with increased speed, accuracy, and safety. In the future, these new methods and the data they generate could make AHD an important tool in the clinic for precision medicine and in the lab for exploring AHD on a new level.

Section 1: Mechanobiology of the TM

1. PIEZO2-POSITIVE MECHANORECEPTORS OF TRIGEMINAL ORIGIN FORM A DISTINCT NEURONAL NETWORK THROUGHOUT THE TRABECULAR MESHWORK AND SCLERAL SPUR OF THE HUMAN EYE

Ernst R. Tamm,Gholamreza Naghibi

Institute of Anatomy, University of Regensburg, Regensburg, Germany

Purpose: To identify specific proprioceptive sensory nerve endings in the human chamber angle that serve as mechanoreceptors to measure stress or strain of the extracellular matrix. Nerve terminals were identified by co-immunoreactivity for Piezo2 and synaptophysin. Piezo2 is a mechanosensitive ion channel that plays a specific role in rapidly adapting mechanically activated currents in somatosensory neurons. Synaptophysin is a glycoprotein characteristically present in synaptic vesicles of nerve terminals.

Methods: Human autopsy eyes (age 70-80 years) without any obvious ocular pathology were investigated. The anterior eye segment was dissected in quadrants. From each quadrant, wedge-shaped specimens with 1.6 mm width on average, and containing trabecular meshwork and ciliary muscle were cut. The specimens were fixed in 2 % paraformaldehyde for immunohistochemistry or Karnovsky's solution for transmission electron microscopy (TEM). Serial tangential 12-20 µm cryosections were cut and immunostained with antibodies against Piezo2. In addition, whole mounts covering the entire uvea were stained. For comparison, flat mounts of the anterior eye of C57BL/6N mice were stained. For positive control, Ruffini-like terminals (Krause's bulbs) were stained in the tongue of both species.

Results: Piezo2/synaptophysin immunoreactivity was detected exclusively in club- or bulb-shaped nerve terminals in scleral spur, posterior trabecular meshwork, and more inwardly, at the apex of the longitudinal portion of the ciliary muscle. The terminals had a diameter of 10-20 µm and were regularly arranged along the entire circumference. The distance between individual terminals was 150-200 µm. Piezo2/synaptophysin-immunoreactive terminals were distinctly absent in other parts of the uvea. TEM confirmed that the nerve endings were identical with nerve endings previously identified as putative mechanosensory based on ultrastructural criteria (Tamm et al., IOVS 1994). No Piezo2/synaptophysin-immunoreactive terminals were identified in the murine chamber angle.

Conclusion: We conclusively confirm the presence of mechanosensory nerve terminals that measure stress or strain of the extracellular matrix in the chamber angle. Such changes are likely induced by ciliary muscle contraction and/or changes in intraocular pressure. The absence of those structures in the murine chamber angle indicates a specific role for the primate eye.

2. MOLECULAR AND FUNCTIONAL CHARACTERIZATION OF CAVEOLAE MECHANOSENSORS IN TRABECULAR MESHWORK

Michael H. Elliott[1], Philip Mzyk[2], Rashad Raman[2], Jennifer Ballheim[1], Olawale Bankole[1], W. Daniel Stamer[2]

[1]Departments of Ophthalmology and Biochemistry & Physiology, Dean McGee Eye Institute, Oklahoma City, OK, USA; [2]Department of Ophthalmology, Duke Eye Center, Duke University, Durham, NC, USA

Purpose: Caveolins are the signature proteins for membrane domains called caveolae, which are abundant features of the conventional outflow pathway including the trabecular meshwork (TM), Schlemm's canal (SC), and distal outflow vessels. Variants in the genes which encode caveolins, are associated with risk of primary open angle glaucoma (POAG) and with elevated intraocular pressure (IOP). Caveolae, via the caveolin scaffolding proteins, have been implicated as membrane mechanosensors in vascular and SC endothelium where they regulate nitric oxide production. However, in the TM less is known about the molecular machinery connecting mechanical stimulation to caveolae mechanosensation. Herein, we examine the caveolae protein interactome in TM cells subjected to mechanical challenge and find novel interactions associated with Rho/ROCK signaling.

Methods: To define the CAV1 interactome in human TM cells, we immunoprecipitated CAV1 with a highly specific antibody from authenticated human TM cell strains (n = 3) that were subjected to one hour of cyclic mechanical stretch (15 % stretch, 1 Hz). Control immunoprecipitations using normal rabbit IgG were done in parallel to evaluate specificity. Immune complexes were evaluated by unbiased, quantitative mass spectrometry (Mass Spectrometry/Molecular Biology Core Module at Duke University Eye Center). Proteins identified with ≥ 2 peptides which were 1.5-fold enriched over the IgG control were compared between stretched and unstretched cells. Interactomes were generated using STRING databases (https://string-db.org/) for proteins with differential abundance of ≥1.5-fold between stretched and control cells. Functional interrogation of stretch-dependent interactomes were evaluated in caveolae-deficient and control mice treated with rho kinase inhibitor.

Results: CAV1 was quantitatively precipitated from stretched and control human TM cell lysates and efficiently eluted for mass spectrometric analyses. We identified 62 proteins with significantly reduced interaction and 80 proteins with increased interaction following stretch. There were 46 proteins which were not significantly different in association between stretch and control cells which included proteins involved in membrane raft assembly (i.e., CAV2, PRKCDBP/CAVIN3, FLOT1). Among proteins with reduced interaction following stretch were EHD proteins which are important for caveolae assembly, GULP1, which is implicated in TM phagocytosis, and PDE5A which is involved in nitric oxide-dependent contractility. Proteins which were increased in interaction after stretch included proteins involved in Rho/ROCK signaling/actin cytoskeleton including ROCK1, MPRIP, and FLNA, proteins involved in caveolae assembly (CAVINS1,2), a protein involved in membrane repair after mechanical stress (MYOF). Given the link to Rho/ROCK1 signaling, we evaluated whether a rho kinase inhibitor (0.02% netarsudil) could lower IOP in mice deficient in caveolae. We found that netarsudil effectively lowered IOP in global CAV1 KO mice similar to littermate controls (ΔIOP in mmHg: WT, 3.0 ± 1.9; Het, 3.6 ± 2.7; KO, 3.1 ± 2.1 (mean ± SD)).

Conclusion: The caveolae interactomes in mechanically-stimulated TM cells are remarkably different than unstimulated cells and reveal novel roles in cell contractility and mechanoprotection. Of particular interest is the increased association of proteins involved in Rho/ROCK signaling. The elevated IOP in Cav1 KO mice is reduced by RKI treatment similar to controls. Further functional validation will likely reveal novel players in mechanotransduction of TM cells with potential relevance to IOP homeostasis and POAG.

Support: R01EY028608, P30EY005722, P30EY021725, R01EY022359, and Research to Prevent Blindness.

3. MODULATION OF TRACTION FORCES AND ECM REORGANIZATION IN GLAUCOMATOUS TM/JCT TISSUES USING ROCK AND YAP/TAZ INHIBITION

Alireza Karimi[1,2], Mini Aga[1], Ansel Stanik[1], Tia Harbaugh[1], Elise Coffey[1], Elizabeth White[1], Mary J. Kelley[1], Ted S. Acott[1,3]

[1]Department of Ophthalmology, Casey Eye Institute, Oregon Health & Science University, Portland, Oregon, USA; [2]Department of Biomedical Engineering, Oregon Health & Science University, Portland, Oregon, USA; [3]Department Chemical Physiology & Biochemistry, School of Medicine, Oregon Health & Science University, Portland, Oregon, USA

Purpose: To investigate how ROCK and YAP/TAZ inhibition affects cellular traction forces and ECM reorganization in normal and glaucomatous trabecular meshwork (TM) and juxtacanalicular tissue (JCT), which play critical roles in regulating intraocular pressure in glaucoma.

Methods: We utilized 3D in situ traction force microscopy (TFM) to quantify cellular contractile forces and analyze ECM reorganization within TM/JCT tissues from both normal and glaucomatous human donor eyes. Human TM/JCT tissues were treated with ROCK inhibitor Y-27632 and YAP/TAZ inhibitor Verteporfin. We tracked the displacement of FluoSpheres embedded in the ECM and examined changes in collagen fibril orientation, tensile strain, divergence, and curl over a 24-hour period using confocal imaging and computational analysis.

Results: Our analysis revealed dysregulated traction forces within glaucomatous tissues, leading to significant ECM reorganization that may contribute to disrupting the homeostasis of the aqueous outflow pathway. Treatments appear to help restore normal ECM structure by adjusting cellular forces. The effect on contractile forces differed between genders, suggesting the significance of gender in treatment response.

Conclusions: Our results suggest that targeting these biomechanical pathways may offer new therapeutic strategies to reduce outflow resistance, laying the groundwork for future therapies aimed at preserving vision by restoring ECM biomechanics and improving outflow.

4. THE EMERGING CASE FOR ALTERED MECHANOEPIGENETICS IN GLAUCOMATOUS TM CELL PATHOBIOLOGY

Rajanya Ghosh[1], Rachel Hadvina[2], Makenzie Miller[1], Souvik Ghosh[1], W. Daniel Stamer[3], Kate E. Keller[4], Preethi S. Ganapathy[1], Yutao Liu[2], Samuel Herberg[1]

[1]Department of Ophthalmology and Visual Sciences, Center for Vision Research,

SUNY Upstate Medical University, Syracuse, NY, USA; [2]Department of Cellular Biology and Anatomy, James & Jean Culver Vision Discovery Institute, Augusta University, Augusta, GA, USA; [3]Department of Ophthalmology, Duke Eye Center, Duke University, Durham, NC, USA; [4]Department of Ophthalmology, Casey Eye Institute, Oregon Health & Science University, Portland, OR, USA

Purpose: Trabecular meshwork (TM) cells from glaucoma eyes retain a pathological phenotype upon isolation and *in vitro* culture. Emerging evidence suggests that this “disease signature” involves abnormal nuclear dynamics compared to normal TM cells. However, the underlying mechanisms are incompletely understood. Here, we investigate the nuclear architecture and epigenetic landscape in glaucomatous vs. normal TM cells and how this impacts gene expression and chromatin accessibility in a tissue-like soft extracellular matrix (ECM) microenvironment.

Methods: Five pairs of age- and sex-matched normal TM (NTM) or glaucomatous TM (GTM) cell strains were cultured on ECM hydrogels (type I collagen, elastin, hyaluronic acid). Nuclear volume, chromatin condensation, and histone 3 (H3) acetylation/methylation were quantified by immunostaining and immunoblotting. Total histone deacetylase (HDAC) activity was measured in nuclear extracts using a direct assay kit, while specific HDACs were quantified by qPCR and immunoblot analyses. Expression of outer and inner nuclear membrane and lamina proteins was assessed by immunostaining and immunoblotting. Trizol-isolated RNA was used to prepare RNA-seq libraries for genome-wide expression profiling using 100 bp paired-end RNA sequencing. Select up- or downregulated genes were validated by qPCR analysis. In parallel, TrypLE-dissociated TM cells were used to extract nuclei and prepare ATAC-seq libraries for chromatin accessibility mapping using 50 bp paired-end ATAC sequencing. All sequencing data were processed using established Partek-Flow pipelines to identify differentially expressed genes / altered genomic peaks, followed by Gene Ontology and Ingenuity Pathway analyses.

Result: Imaris Surface visualizations of DAPI-stained confocal z-stacks showed significantly increased nuclear volume in GTM vs. NTM cells, concurrent with decreased chromatin condensation. This was associated with increased permissive H3K9/14 acetylation, while repressive H3K27 tri-methylation was largely unaffected. Strikingly, total HDAC activity was significantly decreased (>3-fold) in GTM vs. NTM cell nuclei, consistent with nearly abolished HDAC1 mRNA and protein expression. Both nesprin-1 and lamin A/C expression were increased in GTM vs. NTM cells. No difference in overall emerin expression was noted; however, there was a clear nuclear membrane enrichment in NTM cells compared to GTM cells consistent with more condensed heterochromatin. RNA-seq analysis revealed 620 differentially expressed genes in GTM vs. NTM cells with functional enrichment of genes involved in: ECM organization, nuclear membrane protein complex, ECM conferring elasticity. ATAC-seq analysis showed 600 differentially accessible chromatin regions in GTM cells vs. NTM cells with enrichment of genes involved in: regulation of response to stress, nucleus, structural constituent of chromatin. Hierarchical clustering demonstrated overall largely consistent patterns of differentially expressed genes/altered genomic peaks specific to either GTM or NTM cells. qPCR target analysis of differentially expressed genes validated the unbiased sequencing data. Sixteen differentially expressed genes displayed significantly altered open chromatin regions, some with known glaucoma association (e.g., ARID5A, WNT4A). Ingenuity Pathway analysis predicted altered signaling networks involving TGFβ superfamily, cyclic AMP response element-binding protein (CREB)-mediated transcription, and inflammation in GTM cells vs. NTM cells (Fig. 1).

Conclusions: Our data suggest that abnormal nuclear dynamics - including permissive histone acetylation, increased chromatin accessibility and transcriptional activity, and altered nuclear mechanotransduction machinery - is a central component in the complex regulatory network underlying glaucomatous TM cell dysfunction.

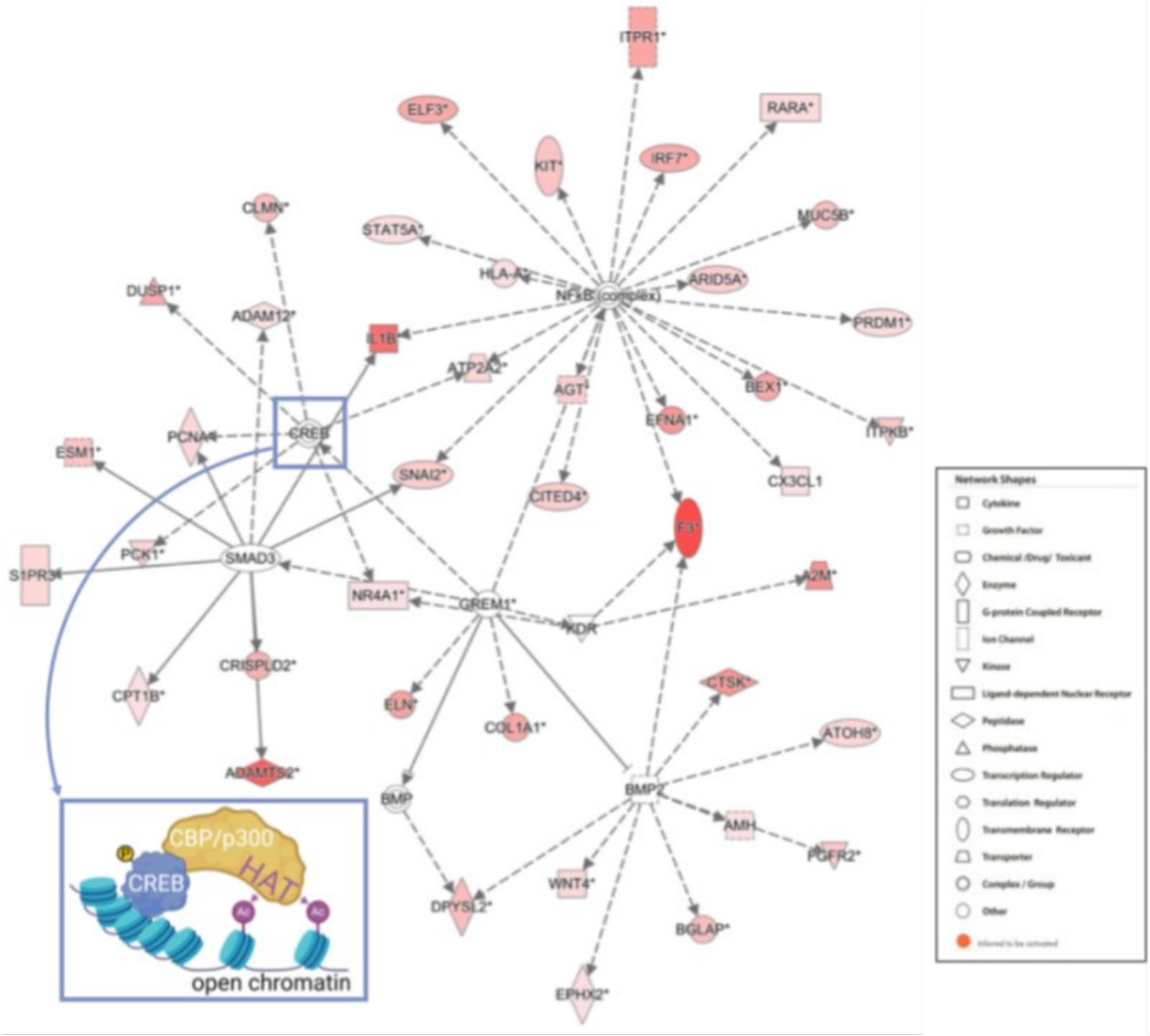

Figure 1: Ingenuity pathway analysis of paired RNA-seq/ATAC-seq data showed activated causal networks between GREM1, BMP2, SMAD3, CREB, and NFkB signaling pathways in GTM cells compared to NTM cells. Inset: schematic of CREB-CBP/p300-mediated histone acetylation; once CREB is phosphorylated, it interacts with its coactivator proteins CREB-binding protein (CBP) or p300 - both type A/nuclear HATs - and initiates transcription by modulating chromatin accessibility through histone acetylation.

5. ALTERED DISTRIBUTION OF VIMENTIN INTERMEDIATE FILAMENTS IN GLAUCOMATOUS SCHLEMM'S CANAL ENDOTHELIAL CELLS

Amir Vahabikashi[1,2]

[1]Department of Bioengineering, Northeastern University, Boston, MA, USA; [2]Institute for Mechanobiology, Northeastern University, Boston, MA, USA

Purpose: Schlemm's canal (SC) cells isolated from glaucomatous donor eyes are stiffer than cells isolated from normal donor eyes (Overby et al. 2014). Increased stiffness of glaucomatous SC cells leads to a decrease in pore-forming ability, likely contributing to increased outflow resistance in ocular hypertension. It is shown that altered distribution and mesh size of intermediate filaments regulate cell stiffness (Sivaramakrishnan et al., 2008). Here, we sought to examine the distribution and to quantify the mean fluorescent intensity (MFI) of vimentin intermediate filaments (VIFs) in cultured normal and glaucomatous SC cells.

Methods: Normal (n=1) and glaucomatous (n=1) SC cells of same passage (n=3) were seeded to glass cover slips and fixed with 4% Paraformaldehyde next day. Fixed cells were permeabilized with 0.1% Triton X-100 and stained for DNA (Hoechst), F-actin (Alexa Fluor® 568 Phalloidin), and vimentin (chicken anti vimentin; Alexa Fluor® 488). A Zeiss 510 LSM confocal microscope with 63x (oil immersion, NA=1.4) objective lens was used to create confocal images from normal (n=22) and glaucomatous (n=24) SC cells. Same microscope settings were used for creating the images. Maximum projection image for each cell was generated from the confocal stacks, and then used to quantify total fluorescent intensity. Cell area was measured as marked by the peripheral cortical actin. MFI was calculated as total fluorescent intensity divided by cell area. MFI values for each cell type (normal or glaucomatous) were normalized to the highest value resulting in a range from zero to one. Student's t-test was used for statistical analysis.

Results: Results from the confocal imaging showed an altered distribution of VIFs in cultured glaucomatous SC cells as compared to their normal counterparts. While VIFs were uniformly distributed in normal SC cells extending from perinuclear region to cell periphery, many glaucomatous SC cells showed aggregates of VIFs referred to as "bundling" (see Figure.1). F-actin looked similar in both cell types showing prominent stress fibers and cortex. Average normal versus glaucoma cell area ($5865\pm351\mu m^2$ vs. $5154\pm380\mu m^2$, p=0.17) and normalized MFI for VIFs (0.68 ± 0.03 vs. 0.64 ± 0.04, p=0.4) were not different.

Conclusions: Confocal images indicated bundling of VIFs in glaucomatous SC cells, a behavior that was lacking in normal SC cells. The F-actin distribution was similar between the two cell types. The normalized MFI for vimentin was similar between the normal and glaucomatous SC cells despite altered distribution of the VIFs. Future studies will determine the effect from VIFs expression level and distribution on the stiffness of SC cells and its consequent effect on pore formation and outflow resistance.

Figure

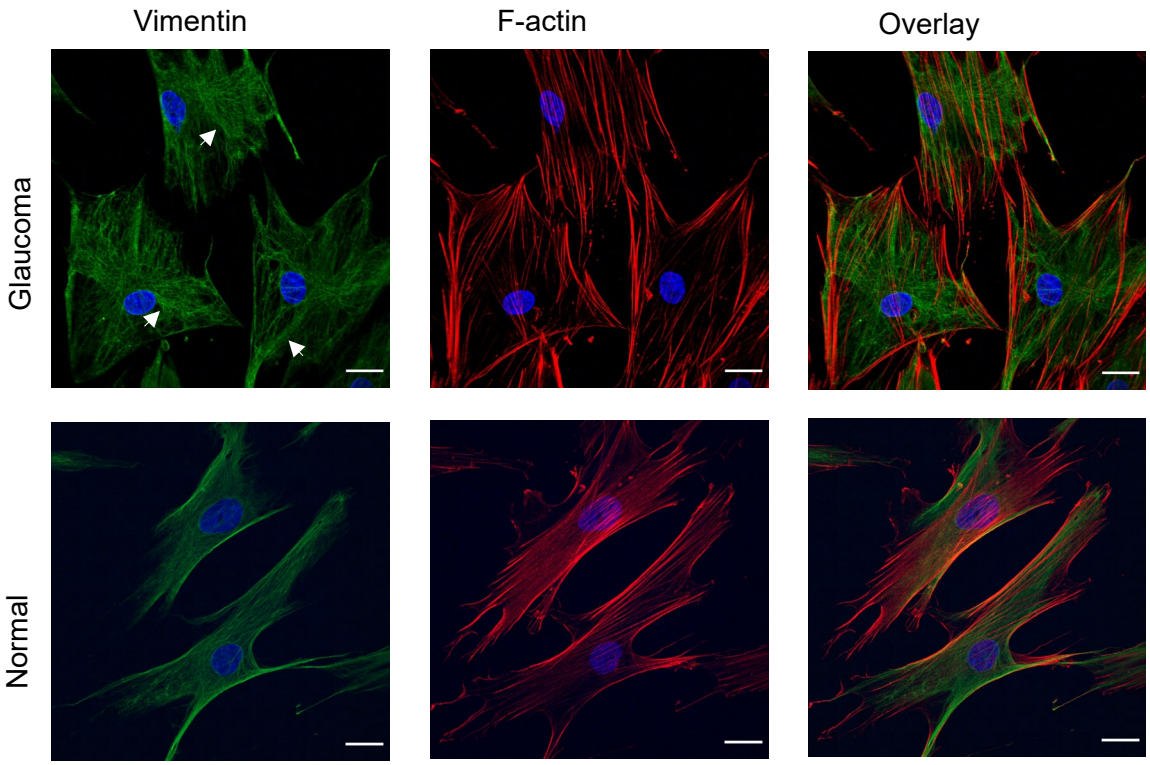

Figure 1: Confocal images for glaucomatous and normal SC cells stained for Vimentin (green), F-actin (red), and DNA (Blue). VIFs bundling is present in glaucomatous SC cells (see arrow). Scale bar is 20μm.

6. TREK-1 CHANNELS REGULATE CONVENTIONAL OUTFLOW AND INTRAOCULAR PRESSURE

Sarah N. Redmon[1], Christopher N. Rudzitis[1], Joseph van Battenberg Sherwood[2], Christina M. Nicou[3], Christopher L. Passaglia[3], Monika Lakk[1], Darryl Overby[2], David Krizaj[1]

[1]Department of Ophthalmology & Visual Sciences, University of Utah School of Medicine, Salt Lake City, UT; [2]Dept. of Bioengineering, Imperial College London, UK

Purpose: To characterize the effect of glucocorticoids on trabecular mechanosensing and conventional outflow.

Methods: Whole-cell patch-clamp recordings, optical imaging, pharmacology, tonometry were used to investigate TRPV4 function in cultured mouse and human trabecular meshwork cells and intact eye. High-speed pressure clamp was used to apply pressure steps to cultured cells. Acute ocular hypertension was induced in mouse and rat eyes through cannulation, and chronic IOP elevations via injection of microbeads and glucocorticoid administration.

Results: REK-1 channels mediate pressure-induced hyperpolarizations in human TM cells. TREK-1 activation promotes outflow and lowers IOP in rat and mouse eyes, as well as in eyes chronically treated with dexamethasone. DEX alone depolarizes human TM cells and suppresses TREK1 expression and activation.

Conclusions: Mechanosensitive TREK-1 channels promote conventional outflow but are also highly susceptible to glucocorticoid modulation. The increase in outflow resistance in glucocorticoid-treated patients may include suppression of protective TREK-1 activity.

Acknowledgements: Funded by the National Eye Institute, Stauss-Rankin Foundation, Crandall Glaucoma Initiative and an unrestricted RPB award to the Department of Ophthalmology at the University of Utah.

7. SCHLEMM'S CANAL CELL MECHANOBIOLOGY AND PORE FORMATION

C. Ross Ethier[1,2], Haiyan Li[1], Cydney Wong[1], Seyed Mohammad Siadat[1], Kristin M. Perkumas[3], Jacques A. Bertrand[4], Darryl R. Overby[4], Todd Sulchek[2], W. Daniel Stamer[3]

[1]Biomedical Engineering, Georgia Institute of Technology/Emory University, Atlanta, GA, USA; [2]Mechanical Engineering, Georgia Institute of Technology, Atlanta, GA, USA; [3]Department of Ophthalmology, Duke University, Durham, NC, USA; [4]Bioengineering, Imperial College London, London, UK

Purpose: Pores in Schlemm's canal (SC) endothelial cells are reduced in glaucomatous eyes, are triggered by mechanical stretch, and influence IOP, yet our mechanistic understanding of pore formation is weak. TRPV4 is expressed in SC cells and has been previously shown to influence IOP. We thus measured the effects of TRPV4 activity on cell phenotype and used an *in vitro* assay to assess how TRPV4 influences intracellular pore (I-pore) formation.

Methods: All experiments used primary normal (N=3) and glaucomatous (N=3) human SC cell strains cultured on either: (i) cell culture plastic; (ii) hydrogels of stiffness 2.4 and 8 kPa (corresponding to normal and glaucomatous TM), or (iii) seeded on 5 um diameter microspheres to induce pore formation. Cells were treated with either the TRPV4 activator GSK101 (100 nM) or the TRPV4 antagonist HC06 (10 uM). mRNA and protein levels of cytoskeletal and ECM proteins were determined by qRT-PCR and fluorescent labeling, respectively. Cell stiffness was measured by atomic force microscopy (AFM). Pores were detected using fluorescently labeled streptavidin tracers (Braakman+, IOVS, 2014).

Results: Treating normal human SC cells with a TRPV4 antagonist for 2 days softened cells and reduced message and expression of F-actin, α-smooth muscle actin and fibronectin. This phenotype could be reversed by treating cells with a TRPV4 activator. Cells cultured on stiff hydrogels showed increased calcium signaling, F-actin and cellular stiffness measured by AFM compared to cells on soft hydrogels. These phenotypes could be reversed by inhibiting TRPV4. Repeating these experiments in glaucomatous SC cells gave qualitatively similar results, but with reduced amplitude compared to that seen in normal cells. In the pore forming assay, TRPV4 activation increased cytoplasmic calcium levels and pore formation, an effect which again was blunted in glaucomatous cells.

Conclusions: Our data shows that TRPV4 is important for mechanosensing in human SC cells, with TRPV4 activation mimicking many of the same phenotypic features that occur when cells are grown on stiff substrates. Importantly, glaucomatous SC cells showed similar trends, but these changes were significantly attenuated in magnitude, suggesting alterations in mechanoresponsive signaling pathways downstream of TRPV4 in glaucomatous SC cells.

Support: BrightFocus Foundation, NIH, Georgia Research Alliance

Section 2: Transcriptomics, Gene Expression Profiling & Genetics

8. FIBROSIS-RELATED GENE EXPRESSION PROFILE IN PRIMARY CELLS CULTURED FROM NORMAL AND GLAUCOMATOUS TRABECULAR MESHWORK

Kate E. Keller[1], Yong-feng Yang[1], Ying Ying Sun[1], Paul Holden[1]

[1]Casey Eye Institute, Oregon Health & Science University, Portland, OR 97239, USA

Purpose: Glaucomatous trabecular meshwork (TM) tissue is characterized by excess fibrotic-like extracellular matrices, which contributes to tissue stiffening and negatively impacts aqueous humor outflow. Due to cellular mechanical memory, primary TM cells placed in culture retain molecular expression profiles of the environment from which they were isolated. In this study, we investigated fibrotic-related gene expression profiles of normal and glaucomatous TM cells in culture using fluorescent barcode technology.

Methods: Primary TM cells were cultured from non-glaucomatous (n=6) and glaucomatous (n=5) cadaver eyes. The donors were age- and sex-matched (NTM: mean age=70. 6 ± 4 years, range=57-80, 3 males/3 females) and (GTM: mean age=73.8 ±5.9 years, range=57-92, 2 males/3 females). All donors were Caucasian. TM cells were cultured in DMEM containing 0.1M ascorbate. RNA was harvested and mRNA profiling of 750 genes was performed using the human fibrosis panel (NanoString). Rosalind software was used to analyze datasets to identify differentially expressed genes. Quantitative PCR, Western immunoblotting, and immunofluorescence microscopy were performed to confirm gene expression results, while immunohistochemistry showed differences in TM tissue. A fluorogenic assay was used to quantitate matrix metalloproteinase (MMP) enzyme activity.

Results: Western immunoblotting showed that GTM cells had up-regulated α-smooth muscle actin and phosphorylated SMAD2/3 compared to NTM cells. RNA from NTM and GTM cells were tagged with fluorescent barcodes and genes showing significant differential expression were identified. Two fibrotic-related genes were up-regulated (*CDH2, VEGFA*), while 28 genes were down-regulated in GTM cells compared to NTM cells. Down-regulated genes included *CHI3L1, COL6A3, F11R (JAM1), IL33, MMP2, POSTN, SERPINF1,* and *VCAM1*. Western immunoblotting confirmed increased protein levels of CDH2 (N-cadherin) and decreased MMP2, CHI3L1, and SerpinF1 (PEDF) proteins in GTM cells. Immunohistochemistry showed the distribution of N-cadherin and CHI3L1 in the juxtacanalicular region and surrounding TM beams in normal and glaucomatous tissue. While MMP2 gene expression and protein levels were reduced, there was increased MMP2 activity.

Conclusions: Our results provide further support that GTM cells display mechanical memory, displaying altered gene expression and protein levels than age-matched NTM cells. In combination with tissue studies, cultured GTM cells are a useful *in vitro* model for studying fibrotic changes associated with glaucoma in the TM.

Support: Supported by R01EY019643, R01EY032590, P30 EY010572, the Malcolm M. Marquis Endowed Fund, and an unrestricted grant to the Casey Eye Institute from Research to Prevent Blindness, NY.

Commercial Relationships: None

9. PROFILING IOP-RESPONSIVE GENES IN ANTERIOR AND POSTERIOR OCULAR TISSUES FOLLOWING A CONTROLLED ELEVATION OF IOP

Diana C. Lozano, Yong-Feng Yang, Eliesa Ing, William O. Cepurna, John C. Morrison, Kate E. Keller

Casey Eye Institute, Oregon Health & Science University, Portland, OR, USA

Purpose: To investigate *in vivo* IOP-related gene responses in the trabecular meshwork (TM) and optic nerve head (ONH) simultaneously from the same animals following a controlled elevation of IOP (CEI).

Methods: An equal number of male and female rats underwent CEI for 8-hours, at pressures of 20 mmHg (mean rat IOP; CEI-20; N=11) and 50 mmHg (2.5x mean IOP; CEI-50; N=12). Naïve animals (n=12), receiving no anesthesia or surgical interventions, served as additional controls. Immediately after CEI, TM and ONH tissues were dissected and RNA isolated. Samples were processed with the Nanostring nCounter PanCancer Immune Profiling Panel, containing 770 genes, following the low input RNA protocol, and raw count data were uploaded to Rosalind® for differential expression analyses. For TM, three comparisons were made: “CEI-50 vs. CEI-20”, “CEI-50 vs. naïve”, and “CEI-20 vs. naïve”. For ONH, our previous RNA-seq study showed no significant gene responses in “CEI-20 vs. naïve”, so only “CEI-50 vs. naïve” ONH samples were compared. Gene functional assessment was evaluated with ShinyGO bioinformatics software.

Results: Mean RNA concentration was 61 ng/TM and 60 ng/ONH. TM and ONH naïve samples clustered separately, indicating distinctive gene profiles. Naïve TM had 34 uniquely enriched genes, while the ONH had 33. For TM, 46 IOP-related genes were found to be significant in “CEI-50 vs. CEI-20” and “CEI-50 vs. naïve” groups, with ‘ECM space’ and ‘membrane raft’ identified as significant GO cellular components. Fifteen genes were common to both comparisons, which were related to the Notch (upregulated) and TGFβ (downregulated) KEGG pathways. For ONH, 22 significantly regulated genes were identified in the “CEI-50 vs. naïve” comparison and significantly affected biological process pathways were ‘response to cytokine’ and ‘immune response’.

Conclusions: This study demonstrated the ability to assay short-term IOP-responsive genes in both TM and ONH tissues simultaneously. In the TM, downregulation of TGFβ pathway genes suggests that TM responses may reduce TGFβ-induced extracellular matrix synthesis. For ONH, the initial response to short-term elevated IOP may be protective. Future studies will investigate TM and ONH changes in response to lower and repeated IOP exposures. One of our goals is to model experimental glaucoma as a series of repeated controlled elevations of IOP.

Funding: This work was supported by the National Institutes of Health (Bethesda, MD) grants R21 EY033073 (KEK), R01 EY019634 (KEK), R01 EY010145-17S1 (DCL), R01 EY010145 (JCM), P30 EY010572 (OHSU), the Malcom M. Marquis, MD Endowed Fund for Innovation, and an unrestricted grant from Research to Prevent Blindness (New York, NY) to Casey Eye Institute, Oregon Health & Science University.

10. TM TRANSCRIPTOMES FROM MICE THAT DEVELOP DEXAMETHASONE-INDUCED OCULAR HYPERTENSION (RESPONDERS) COMPARED TO STRAINS RESISTANT TO DEVELOPING DEX-OHT (NONRESPONDERS)

Pinkal Patel[1], J. Cameron Millar[1], Gaurang Patel[1], Sherri Feris[1], Stacy Curry[1], Eldon E. Geisert[2], Abbot F. Clark[1]

[1]Department of Pharmacology & Neuroscience, North Texas Eye Research Institute, U. North Texas Health Science Center, Fort Worth, TX, USA; [2]Department of Ophthalmology, Emory University, Atlanta, GA, USA

Purpose: Glucocorticoid-induced ocular hypertension (GC-OHT), which can lead to iatrogenic OAG, is a serious side effect of prolonged GC therapy. However, only approximately 40% of the general population is susceptible to developing GC-OHT (i.e. steroid responders). GC-OHT and the resulting glaucoma is clinically and molecularly similar to POAG, and POAG patients as well as family members have a higher risk of developing GC-OHT. We developed a reproducible mouse model of GC-OHT in order to discover the following: (1) do all mouse strains develop GC-OHT?; (2) what are the molecular mechanisms responsible for GC-OHT?; and (3) if GC-OHT is genetically determined, what genes are involved?

Methods: Five genetical distinct mouse strains (C57BL/6J, C3H/HeJ, DBA/2J.*Gpnmb*$^{+}$, 129P3/J, and BALB/cJ) were bilaterally injected periocularly with a dexamethasone (DEX) formulation weekly for 5 weeks. Conscious or isoflurane anesthetized IOPs were measured weekly using a TonoLab rebound tonometer. At the end of 5 weeks, TM tissues were carefully dissected from each eye, and total RNA isolated for RNA seq analysis. To map the genes responsible for GC-OHT, recombinant inbred BXD mice were evaluated for their ability to develop GC-OHT.

Results: Two of the five mouse strains tested (C57BL/6J and C3H/HeJ) developed significant DEX-OHT (i.e. responders) while the other 3 mouse strains were resistant to DEX-OHT (non-responders). This equates to a 40% responder rate, which is quite similar to the responder rate in man. These mice developed glaucomatous optic neuropathy with loss of RGC soma and axons as well as decreased RGC functional response (PERG) mimicking POAG in man. Since B6 mice are responders and D2 non-responders, we are taking advantage of the BXD recombinant inbred mouse strains to map the genes responsible for DEX-OHT. The TM transcriptomes of the 2 responder strains were quite similar. The TM transcriptomes of the non-responder strains also were very similar but quite different from the responder strains. Top pathways affected in the responder strains included: cytokine signaling, integrin signaling, ECM organization, fibrosis signaling pathways, wound healing pathways, and actin cytoskeletal signaling. Top pathways in the nonresponder TM transcriptomes were: potassium channels, calcium signaling, Gα(i) signaling, NFAT in cardiac hypertrophy, nNOS signaling, and PKA signaling.

Conclusions: GC-OHT is genetically determined in mice, and the genes responsible will be identified using BXD recombinant inbred mice. The orthologous genes in man will be independently confirmed using banked DNA from clinically documented steroid responders. TM tissue transcriptomes are extremely different from responder vs nonresponder mice, and we are using these data to discover the molecular mechanisms responsible for GC-OHT.

11. TRANSCRIPTOMICS, MODELS, AND MECHANISMS OF CONGENITAL GLAUCOMA

Abdul Hannan, Violet Bupp-Chickering, Revathi Balasubramanian

Department of Ophthalmology, Columbia University Irving Medical Center, New York, NY, USA

Purpose: Schlemm's canal (SC) and trabecular meshwork (TM) play a central role in ocular physiology. Impaired SC and TM development has implications in regulation of ocular physiology and congenital glaucoma. SC develops from blood vessels through a process recently described as canalogenesis. The transcriptomic control of SC development is unknown. It is essential that we understand the underlying biology of normal development of SC to understand how genetic changes in disease impacts SC development in congenital glaucoma.

Method: Recent advances in genomics and sequencing have enhanced our understanding of the interplay between signaling networks and gene regulation during ocular development. Single cell RNA sequencing allows for complex assessment of inter-cellular and intra-cellular dynamics during development. We previously generated single cell profiles for ~150,000 cells across multiple developmental ages – postnatal days P2, P4, P6, P10, P14, P21 and P60, that are crucial for SC and TM development. Dynamic gene expression studies highlighted the crucial need for Apelin signaling in SC development. Using loss-of-function mouse models, we are studying the mechanism of Apelin signaling in SC development and as a model for congenital glaucoma.

Results: We observe dynamic populations of cells charting the course of SC and TM development. We identify the developmental trajectory of vascular progenitors and changes in key gene expression leading to SC development and the specification of inner and outer wall endothelial cells of SC. Upon loss of Apelin signaling in vascular progenitor during key stages of SC development, we observe changes to SC morphology. We also observe changes to the anterior chamber depth indicating changes in intraocular pressure.

Conclusions: Apelin signaling is an important pathway in vascular development that has not been studied in the context of SC development. Our study illuminates the role of Apelin signaling in SC development and as a potential mouse model to study congenital glaucoma.

Funding: Glaucoma Research Foundation Shaffer award (RB), BrightFocus Foundation NGR G2021007S (RB)

12. GENETIC INTERACTION BETWEEN TRANSCRIPTION FACTORS IN THE MAINTENANCE OF OCULAR DRAINAGE TISSUE

Kiran Gangappa[1], Durairaj Duraikannu[1], Emre Uludag[1], Yien Ming Kuo[1], Saidas Nair[1,2]

[1]Department of Ophthalmology, [2]Department of Anatomy, University of California, San Francisco, CA , USA

Purpose: This study aims to identify genetic factors and molecular mechanisms that contribute to elevated intraocular pressure (IOP) and primary open-angle glaucoma (POAG). Understanding genetic interactions that influence disease risk remains a significant challenge in glaucoma research. We seek to uncover interactions between Glis1 and Foxc1, transcription factors crucial for ocular drainage tissue health. Genetic variants of *GLIS1* have been associated with POAG, and our previous studies demonstrated that mice lacking Glis1 develop progressive trabecular meshwork (TM) degeneration, leading to elevated IOP. Chip-seq analysis revealed that Glis1 binding sites colocalize with motifs of other transcription factors, including Fox family members, within TM cells, implicating a potential interaction with Foxc1 in IOP regulation. We hypothesize that Glis1 and Foxc1 function within a shared transcriptional network governing TM structure and function, essential for maintaining ocular drainage tissue integrity and normal IOP.

Methods: To investigate the genetic interaction between Glis1 and Foxc1, we utilized genetic mouse models and molecular techniques. Our approach involved generating mice with specific combinations of *Glis1* and *Foxc1* alleles to mimic subtle genetic changes relevant to complex diseases like POAG. We tested whether loss of one or two alleles of *Glis1*, in conjunction with a hypomorphic *Foxc1* allele (Hith), would lead to TM abnormalities and elevated IOP. The $Foxc1^{Hith}$ allele is an ENU-induced mutation (T-to-C transition) resulting in an F107L substitution in the forkhead domain, which reduces Foxc1 activity and serves as a model of its partial loss of function. C57BL/6J mice heterozygous for either Glis1 ($Glis1^{+/-}$) or the *Hith* allele ($Foxc1^{Hith/+}$) exhibit normal IOP, serving as controls. B6.$Foxc1^{Hith/+}$ mice were bred to B6.$Glis^{+/-}$ or $Glis1^{-/-}$ mice to generate experimental mice that are heterozygous for both *Glis1* and *Foxc1* mutations ($Glis1^{+/-}Foxc1^{Hith/+}$) or homozygous for *Glis1* and heterozygous for Foxc1 mutations ($Glis1^{-/-}Foxc1^{Hith/+}$). Ocular phenotypes were assessed via spectral-domain optical coherence tomography (SD-OCT) and slit-lamp biomicroscopy, with bi-weekly IOP measurements from one month of age. Histological analysis was performed on plastic-embedded eye sections stained with Hematoxylin and Eosin (H&E), and retinal imaging was conducted using Micron OCT.

Results: Our findings indicate that $Glis1^{+/-}Foxc1^{Hith/+}$ double heterozygous mice, aged up to seven months, exhibit an ocular drainage tissue phenotype similar to that of wild-type or single heterozygous mutants, with normal IOP levels. This suggests that reduced activity of both Glis1 and Foxc1 in the double heterozygotes is not sufficient to induce significant TM defects or elevate IOP. In contrast, $Glis1^{-/-}Foxc1^{Hith/+}$ mice displayed severe TM degeneration and elevated IOP at an early age, with glaucoma-related changes, including optic nerve excavation, observed as early as three months. In comparison, $Glis1^{-/-}Foxc1^{+/+}$ mice showed a relatively delayed phenotype, including high IOP induced optic nerve excavation being observed at around five to six months of age. These results suggest that reduced Foxc1 activity exacerbates the ocular phenotype and IOP elevation associated with Glis1 deficiency, indicating an additive or synergistic effect of these transcription factors in maintaining TM integrity and IOP homeostasis.

Conclusion: Although *Glis1/Foxc1* double heterozygous mice did not display overt TM defects, molecular analyses may uncover altered expression of genes co-regulated by Glis1 and Foxc1, shedding light on pathways critical for TM function and IOP regulation. It is also possible that the minor changes in IOP in *Glis1/Foxc1* double heterozygotes might have gone undetected, suggesting that more sensitive techniques, such as outflow measurements, may be needed to capture subtle differences. Nevertheless, our findings support the idea that Glis1 and Foxc1 may participate in a shared transcriptional network necessary for TM maintenance and IOP regulation, with Foxc1 potentially compensating in the context of Glis1 deficiency. Future studies

will focus on dissecting the molecular interactions between Glis1 and Foxc1 to further elucidate their roles in TM function.

13. FROM GENETIC ASSOCIATION TO FUNCTIONAL MECHANISMS: THE PROTECTIVE ROLE OF *ANGPTL7* CODING VARIANTS IN OCULAR HYPERTENSION AND GLAUCOMA

Inas F. Aboobakar[1], Edward Ryan A. Collantes[1], Michael A. Hauser[2,], W. Daniel Stamer[2,3], Janey L. Wiggs[1]

[1]Department of Ophthalmology, Massachusetts Eye and Ear, Harvard Medical School, Boston, MA, USA; [2]Department of Ophthalmology, Duke University School of Medicine, Durham, NC, USA; [3]Department of Biomedical Engineering, Duke University School of Medicine, Durham, NC, USA

Purpose: Rare missense and nonsense variants in the *Angiopoietin-like 7* (*ANGPTL7*) gene are associated with lower intraocular pressure (IOP) and confer protection from primary open-angle glaucoma (POAG), though the functional mechanism remains uncharacterized. Here, we investigate the underlying mechanism using *in silico* and *in vitro* models.

Methods: Protein stability of wild-type (WT) *ANGPTL7* and five protective variants was estimated using FoldX software and correlated with variant effects on corneal-compensated IOP (IOPcc) in the UK Biobank. In parallel, primary cultures of human trabecular meshwork (TM) cells were transfected with an expression vector containing either WT *ANGPTL7* or one of five protective variants (2 TM strains each tested in duplicate). Cells were processed for immunohistochemistry 24 hours post-transfection to assess Angptl7 localization. Cell lysate and conditioned media were collected 48 hours post-transfection to measure levels of Angptl7 and endoplasmic reticulum (ER) stress markers (Grp78 and Atf4). Human TM and Schlemm's canal (SC) cells were subjected to 48 hours of cyclic mechanical stress (CMS) using the Flexcell strain unit (15% stretch at a frequency of 1Hz); control cells were plated on Flexcell plates but were not subjected to CMS. Real-time PCR was performed to measure changes in *ANGPTL7* expression (3 TM and 3 SC strains each tested in triplicate).

Results: More efficacious IOPcc lowering strongly correlates with in silico predictions of increased protein instability ($r= -0.98$, $p<0.001$). Missense and nonsense variants cause aggregation of mutant Angptl7 protein in the ER and decreased levels of secreted protein in TM cells. A lower secreted:intracellular protein ratio strongly correlates with variant effects on IOPcc in the UK Biobank ($r= 0.87$, $p=0.04$), suggesting that protective variants lower Angptl7 protein levels. Interestingly, accumulation of mutant protein in the ER does not increase expression of ER stress markers ($p>0.05$ for all). CMS, a glaucoma-relevant physiologic stressor, also significantly lowers ANGPTL7 expression in SC cells (-2.4 fold-change, $p=0.01$).

Conclusion: These data suggest that the protective effects of ANGPTL7 variants in ocular hypertension and POAG stem from lower levels of secreted protein, which may modulate responses to physiologic and pathologic ocular cell stressors. Downregulation of ANGPTL7 expression may therefore serve as a viable preventative and therapeutic strategy for this common, blinding disease.

Funding: NIH/NEI K23EY035734 (IFA), R01EY022305 (JLW), R01EY030617 (WDS), P30EY014104 (Mass Eye and Ear), P30EY005722 (Duke University), Research to Prevent Blindness Departmental Grants (Mass Eye and Ear and Duke University)

14. DIFFERENTIAL EXPRESSION OF MMPS IN TM CELLS AND TM STEM CELLS AND THE EFFECTS

Yiqin Du, Minwen Zhou, Enzhi Yang

Department of Ophthalmology, Morsani College of Medicine, University of South Florida, Tampa, FL, USA

Purpose: Human trabecular meshwork (TM) extracellular matrix (ECM) turnover plays important roles in intraocular pressure (IOP) regulation. Matrix metalloproteinases (MMPs) are involved in TM ECM turnover. Human TM stem cells (TMSCs) are able to home to the TM region after intracameral injection in mice. The study hypothesis is that TMSCs are functional in ECM turnover via MMPs for TM regeneration and IOP control.

Methods: Human TM cells and TMSCs were used between passages 4 to 6 from at least 3 different donors for this study. Using quantitative polymerase chain reaction (qPCR), expression levels of *MMP1, MMP2, MMP3, MMP8, MMP9, MMP12, MMP13* and *MMP14* in TM cells and TMSCs were compared. An ECM degradation assay was performed to compare the functions of TM cells and TMSCs. Specific and broad MMP inhibitors were used to block MMP activities to explore specific functional MMPs in TM cells and TMSCs. *T-test* was used for statistical analysis.

Results: Both TM cells and TMSCs produced detectable basal amounts of MMPs. The expression of *MMP1, MMP3, MMP12, and MMP14* was significantly higher in TMSCs than in TM cells. The expression of *MMP2, MMP8*, and *MMP9* was comparable between the two cell types. However, the expression of *MMP13* was significantly higher in TM cells than in TMSCs. Both TM cells and TMSCs were able to digest pre-coated labeled collagen gel. With a broad-spectrum MMP inhibitor GM6001, the collagen degradation was blocked within 24-hr in TMSCs and up to 5 days in both TM cells and TMSCs. Most selective MMP inhibitors could block collagen degradation in both cell types. However, this inhibition of ECM degradation function was insignificant in TMSCs when the cells were treated with MMP3/12 inhibitor UK370101 and MMP2 inhibitor ARP101. The MMP inhibitors could inhibit the corresponding MMP expression in TM cells but not TMSCs.

Conclusion: TMSCs have higher MMP expression and activities than TM cells. Both TMSCs and TM cells can degrade collagen, which could be blocked by MMP inhibitors. This study unveils the TMSC function in TM ECM turnover, which is one of the mechanisms for TM regeneration.

Section 3: New Models and Tools to Study the TM and SC

15. A NOVEL CRE-INDUCIBLE MOUSE MODEL OF MYOCILIN GLAUCOMA FOR STUDYING TRABECULAR MESHWORK OUTFLOW AND NEURODEGENERATION IN GLAUCOMA

Balasankara Reddy Kaipa[1], Sam Yacoub[2], Ramesh Kasetti[2], Linya Li[1], J. Cameron Millar[2], William Cho[1], Dorota Skowronska-Krawczyk[1], Prabhavathi Maddineni[3], Yogapriya Sundaresan[1], Gulab S. Zode[1]

[1]Gavin Herbert Eye Institute-Center for Translational Vision Research, Department of Ophthalmology, Department of Physiology and Biophysics, University of California Irvine School of Medicine, Irvine, CA, USA; [2]Department of Pharmacology and Neuroscience, North Texas Eye Research Institute, University of North Texas Health Science Center at Fort Worth, TX, USA; [3]Department of Ophthalmology, School of Medicine, University of Missouri, Columbia, MO, USA

Purpose: The trabecular meshwork (TM) plays a vital role in aqueous humor outflow to maintain intraocular pressure (IOP) homeostasis. Elevation of IOP due to TM dysfunction and retinal ganglion cells (RGCs) loss are the pathological hallmarks of Primary Open Angle Glaucoma (POAG). However, a robust mouse model that faithfully recapitulates all pathological features of human POAG are lacking. Here, we report the generation and characterization of a novel Cre-inducible mouse model expressing DsRed-tagged Y437H mutant of human myocilin (*Tg.CreMYOC*^{Y437H}).

Methods: We generated a Cre-inducible transgenic mouse model expressing DsRed-tagged Y437H mutant of human myocilin (*Tg.CreMYOC*^{Y437H}). A single intravitreal injection of helper adenovirus (HAd) 5 expressing empty cassette or Cre was performed in adult *Tg.CreMYOC*^{Y437H} mice. MYOC expression, endoplasmic reticulum (ER) stress, fibronectin and actin changes were examined via RNA scope, transmission electron microscopy (TEM), immunostaining and Western blot analysis. Glaucoma phenotypes including IOP, outflow facility, structural and functional loss of RGCs, ON degeneration, and axonal transport deficits were examined at various stages of IOP elevation.

Results: A single intravitreal injection of HAd5-Cre led to selective *MYOC* expression in the TM at the level similar to endogenous *Myoc*. Expression of MYOC in TM induced significantly reduced outflow facility and sustained IOP elevation. Expression of mutant MYOC leads to accumulation of MYOC aggregates inducing chronic endoplasmic reticulum (ER) stress, fibrosis and increased actin in the TM. Sustained IOP elevation led to significant loss of RGCs and progressive ON degeneration. Notably, chronic IOP elevation blocked anterograde axonal transport at the optic nerve head prior to axonal loss.

Conclusion: Our studies indicate that Cre-inducible *Tg.CreMYOC*^{Y437H} mice recapitulates all glaucoma phenotypes observed in POAG patients and represents an ideal model for studying TM dysfunction and neuronal loss in POAG.

Funding: These studies were supported by the National Institutes of Health (EY034333 and EY026177). The authors acknowledge support from NIH grant EY034238 and from an unrestricted grant from Research to Prevent Blindness to the Gavin Herbert Eye Institute at the University of California, Irvine.

16. NEW TOOLS FOR GENETIC TARGETING OF THE SCHLEMM'S CANAL ENDOTHELIUM

Sofia L. Ochoa[1], Mark Johnson1, Evan A. Scott[1,2], Benjamin R. Thomson[3]

[1]Northwestern University McCormick School of Engineering, Department of Biomedical Engineering, Evanston, IL, USA; [2]University of Virginia School of Engineering and Applied Science, Department of Biomedical Engineering, Charlottesville, USA; Northwestern University Feinberg School of Medicine Department of Ophthalmology and Feinberg Cardiovascular and Renal Research Inst. Chicago, IL, USA

Purpose: The conventional outflow pathway, comprised of the trabecular meshwork and Schlemm's canal (SC), is responsible for the majority of aqueous humor outflow and is a key mediator of intraocular pressure (IOP). As small changes in these tissues have large impacts on IOP, understanding genes and pathways regulating SC function is crucial to the next generation of glaucoma therapies. Tamoxifen-inducible cre-loxp gene deletion systems (Cre-ERT2) have emerged as critical tool for these studies, allowing time and cell-type specific gene deletion in mice and generation of new ocular hypertension models. However, these tools depend on robust tissue-specific promotors to drive cre recombinase expression and to date, no ideal cre-recombinase expressing mouse lines have been generated for SC. Instead, SC deletion has been achieved using nonspecific cre drivers that also target other endothelial cells (*Cdh5, Tek, Prox1*) neurons and lens cells (*Prox1*) or even the whole body (*Ubc, Rosa26, EIIa*, *Bact*) and studies have depended on careful phenotypic analysis to disentangle SC-driven from systemic phenotypes. While this approach has led to numerous insights, its limitations become apparent when studying genes and pathways where widespread deletion would lead to overt systemic phenotypes or death. To overcome these limitations, we have developed a new method to deliver the active tamoxifen metabolite 4-OH-tamoxifen using SC-targeted nanocarriers. By delivering 4-OH tamoxifen directly to the SC endothelium, this system provides an additional level of specificity and eliminates systemic phenotypes by minimizing the dose of tamoxifen required. Moreover, this method permits targeted deletion in a single eye and allows the contralateral eye to serve as a same-animal control.

Methods: We have previously reported that poly(ethylene glycol)-b-poly(propylene sulfide) (PEG-b-PPS) nanocarriers decorated with a VEGFC-derived targeting peptide provide a robust tool for SC-specific delivery of hydrophobic small molecules and lead to IOP lowering when loaded with the actin depolymerizing agent latrunculin A.[1,2] Here, we use our previously published methods to generate SC-targeting PEG-b-PPS particles and load them with 4-OH tamoxifen. Particles were then delivered by intracameral injection and cre-mediated recombination was validated using *Cdh5*Cre-ERT2 in combination with the *Rosa26*-mTmG reporter mouse strain.

Results: Cre recombined endothelial cells were observed in SC following intracameral injection of 4-OH-tamoxifen loaded PEG-b-PPS nanocarriers, while no recombination was observed in contralateral eyes receiving injections of empty nanocarriers. Recombination efficiency was increased following a second injection 24 hours after the first, consistent with commonly used protocols for systemic tamoxifen administration. As expected due to their expression of the VEGFC receptor VEGFR3 (FLT4), targeted recombination was also seen in lymphatic capillaries of the limbus. Low levels of recombination were also observed in distal outflow vessels immediately adjacent to the canal. As these vessels do not express VEGFR3, this recombination may indicate nonspecific nanocarrier uptake or tamoxifen escape after nanocarrier degradation in the canal. No recombination was observed outside of the eye.

Conclusions: Here, we demonstrate that 4-OH-tamoxifen loaded nanocarriers facilitated robust cre activity in SC endothelial cells when used in combination with the pan-endothelial *Cdh5*CreERT2 mouse line. Nanocarrier delivery allowed deletion in the canal of a single eye and eliminated the need for hydrophobic vehicles such as corn oil or DMSO that are routinely used to deliver tamoxifen and its metabolites. Moreover, lack of recombination in the contralateral eye or other organs highlighted the potential of this system for studies of systemically lethal knockouts in SC and phenotypic comparison of matched pairs of eyes.

References

1. Stack, T., et al., Targeted Delivery of Cell Softening Micelles to Schlemm's Canal Endothelial Cells for Treatment of Glaucoma. Small, 2020. 16(43): p. 2004205.
2. Vincent, M.P., et al., Surface Engineering of FLT4-Targeted Nanocarriers Enhances Cell-Softening Glaucoma Therapy. ACS Applied Materials & Interfaces, 2021. 13(28): p. 32823-32836.

17. MAGNETIC STEERING OF ADIPOSE TISSUE DERIVED MESENCHYMAL STEM CELLS IN HUMAN OCULAR PERFUSION CULTURE

Markus Kuehn[1,2]

[1]University of Iowa, Ophthalmology and Visual Sciences, Iowa City, USA, [2]Iowa City VA Center for the Prevention and Treatment of Visual Loss, Iowa City, USA

Introduction: Reduced cellularity in the trabecular meshwork (TM) cells is strongly associated with aging, the development of elevated intraocular pressure (IOP) and Primary Open Angle Glaucoma (POAG). Efforts to replace lost TM cells have been focused on transplantation of various stem cell types, including iPSC derived material, TM stem cells and derived mesenchymal stem cells (MSC). Transplantation of these cells has resulted in reduced IOP in the eyes of mouse models of the disease, but their utility has been less well established in human eyes. The objective of this study was two-fold: First, we desired to evaluate whether human adipose tissue derived MSC can implant and survive in the human TM. Second, we evaluated whether magnetic steering of iron oxide particle labeled MSC into the iridocorneal angle is a feasible approach to improve targeted delivery of cells.

Methods: Human MSC were isolated from adipose tissue and maintained in cell culture up to passage 7. Human donor eyes (n=10) were obtained from the Iowa Lions Eye Bank and ocular perfusion cultures were established within 16 hours post-mortem. MSC were labeled with Cell Tracker DeepRed dye and incubated with superparamagnetic iron oxide particles. Labeled MSC were then isolated using magnetic separation and $2x10^5$ cells were transplanted into the anterior chamber of donor eyes by transcorneal injection. Cells were then steered toward the iridocorneal angle by positioning a Neodymium magnet slightly posterior of cornea on the exterior of the eye. Magnetic steering was only applied to the superior half of the eye, and the posterior portion was left untreated. Additional control eyes did not undergo magnetic steering. After 2 and 48 hours the tissue was fixed in paraformaldehyde and the number of MSC observed in the TM was determined in radial sections.

Results: Implantation of MSC in the TM was sparse in the absence of magnetic steering or in those portions of the eyes that did not undergo steering (<0.2 cells/section). Portions of the eye that were targeted by steering displayed significantly higher rates of implantation (1.2±0.5 cells/section, $p<0.001$). A significant difference in the number of MSC implanted into the TM was not observed between eyes harvested 2 or 28 hours after transplantation.

Conclusion: These data demonstrate that magnetic steering of MSC dramatically improves the successful delivery of cells to the target tissue. Our data also indicate that adipose derived MSC are capable of implanting into the human TM. These findings are in concert with recently published data demonstrating the feasibility of magnetic steering of MSC in rodent models of glaucoma.

18. SEGMENTAL OUTFLOW PATTERNS COINCIDE WITH LOCAL HYPOXIA AND VEGF EXPRESSION IN THE TM

Ester Reina-Torres, Darryl R. Overby

Dept. of Bioengineering, Imperial College London, London, UK

Purpose: To investigate how segmental aqueous humour outflow patterns change over time in mice and examine whether local hydraulic conductivity of the outflow pathway is determined by local metabolic demand mediated by hypoxia and vascular endothelial growth factor (VEGF).

Methods: Segmental outflow patterns mapped at different time points (Reina-Torres *et al*. 2022, EER) were used to determine how high (HF), medium (MF) and low flow (LF) regions redistribute over a 2-week time frame in C57BL/6J mice. Moran's I statistics were used to measure spatial autocorrelation and classify flow regions as HF, MF or LF in an unbiased way. This classification enabled us to calculate whether the areal fraction of each flow type was maintained over time and how regions changed from one type to another. Additionally, immunofluorescence analysis was performed to evaluate VEGF (n=4 eyes), the hypoxia marker CA-IX (n=5 eyes), and eNOS (n=10 eyes) expression in relation to tracer accumulation. VEGF and CA-IX correlations were determined from cross sections (27-47 sections/eye) while eNOS correlations were obtained from eyes that were flat mounted, and the entire outflow pathway was binned and analysed. Protein expression and tracer intensity correlations were assessed using ANCOVA. Image and data analyses were carried out using MATLAB.

Results: Despite temporal decorrelation between tracers, the overall distribution of flow regions remained stable across all time points: HF = 26±3%, MF = 40±6%, and LF = 34±6%. Spatial analysis revealed that regions predominantly shifted between HF and MF areas, with minimal change of LF areas. VEGF expression showed significant positive correlation with tracer accumulation ($p<0.001$), with difference in slope between eyes ($p<0.001$). CA-IX demonstrated consistent correlation with tracer intensity across all eyes ($p<0.001$, no significant slope differences between eyes, $p=0.12$). eNOS expression also significantly correlated with tracer intensity ($p<0.001$, with inter-eye slope variations $p=0.02$).

Conclusions: This study demonstrates that, within 2 weeks, aqueous humour outflow segmental patterns maintain an overall proportion of HF, MF and LF regions. However, patterns are dynamic and there is a shift between HF and MF regions while LF regions remain mainly unchanged, suggesting the presence of regulatory mechanisms controlling these changes. The correlation between high-flow regions and expression of VEGF, the hypoxia marker CA-IX, and eNOS suggests that local metabolic demands may regulate outflow function through VEGF-dependent pathways. These findings provide new insights into mechanisms required to maintain the outflow pathway's health and might explain the segmental nature of aqueous humour outflow.

Acknowledgements: This work was supported by the BrightFocus Foundation (G2021004F) and the NIH (EY022359).

Section 4: Schlemm's Canal and Distal Outflow

19. EFFECT OF CGRP ON SC AND TM CELL FUNCTION

Colleen M. McDowell, Timur Mavlyutov

Department of Ophthalmology and Visual Sciences, University of Wisconsin-Madison, Madison, WI, USA

The aqueous humor (AH) outflow pathway through the trabecular meshwork (TM) and Schlemm's canal (SC) is known to have regions of both high and low flow. Increased areas of low-flow regions increase risk for elevated IOP. The mechanism of how high and low-flow regions are developed and regulated is unknown. CGRP positive C-fibers are the major type of sensory neurons innervating the TM and SC. Upon activation afferent neurons secrete CGRP locally, and CGRP receptors are known to be expressed in TM and SC cells. It has previously been shown in other cell types that CGRP can modulate ECM protein expression and remodeling as well as enhance phagocytosis, both important aspects of TM function and IOP regulation. The goal of this project was to determine whether CGRP positive neurites innervating the TM and SC are involved in formation of high and low-flow regions.

High and low-flow regions were determined in 3 and 9-month-old wild-type C57BL/6J mice using yellow-green fluorescent tracer latex beads (0.02 μm) with or without Ad5.TGFβ2 induced ocular hypertension. Beads were injected intracamerally with a 35G needle at a rate 4 nL/s using a syringe pump controller. Anterior segment flat mounts were co-labeled with antibodies against CGRP (afferent neurons), CALCRL (CGRP receptor), and PECAM1 (SC endothelium), and imaged by confocal microscopy to acquire tiled Z-stacks of entire outflow area. Density of CGRP neurites in each flow region was determined by volumetric analysis in ImageJ. Primary human TM cells in culture were exposed to fluorescently labeled beads with or without CGRP (0.1 nM-5μM) for 24 hours and processed for immunocytochemistry. Phagocytosed beads were imaged and quantified using ImageJ analysis. Primary TM cells were exposed to 1μM CGRP with or without 5ng/mL TGFβ2 for 72 hours and expression of αSMA and COL1 assessed by western blot. Primary SC cells were exposed to 1μM CGRP for 24 hours and nitrite, a byproduct of nitric oxide (NO) degradation, was measured using the Griess reagent analysis kit.

Both high and low-flow regions were identified in 9-month-old C57BL/6J mice, with significantly more CGRP positive neurites per square area of high-flow regions compared to low-flow regions ($p<0.05$, n=10 eyes). CGRP positive neurite innervation significantly correlated with high flow regions in young 3-month-old ocular hypertensive C57BL/6J mice ($p<0.001$, n=3 eyes). The CGRP receptor, CALCRL, is expressed in both TM and SC cells and there is significantly more CALCRL expression in high-flow regions compared to low-flow regions ($p<0.01$, n=5 eyes). CGRP significantly increased phagocytosis in primary TM cells in culture compared to untreated controls ($p<0.01$), while Substance P treated cells had no significant differences in phagocytosis. TGFβ2 induced increases in αSMA and COL1 expression while exposure to CGRP blocked the effect ($p<0.05$). CGRP significantly increased production of NO as measured by concentration of nitrite compared to controls ($p<0.001$).

These data suggest CGRP positive nerve innervation favors a region to be high flow and suggest CGRP influences the development and regulation of high and low-flow regions of AH outflow.

20. INVESTIGATION OF TWO PORE TYPES IN SCHLEMM'S CANAL INNER WALL ENDOTHELIUM IN DIFFERENT FLOW-TYPE AREAS USING SERIAL BLOCK-FACE SCANNING ELECTRON MICROSCOPY

David L. Swain[1,2], Thuy Duong Le[2], Connie Lam[2], Haiyan Gong[2,3]

[1]Department of Ophthalmology, Northwestern University Feinberg School of Medicine, Chicago, Illinois, USA; [2]Department of Ophthalmology, Boston University Chobanian & Avedisian School of Medicine, Boston, Massachusetts, USA; [3]Department of Anatomy and Neurobiology, Boston University Chobanian & Avedisian School of Medicine, Boston, Massachusetts, USA

Purpose: With the introduction of advanced automated serial block-face imaging, we can now further investigate the characteristics of pores in the inner wall Schlemm's canal endothelium. Previous studies of the pores using 2D scanning or transmission electron microscopy were limited to *en face* or random cross-sectional imaging and may have missed pores. Additionally, the morphological characteristics of pores in different segmental flow areas have not been fully explored. This study aimed to further characterize the two types of pores in different flow areas of human eyes using serial block-face scanning electron microscopy (SBF-SEM).

Methods: In this study, two normal human eyes were perfused at 15 mmHg with fluorescent tracers to label high-, low-, and non-flow areas of outflow, which were dissected from each eye, sectioned serially (thickness = 0.13 μm), and imaged using SBF-SEM. 10,832 serial images were examined to identify all intracellular pores (I-pores) and intercellular or border pores (B-pores). Pore densities per unit inner wall area or per inner wall cell nucleus and pore sizes were determined. Locations of I-pores on giant vacuoles (GVs), whether on the side or tops of GVs was determined. Pores that would be potentially missed using 2D scanning electron microscopy and I-pores on the edges of inner wall cells that could be mistaken for B-pores were identified.

Results: We observed 729 pores, of which 656 (90.0%) were GV-associated I-pores, 25 (3.4%) were non-GV-associated I-pores, and 48 (6.6%) were B-pores. Of all pores, there were significantly more I-pores (93.4%) than B-pores (6.6%). Of all I-pores, the majority (96.3%) were associated with GVs. Significantly more GV-associated I-pores were located on the side of GVs (413/656, 63.0%), compared to the top of GVs (243/656, 37.0%; $P \leq 0.01$), which was observed similarly in all flow-type areas. I-pore density was higher in high-flow areas compared to low- or non-flow areas in both eyes, whereas B-pore densities did not appear to differ between flow-type areas. From *en face* view via traditional SEM, 6.6% of I-pores on the side of GVs and/or near the edge of cells could have been mistaken as B-pores. 32.0% of all pores could have been missed by 2D-SEM due to obstruction of view by neighboring cells/GVs (31.4% of I-pores and 39.6% of B-pores). Median major and minor axes of I-pores were significantly smaller in high-flow areas, compared to non-flow areas ($P = 0.024$ and $P = 0.048$, respectively). B-pores were not significantly different in size among flow-type areas.

Conclusions: SBF-SEM and 3D-reconstruction provided an in-depth method to identify the pores of Schlemm's canal inner wall, as the cells could be freely rotated to any viewpoint. This study applied a novel method to investigate the morphological characteristics of pores and found that pores in high-flow areas were more numerous and smaller than in non-flow areas, suggesting that pore morphology and density may play a role in the regulation of segmental outflow.

Financial Support: National Institute of Health (NIH) EY022634 (HG), EY030318 (DLS), BrightFocus Foundation 2016099 (HG), Posse Foundation Scholarship (CL), and The Massachusetts Lions Eye Research Fund.

21. INVESTIGATION OF THE EFFECT OF NETARSUDIL ON THE INNER WALL ENDOTHELIAL CELLS OF SCHLEMM'S CANAL OF HUMAN EYE USING SERIAL BLOCK-FACE SCANNING ELECTRON MICROSCOPY

Haiyan Gong, Cameron Ashrafzadeh, Roviel Arquiza, Tianyang Chen, Sarah Park, David L. Swain

Department of Ophthalmology, Chobanian & Avedisian School of Medicine, Boston, MA, USA

Purpose: Netarsudil, a rho-kinase/norepinephrine inhibitor, is a new class drug to decrease IOP in glaucoma. A previous study showed that netarsudil increases outflow facility by increasing active filtration area through inducing trabecular meshwork expansion and dilating episcleral veins. The inner wall (IW) endothelial cells of Schlemm's canal (SC) play an important role in regulating aqueous outflow. However, the effect of netarsudil on the IW endothelial cells of SC has not been fully studied. Additionally, aqueous outflow is not uniform with high-, low-, and non-flow regions, and whether netarsudil affects the IW cells differently in the different flow regions has not yet been studied. This study investigated the morphological changes in the IW endothelial cells between netarsudil-treated and control eyes in high-, low-, and non-flow regions using serial block-face scanning electron microscopy (SBF-SEM).

Methods: Two pairs of normal human donor eyes were obtained from eye banks. Eyes were perfused with Dulbecco's phosphate-buffered saline with 5.5 mM D-glucose (GPBS) to establish a baseline outflow facility at a constant pressure of 15 mmHg. The anterior chambers of all eyes were exchanged and perfused with green fluorescent tracer to label the areas of active flow before the treatment. One eye from each pair was then exchanged and perfused with GPBS, and the other eye was exchange and perfused with 0.3 uM Netarsudil-M1 (Aerie Pharmaceuticals, Inc.) for 3 hours. Eyes were exchanged and perfused with red fluorescent tracer to record the changes in the areas of active flow, followed by perfusion-fixation with Karnovsky's fixative. The green and red fluorescent tracers were visualized via global imaging. Six radial wedges of trabecular meshwork including SC (2 each from high-, low-, and non-flow areas) were imaged using SBF-SEM (1500-2000 images for each block). SBF-SEM images were traced using Reconstruct software, and each cell was 3D reconstructed (n= 10 for each group). Cell and nuclear volume of each cell, volume and types of giant vacuoles (GVs) were analyzed and compared to controls using two-way ANOVA.

Results: Two-color tracer perfusion successfully identified areas that increased in flow after treatment with netarsudil. Compared to controls, netarsudil treatment significantly increased cell volume in the high-flow ($p<0.0001$) and low-flow regions ($p<0.05$) but not non-flow regions; and also significantly increased nuclear volume in the high-flow ($p<0.0001$) and low-flow regions ($p<0.0001$) but not non-flow regions. The cell and nuclear volume were the largest in the high-flow regions of netarsudil-treated eyes compared to other groups. Netarsudil treatment significantly increased total GV volume in the high-flow ($p<0.01$) and low-flow ($p<0.001$) regions but not non-flow regions. Netarsudil significantly increased the volume of Type IV GVs (GVs with basal opening and I-pores) and percentage of Type IV GVs per cell in high-flow regions (24 % in treated vs. 10% in control).

Conclusions: Netarsudil treatment significantly increased cell, nuclear, and total GV volume. It also significantly increased the volume and percentage of Type IV GVs in high-flow regions, which increased the area of high-flow. The morphological changes in the IW endothelial cells induced by netarsudil are not uniform, mainly in high- and low-flow regions.

Financial Support: The Student Research Award from Boston University Undergraduate Research Opportunities Program, NIH grants EY022634, EY030318, and the Massachusetts Lions Eye Research Fund.

22. MICROENVIRONMENTAL FACTORS INFLUENCING BARRIER FUNCTION IN CULTURED HUMAN SCHLEMM'S CANAL ENDOTHELIAL CELLS

Darryl R. Overby[1], Haoyu Xia[1], Jacques A. Bertrand[1], W Daniel Stamer[2]

[1]Dept. of Bioengineering, Imperial College London, London, UK; [2]Department of Ophthalmology, Duke University, Durham, NC, USA

Purpose: The inner wall endothelium of Schlemm's canal (SC) is the sole continuous barrier to conventional outflow and the main site of outflow resistance generation. A major limitation is that cultured human SC cells fail to recapitulate the inner wall barrier that exists *in vivo*. In this project, we aim to restore lost barrier function in cultured SC cells by focusing on the role of cell shape confinement, which promotes barrier formation in other cell types[1].

Methods: This study integrates two established tools of cellular mechanobiology: (i) *micropatterning*, where cells are confined to adhere and spread within islands of specific shape, and (ii) *permeability mapping*, which identifies locations of high permeability between neighbouring cells. Micropatterning was achieved using ultraviolet degradation[2]. We investigated circular, square and triangular islands of equal area (5,000 μm^2), and compared against SC cells that were allowed to spread freely on non-patterned surfaces. For permeability mapping, SC cells were seeded on micropatterned islands coated with biotinylated gelatin. After 24 hours, cells were exposed to Texas-red avidin (25 µg/ml) for 1 minute to label permeable locations where fluorescent avidin crosses the inter-cellular junctions to bind to the biotinylated substrate. Cells were treated with EDTA (5 mM) or BV9 (1 µg/ml) for 5 minutes, which disassemble junctions by chelating calcium or blocking the extracellular domains of VE-cadherin, respectively. Cells were fixed and immunolabelled for ZO-1, VE-cadherin or claudin-11 and stained for F-actin and DAPI. Two SC cell strains (SC60, SC68) from 58- and 30-year-old non-glaucomatous donors were used. Images from at least 50 patterned SC cells were compared to non-patterned SC cells.

Results: Micropatterned SC cells showed reduced stress fiber formation and a lower nuclear aspect ratio compared to non-patterned SC cells. ZO-1 labelling revealed a prominent band between SC cell doublets on circular, square and triangular micropatterns (Figure), although there was a tendency for the ZO-1 band to be straighter on square islands, oriented along the diagonal. In non-patterned SC cells, ZO-1 labelling was punctate without continuous cell border labelling. On micropatterns, regions of cell-cell contact were devoid of permeability label whilst non-patterned SC cells showed pronouced permeability label between cells. EDTA, but not BV9, caused junctional disruption, as indicated by increased permeability label on circular islands ($p<0.05$; N=54 vs 65 cells). VE-cadherin and claudin-11 labelling was absent in all cases, regardless of pattern.

Conclusions: Cell shape confinement promotes junctional formation between adjacent human SC cells. Current research aims to identity the nature of the inter-cellular junctions formed between micropatterned SC cells. Combining micropatterning and permeability mapping provides an opportunity to screen for compounds to disrupt intercellular junctions and SC barrier function as potential outflow-enhancing drugs to lower IOP.

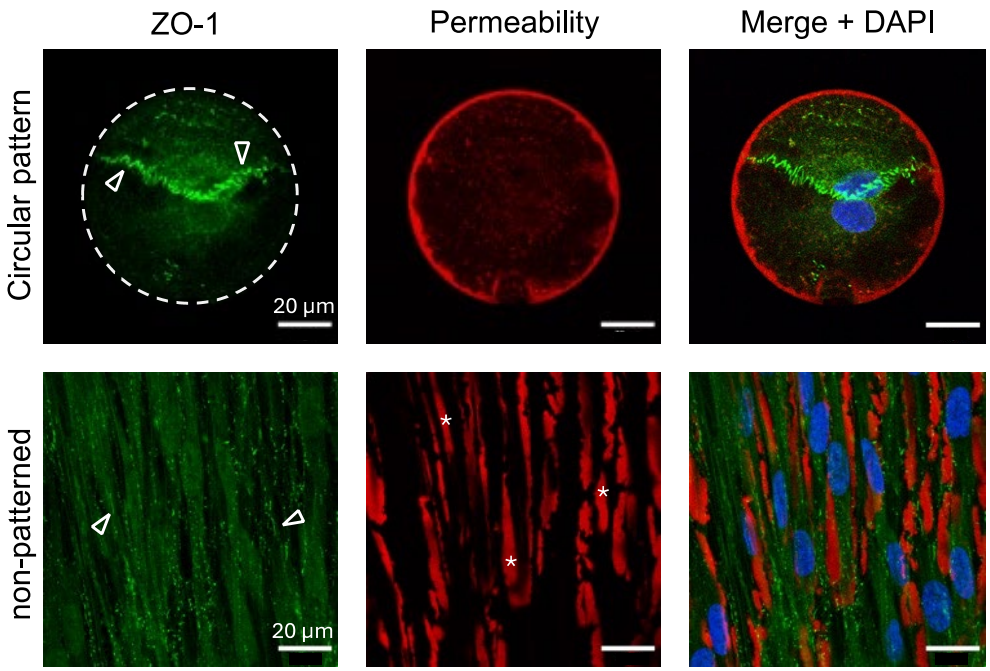

Figure: Micropatterned SC cell doublets (SC60p6) seeded on circular islands (top row) relative to non-patterned SC cells allowed to spread freely (bottom row). Note the appearance of a dense ZO-1 labelled band between micropatterned SC cells (arrowheads), which is largely absent from non-patterned SC cells. Patterned SC cells allow very little permeability tracer through the cell-cell border, while permeability tracer freely labels spaces between non-patterned SC cells.

References

1. Sri-Ranjan, K. *et al.* Intrinsic cell rheology drives junction maturation. *Nat. Commun.* 202213, 4832 (2022).
2. Azioune et al. Protein micropatterns: A direct printing protocol using deep UVs. *Methods in Cell Biology*. 97:133-146, 2010.

Financial Support: BrightFocus Foundation (G2023011S), NIH (EY022359) and BBSRC (BB/Z516375/1). We acknowledge the efforts of Kristin Perkumas for isolation and characterisation of human SC cells.

23. VALVE-LIKE STRUCTURES DISTAL TO SC IN THE HUMAN EYE: AN SEM STUDY

Murray Johnstone[1], Elizabeth Martin[1], Steven Padilla[1], Ronald L Fellman[2], Chen Xin[3], Ruikang Wang[1,4]

[1]Department of Ophthalmology, University of Washington, Seattle, WA, USA; [2]Glaucoma Associates of Texas, Dallas, TX, USA; [3]Beijing Tongren Hospital, Capital Medical University, Beijing, P.R. China; [4]Department of Bioengineering, University of Washington, Seattle, WA, USA

Purpose/Relevance: Collector channels (CC) exit Schlemm's canal (SC), then immediately enter circumferential vascular channels (CVC) parallel to SC, as shown by definitive embryogenesis, microvascular casting, and OCT studies.(1,2) CVC have distal radial channels leading to the episcleral veins that are noncontiguous with the CC or SC. (2) OCT imaging shows mobile pressure-dependent septa between SC and the CVC, providing a valve-like distal control system as also demonstrated by SEM.(3, 4) The distal highly organized CVC aqueous pathway suggests an important role in controlling aqueous flow and IOP. The study explores CVC relationships quantitatively using SEM.

Methods: A < 24 hours postmortem eye of a 74 y/o C/M was divided into 4 quadrants and each quadrant dilated with viscoelastic. Meridional sections bisected the entire 360º SC circumferential axis. To prevent double counting, only the corneal side of each bisected area was analyzed. Standard procedures were used for SEM. ImageJ was used to measure and analyze images.

Results: A total of 40 SEM segments processed: 9, 9, 11, 11 for IT, IN, ST, & SN quadrants, respectively. SC data: full length measured, 30,116 µm; mean SC segment length, 752±150 µm (range (R) 392-1069 µm); mean SC height at cut front edge perpendicular to the long axis, 69.5±23.6 µm (R 34.3-134.5); mean SC area 51,687±21,760 µm^2. CC data: n=10. Mean height perpendicular to SC, 13.9±6.6 µm (R 6.0-28.4); width parallel to SC 44.3±24.9 µm (R 17.8-88.9); mean area 570.8±494.9 um^2. CVC Data: Distance from SC, 100.2±50.9 µm (R 6.4-221.8); mean CVC height, 21.9±11.5 µm (R 8.3-64.4); mean length, 150.6±113.8 µm (R 35.4-691); Mean aspect ratio, 7.3 ±4.6 µm (R 1.6-29.5). Mean ISCC angle subtended from SC outer wall 9.5±9.80 (R 0.0-51.7)

Discussion: CC extended a mean of 13.9 µm & a maximum of 28 µm into the sclera before abruptly turning circumferentially to join CVC. Collagenous septum separated the SC and CVC lumens creating flap-like relationships at CC entrances. Consistent with MVC findings, CVCs typically coursed for a long distance nearly parallel to SC. (1). Long septa partitioned the CVC from SC with a mean 100.4 µm thickness. The 7.3 mean septa aspect ratio mirrored that of the CVC. The elongated septa separate the CVC from SC, creating a noncontiguous separation of CC and distal radial channel lumens.

Conclusion: SEM confirms the CVC anatomy and relationships demonstrated by MVC and embryogenesis studies. The CVCs experience pressure-dependent motion documented by OCT, permitting them to act as compressible conduits involved in controlling outflow pathway size, aqueous outflow, and IOP.

Selected References

1. Ramírez JM, Ramírez AI, Salazar JJ, Rojas B, De Hoz R, Triviño A. Schlemm's canal and the collector channels at different developmental stages in the human eye. Cells Tissues Organs. 2004;178:180-185.
2. Johnstone M, Xin C, Tan J, Martin E, Wen J, Wang RK. Aqueous outflow regulation–21st century concepts. Progress in retinal and eye research. 2021;83:100917.
3. Hariri S, Johnstone M, Jiang Y et al. Platform to investigate aqueous outflow system structure and pressure-dependent motion using high-resolution spectral domain optical coherence tomography. J Biomed Opt. 2014;19:106013 1-10601311.
4. Xin C, Wang RK, Song S et al. Aqueous outflow regulation: Optical coherence tomography implicates pressure-dependent tissue motion. Exp Eye Res. 2017;158:171-186

Figures

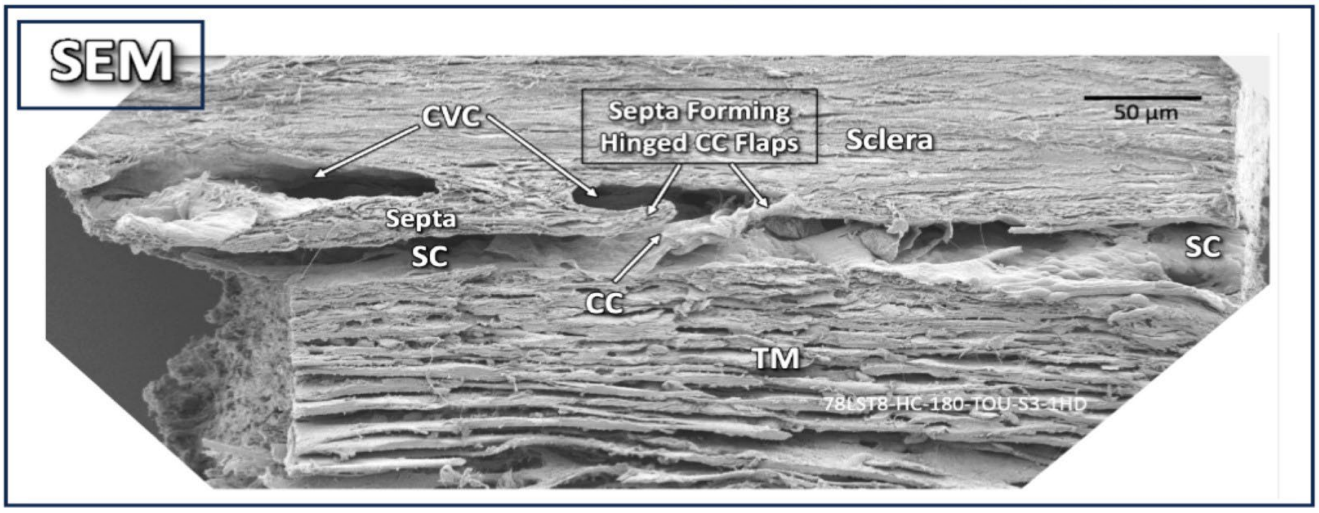
SEM
CVC
Septa Forming
Hinged CC Flaps
Sclera
50 µm
Septa
SC
SC
CC
TM

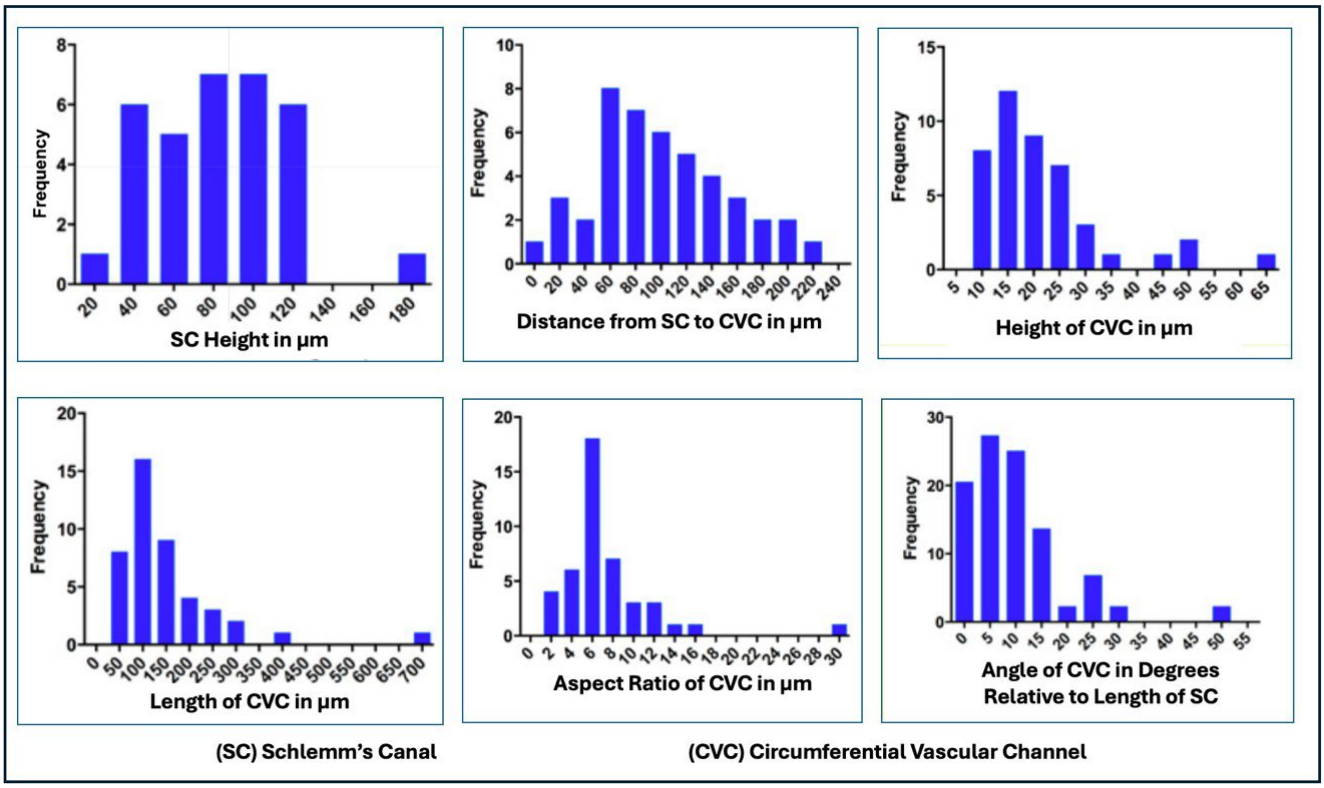
Frequency
SC Height in µm
Distance from SC to CVC in µm
Height of CVC in µm
Length of CVC in µm
Aspect Ratio of CVC in µm
Angle of CVC in Degrees
Relative to Length of SC
(SC) Schlemm's Canal
(CVC) Circumferential Vascular Channel

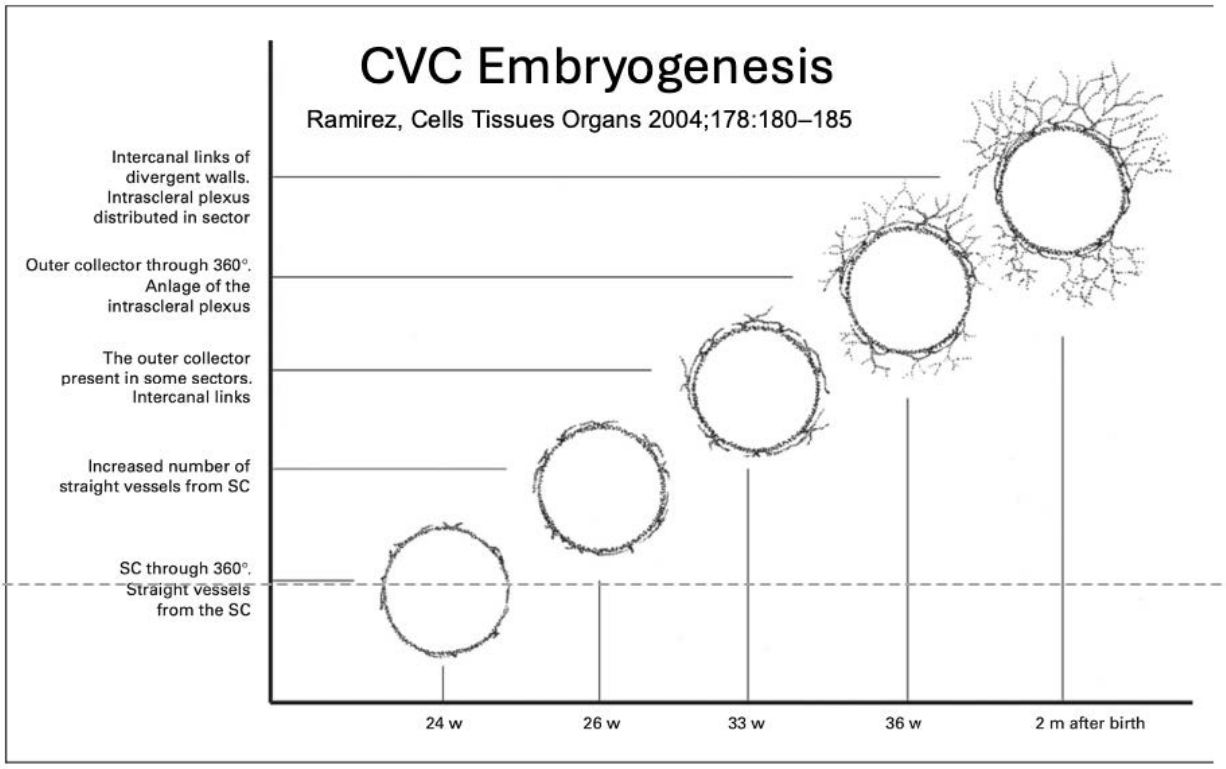

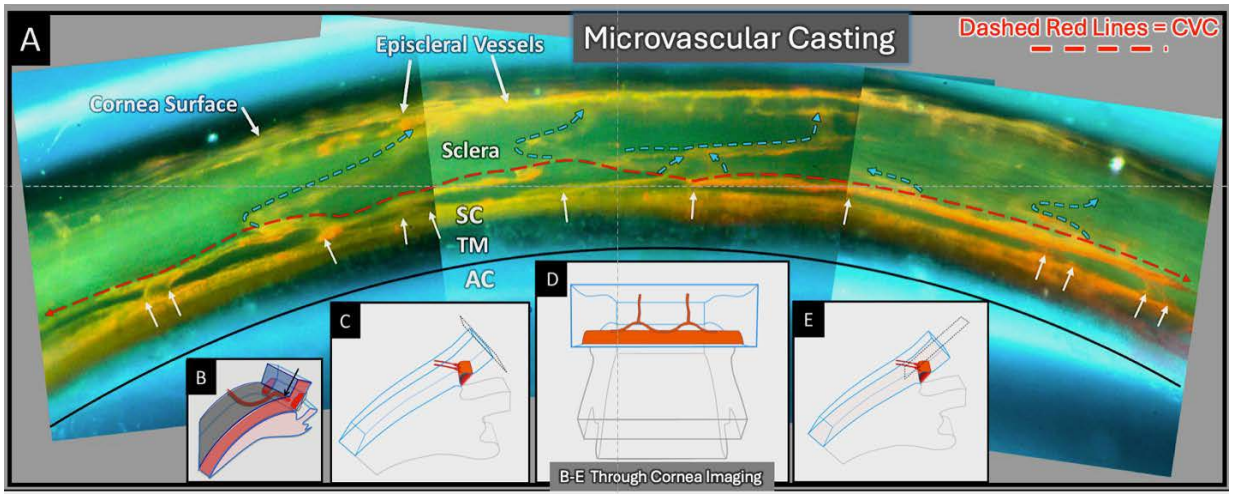

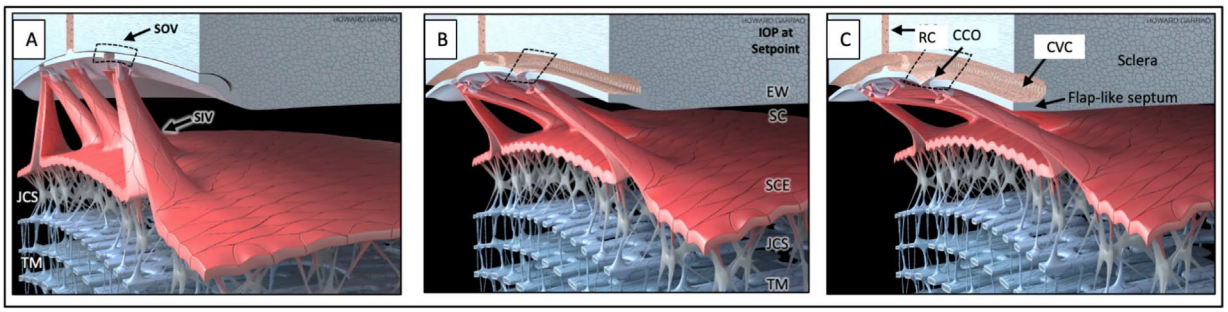

(A) IOP Below Setpoint (B) IOP at Set Point (C) IOP Above Setpoint.
SC Inlet Valve (SIV); SC Outlet Valve (SOV); Collector Channel Ostia (CCO); Radial Channel (RC); Circumferential Vascular Channel (CVC), SC endothelium (SCE); Juxtacanicular Space (JCS)

24. PAST, PRESENT AND FUTURE OF AQUEOUS HUMOR DYNAMICS RESEARCH: IT'S ABOUT MORE THAN JUST THE TM

Carol B. Toris

The Ohio State University, Department of Ophthalmology and Visual Sciences, Columbus, OH, USA

Aqueous humor dynamics (AHD) has been a topic of interest since the 1940s with work by Friedenwald and Goldmann. Then along came the Goldmann equation. Bill identified uveoscleral outflow in the 1960s. I came into the picture in the 1980s. My PhD thesis consisted of the study of aqueous humor dynamics in iridocyclitis. In the 1990s interest in uveoscleral outflow increased when prostaglandin analogs were found to lower IOP by improving this drainage. Outflow facility was identified as the predominant location of pathology in the drainage pathways causing IOP elevation. New treatments for IOP elevation mainly target this region. Currently, this is an area of major research interest and grant funding.

My investigation of aqueous humor dynamics (AHD) and intraocular pressure (IOP) regulation has taken me in many directions. Our clinical work includes the study of ocular pathologies affecting IOP and normal changes that take place during aging and over a 24-hour period. We also investigate novel IOP lowering drugs when dosed alone or together, during the day and at night, and under different pathological conditions. Our rabbit work included the study of novel treatments affecting IOP and normal changes that take place during development. We have spent some time studying mice with glaucoma where we found normal aqueous flow, but reduced outflow facility. This is consistent with studies in humans. Our methods to measure aqueous humor dynamics by fluorophotometry in the tiny eye of a mouse took years to develop but the methods are now published and available for other labs to use. I have worked with a trained NHP colony for 3 decades. With these precious animals, we have done many preclinical AHD studies in collaboration with industry from many countries.

My crystal ball sees the study of AHD well into the future. While research on AHD of the whole eye of humans and research animals has fallen behind molecular and cellular research in the outflow pathways, replacement of old AHD techniques with promising new methods should rapidly advance the field. AHD

findings in eyes where blood is flowing, hormones are circulating, and axons are firing could inform the direction of the molecular/cellular research in the near future and will fill in the many gaps in our knowledge of normal ocular health and pathologies. Aqueous humor dynamics measurements soon may be utilized for individualized medication, laser, and surgical recommendations for each patient. It could revolutionize the way glaucoma is practiced and truly pave the way for individualized glaucoma treatment paradigms.

Section 5: ECM, Extracellular Vesicles, and Macrophages in the TM

25. REVERSING DEX-INDUCED ECM CHANGES IN TM CELLS WITH EXTRACELLULAR VESICLES

Reynolds Ablordeppey[1], Maral Namdari[1], Fiona S. McDonnell[1]

[1]Moran Eye Center, Salt Lake City, UT, USA

Introduction: Dysregulation in the trabecular meshwork (TM) tissue of the conventional outflow pathway leads to elevated IOP and glaucoma. A key element of outflow homeostasis is extracellular matrix (ECM) maintenance and turnover within the TM. Extracellular vesicles (EVs) from glaucomatous TM cells have previously been shown to have significantly different ECM proteins bound to them when compared with non-glaucomatous TM EVs. EVs are involved with cell-cell and cell-matrix signaling through many pathways.

Methods: We isolated EVs from non-glaucomatous TM cells using double-cushioned ultracentrifugation, followed by rigorous characterization of size and concentration using nanoparticle-tracking analysis (NTA). Western blotting for known EV markers was used to characterize EVs. We then treated non-glaucomatous TM cells with the corticosteroid dexamethasone (Dex) with and without healthy EVs (2x10^8 nanoparticles). Western blotting was used to determine the effect of EVs on ECM proteins (fibronectin, α-smooth muscle actin and integrin β3 synthesized by TM cells. Data is presented as mean [95%confidence interval].

Results: Isolated EVs from NTM cells show an average size of 139.7 [130.0, 149.4]. EVs were positive for CD63 and TSG101, and negative for calnexin and albumin, consistent with guidelines for characterization. TM cells treated with Dex showed upregulation of fibronectin (fold change 1.57 [0.49, 2.66], $p<0.05$), α-smooth muscle actin (fold change 1.37 [-0.56, 3.31]), and integrin β3 (fold change 1.61 [0.60, 2.62]) compared to vehicle controls. Healthy EVs attenuated this response; fibronectin (fold change 1.22, [0.60, 1.84]), α-smooth muscle actin (fold change 0.89, [-0.07, 1.85]), and integrin β3 (fold change 1.12, [0.59, 1.65], $p=0.06$).

Conclusion: This data indicates that EVs can be used therapeutically to reverse ECM changes induced by dexamethasone, and therefore could be used to treat similar ECM dysregulation such as occurs in glaucoma.

26. CLUSTERIN AS A SIGNAL ATTENUATOR AND A BONAFIDE ECM SENSOR - A MECHANISTIC STUDY

Avinash Soundararajan, Rodahina Pasteurin, Anusha Shivashankar, Padmanabhan P Pattabiraman

Department of Ophthalmology, Indiana University School of Medicine, Indianapolis, IN, USA

In our previous study, we demonstrated that the clusterin knockout mice showed increased intraocular pressure (IOP). The loss of clusterin function *in vivo* significantly elevated IOP due to increased deposition of ECM like collagen and fibronectin, in TM-JCT region Conversely, clusterin gain of function provided evidence on clusterin as an antifibrotic agent. To better understand the mechanism, we aimed to elucidate the impact of clusterin gain-of-function on IOP and TM biology.

Using adenovirus to constitutively express clusterin (AdCLU) in comparison with control (AdMT), recombinant human clusterin (rhCLU) in comparison to sham control, and knocking down clusterin using siRNA (siCLU) compared to scrambled (siScr) - we performed - **A)** IOP measurements in - *ex vivo* - human anterior segment perfusion cultures, and *in vivo* – in C57BL/6 mice, and *in vitro* primary human TM (HTM) cells. **B)** TMT labeled proteomic analysis. Screening criteria protein level changes included $p \leq 0.05$ and mean$\pm 2\sigma$ of $\log2 \geq 0.3$ as the confidence fold change (FC). **C)** Coimmunoprecipitation (Co-IP) with Clusterin antibody to determine its interactors. Statistical analyses were performed using a Student's t-test with significance at $p \leq 0.05$.

We have identified that – **1.** Clusterin knockdown *in vitro* significantly induced actin and actin regulators. **2.** Conversely, constitutive clusterin expression in the TM tissue lowered IOP by modifying ECM expression in human anterior segment perfusion cultures *ex vivo*. **3.** Exogenous supplementation of clusterin using recombinant human clusterin *ex vivo* lowered transforming growth factor b2 (TGFb2)-induced pathological IOP elevation. **4.** Constitutive clusterin expression in TM lowered the levels of - G-proteins - G(q)a (GNAQ), Gb-1 (GNB1), Gg-12 (GNG12); Ras-like GTPase - RRAS2; focal adhesion proteins of Tensin family – TNS3 (contains actin-binding and integrin-binding domains) and TNS4; and signaling molecules - SMAD3 and STATs. **5.** Clusterin decreased actin contractility, cell adhesive interactions, and fibrogenic machinery. Interestingly, clusterin immunoprecipitation brought down fibronectin, HSPG, laminin, and collagen IV in the TM secretome.

This novel study presents the firsthand report on how clusterin employs distinct regulatory mechanisms as “signal attenuator” and “bonafide ECM sensor” within the TM outflow pathway to control G protein-mediated actin polymerization and tensin-based cell-adhesive interactions and fibrogenic process, ultimately contributing to IOP homeostasis.

Acknowledgements: Funding from NIH/NEI-R01EY029320, R01EY035412, R01EY036107, Showalter Research Award, Research Support Funds Grant, Research to Prevent Blindness Grants to IU.

27. MACROPHAGES IN THE CONVENTIONAL OUTFLOW TRACT

Katy Liu

Glaucoma Division, Duke Eye Center

Purpose: Macrophages are found in all tissues of the body, and their function is determined by their developmental origin and tissue microenvironment. Tissue resident macrophages (RTMs) are derived prenatally and are long-lived, while short-lived macrophages are derived from monocytes from the adult bone marrow. Our previous work has shown that macrophages are abundant in the outflow tract and are of dual origin – comprised of RTMs are short-lived macrophages. The function of macrophages in the outflow tract has not been elucidated which is the topic of our current studies.

Methods: Using *Cx3cr1-YFP*$^{CreER/+}$ mice with various Cre reporters, RTMs are conditionally labeled and specifically depleted by targeting Cre driven iDTR. Short-lived macrophages were genetically depleted using the *CCR2*$^{RFP/RFP}$ (KO) mice (CCR2 is the chemokine needed for monocytes to exit the bone marrow). Intraocular pressure (IOP) was measured by rebound tonometry, and outflow facility was measured *ex vivo* using the iPerfusion system. Extracellular matrix turnover was studied by quantifying the basement membrane material of the beneath the inner wall of Schlemm's canal by transmission electron microscopy. Statistical analysis was performed by Student's t test with $p<0.05$ considered significant.

Results: With RTM depletion, there was a significant increase in IOP and a corresponding reduction in outflow facility. RTM depletion resulted in increase in extracellular matrix basement membrane material. In contrast, short-lived macrophage depletion reduced IOP, but outflow facility was unchanged. There was no change in the quantification of extracellular matrix basement membrane material in short-lived macrophage depleted eyes.

Conclusions: Macrophages in the conventional outflow tract affect IOP homeostasis with RTM depletion raising IOP and lowering outflow facility. Thus, RTMs act on the proximal outflow tract to maintain IOP, likely by altering extracellular matrix turnover. This is in contrast to short-lived macrophages which likely act on other regions of the outflow tract.

Section 6: TM Cell Biology

28. THE MIRNA-MRNA INTERACTIVE NETWORKS IN REGULATING ESTROGEN AND TGFB SIGNALING IN HTM CELLS UNDER CYCLIC MECHANICAL STRETCH

Jingwen Cai[1], Hannah Youngblood[2], Hongfang Yu[1], Louis R Pasquale[3], W Daniel Stamer[4], Yutao Liu[1,5,6]

[1]Department of Cellular Biology and Anatomy, Augusta University, Augusta, GA, USA; [2]School of Chemistry & Biochemistry, Georgia Institute of Technology, Atlanta, GA, USA; [3]Department of Ophthalmology, Icahn School of Medicine at Mount Sinai, New York, NY, USA; [4]Department of Ophthalmology and Biomedical Engineering, Duke University, Durham, NC, USA; [5]James & Jean Culver Vision Discovery Institute, Augusta University, Augusta, GA, USA; [6]Center for Biotechnology and Genomic Center, Augusta University, Augusta, GA, USA

Purpose: Our previous study suggested the role of estrogen signaling in IOP regulation. Estrogen has been shown to remodel extracellular matrix (ECM) and antagonize the effect of glaucoma-associated TGFβ signaling. This study aims to investigate the underlying genetic mechanisms of estrogen's anti-TGFβ2 effect using human trabecular meshwork (HTM) cells under cyclic mechanical stretch (CMS).

Methods: Validated primary HTM cells from non-glaucomatous donors (6 females and 4 males) were treated with DMSO, TGFβ2 (10ng/μl), or TGFβ2 + estradiol (E2, 50μM) under CMS (15%, 1 cycle/second, 24 hours). Extracted total RNAs (200 ng per sample) were used to prepare sequencing libraries for mRNAs/lncRNAs and miRNA, respectively, followed by sequencing using Illumina NovaSeq 6000. Sequence reads were processed using our established pipelines with Partek-Flow for alignment, annotation, normalization, and differential expression analysis. Two-tailed paired t-test was used to identify differentially expressed (DE) miRNAs. Gene ontology and KEGG pathway analysis were done using WebGestalt 2019. The interaction of differentially expressed miRNAs and mRNAs in these HTM cells were analyzed using Ingenuity Pathway Analysis (IPA).

Results: We identified 327 significant DE genes after TGFβ2 treatment (FDR≤0.05, |FC|≥2). However, 285 of these DE genes became non-significant after the combined E2 treatment. At the same time, we identified 65 DE miRNAs with TGFβ2 treatment (p≤0.05), and 54 of them became non-significant in the combined E2 treatment. These 285 genes targeted by E2 were enriched in growth factor receptor binding and cell adhesion molecule binding. Our miRNA-mRNA interaction analysis identified 58 of these 285 genes could be targeted by 28 DE miRNAs using IPA. For example, miR19b-3p may bind to estrogen receptor 1 and increase the expression of 8 genes, including *EFNB2, H3C3, KBTBD8, PDCD1LG2, PPP1R13L, RHOB, RNF152,* and *SDC1*. Moreover, let-7a-5p may be regulated by E2 and increase the expression of 7 genes, including *COL4A1, RHOB, RRM2, TAGLN, TRIM6, TRIP13* and *UHRF1*. The glaucoma related miR-204-5p was inversely paired with TGFβ downstream molecule IL11.

Conclusion: Our study suggested that estradiol has anti-TGFβ2 activity in HTM cells undergoing CMS, potentially mediated by the miRNA-mRNA interactive network induced by E2 treatment.

Funding: We acknowledge the support from NIH/NEI (P30EY031631, F31EY031973, R21EY033961, R01EY023242, R01EY032960, R01EY022359 and R21EY028671), The Glaucoma Foundation, the Glaucoma Research Foundation, the BrightFocus Foundation, and the Medical College of Georgia at Augusta University

29. THE ASSOCIATION BETWEEN CROSS-LINKED ACTIN NETWORKS (CLANS) AND TRABECULAR MESHWORK CELL PROLIFERATION AND SENESCENCE

Weiming Mao, Devon Harvey, Joseph M. Dalloul, Jiannong Dai, Chenna Kesavulu Sugali, Kamesh Dhamodaran, Shaohui Liu

Department of Ophthalmology, Eugen and Marilyn Glick Eye Institute, Indiana University School of Medicine, Indianapolis, IN, USA

Purpose: Cross-linked actin networks (CLANs) are a special type of F-actin structure. In confluent trabecular meshwork (TM) cells, CLANs are often found in the perinuclear region. CLANs appear to be geodesic spheres consisting of hubs (F-actin) and spokes (containing many calcium binding proteins). CLANs are closely associated with glaucoma because 1) there are more CLANs in glaucomatous TM cells and tissues; 2) glaucomatous insults such as TGFβ2 and steroids induce CLAN formation in the TM. Our published studies show that CLANs contribute to TM cell stiffness and compromise phagocytosis in a transformed TM cell line. In this study, we determined whether CLANs are associated with cell proliferation and senescence in primary human TM (pHTM) cells.

Methods: pHTM cells characterized according to published consensus were seeded onto 96-well plates. To induce CLAN formation, the cells were treated with or without 5ng/ml TGFβ2 or 100nM dexamethasone (DEX) or 0.1% ethanol (EtOH; as a vehicle control for DEX) for 1 week. At the end of treatment, the cells were fixed and immunostained for CLANs (phalloidin Alexa 488) together with cell proliferation (Ki67) and senescence (p21, H2AX, and β-galactosidase) markers. Cell nuclei were stained with DAPI. The number of CLAN positive/negative, DAPI positive, and cell mark positive/negative cells was counted. Different ratios were compared using Student's t-tests with p values <0.05 considered statistically significant.

Results: TGFβ2 or DEX-treated pHTM cells formed significantly more CLANs compared to controls. Regardless of TGFβ2 or DEX treatment, there was no difference in the ratio of the cell proliferation marker Ki-67 over DAPI. However, in both control and treated (TGFβ2 or DEX) cells, Ki-67 was found only in CLAN- cells (untreated TM cells also form CLANs at low levels), not in CLAN+. The expression of senescence markers p21 and H2AX did not seem to be affected by TGFβ2 or DEX. However, the expression of individual senescence marker in CLAN+ cells were cell strain dependent.

Conclusion: We believe that CLAN formation and Ki67 expression are mutually exclusive in pHTM cells. The effect of CLAN formation on cell senescence markers varies and is also cell strain and treatment type dependent.

30. AGE-RELATED DYSREGULATION OF α5β1 AND αVβ3 INTEGRIN ACTIVITY PROMOTES PROFIBROTIC PHENOTYPE IN TRABECULAR MESHWORK (TM) CELLS

Kassidy Johns[1], Jennifer A. Faralli[1], Mark S. Filla[1], Nandini S. Shah[1], Ying Ying Sun[3], Kate E. Keller[3], Donna M. Peters[1,2]

[1]Department of Pathology & Laboratory Medicine, University of Wisconsin, Madison, WI, USA; [2]Department Ophthalmology & Visual Sciences University of Wisconsin, Madison, WI, USA;[3]Casey Eye Institute, Oregon Health & Science University, Portland, OR, USA

Purpose: Age is a major risk factor for primary open-angle glaucoma (POAG), an ocular disease associated with elevated intraocular pressure (IOP) due to the restricted outflow of aqueous humor fluid from the anterior chamber. The development of a profibrotic phenotype associated with an endothelial-to-mesenchymal transition (EndoMT) is believed to contribute to the increased restriction of outflow. Despite our current understanding of these changes, it is unknown what tips a healthy eye toward the EndoMT phenotype and ultimately POAG. In this study, we investigated whether age-related changes in integrin expression and activity signifies an early event in initiating fibrotic-like changes in the TM.

Methods: Human TM cells were isolated from young (n=3) and old (n=3) human donor eyes or corneal rims. Tissues from both males and females were used and all donors were Caucasian with no known history of ocular disease. The age of young donor eyes ranged from 25-27 yrs, while the age of old donor eyes ranged from 74-77 years. Flow cytometry and RT-PCR were used to analyze the cell surface expression of integrins and their mRNA levels, respectively. Immunofluorescence microscopy was used to detect integrin expression in the TM in paraffin embedded anterior segments, as well as integrin expression in focal adhesions and the formation of αSMA stress fibers in cultured TM cells. A lenti shRNA viral vector was used to knock down expression of the α5 integrin subunit in young TM cells. Age-related changes in fibronectin mRNA expression of its EDA and EDB isoforms and assembly in fibrils was determined using RT-PCR and an on-cell western.

Results: Flow cytometry, RT-PCR and immunofluorescent microscopy revealed a significant decrease in α5 integrin expression in TM cells from older individuals. Similarly, α5 integrin was reduced in the juxtacanalicular tissue and along the beams in the TM from older individuals. TM cells from older donors expressed higher levels of αSMA mRNA, assembled αSMA-containing stress fibers, and contracted collagen gels significantly more than young TM cells. This loss in α5 integrin expression was accompanied by an increase in activated, but not total αvβ3 integrin in focal adhesions. shRNA knockdown of α5 integrin subunits suggested the increase in αvβ3 integrin activity was due to lower levels of α5 integrin expression. Studies showed that TM cells from old donors also assembled higher levels of insoluble fibronectin fibrils and contained higher levels of the EDB+ isoform of fibronectin in their extracellular matrix.

Conclusions: These studies suggest that age-related dysregulation of α5β1 and αvβ3 integrin signaling may represent an important early molecular event in inducing fibrogenic pathways associated with POAG.

Commercial Relationships: None

Support: This work was funded in part by NIH/NEI grants R01EY017006 (DMP), R01EY032905 (DMP), P30 EY016665 (DMP), R01EY019643 (KEK), R01EY032590 (KEK), P30 EY010572 (KEK), and unrestricted grant to the Casey Eye Institute from Research to Prevent Blindness, NY.

31. TUBULIN ACETYLATION ENHANCES MICROTUBULE STABILITY IN TRABECULAR MESHWORK CELLS UNDER MECHANICAL STRESS

Paloma B. Liton[1], Vaibhav Desikan[1], Kevin Betsch [1], Myoung Sum Shim[1], Kate E. Keller[2], Chien-Chia Su[1]

[1]Department of Ophthalmology, Duke Eye Center, Duke University, Durham, NC, USA; [2]Casey Eye Institute, Oregon Health & Science University, Portland, OR, USA

Purpose: To study the role of tubulin acetylation and cyclic mechanical stretch (CMS) in trabecular meshwork (TM) cells and their impact on outflow pathway physiology and pathology

Methods: Primary TM cell cultures were subjected to CMS (8% elongation, 24 hours); acetylated α-tubulin at lysine 40 (Ac-TUBA4) was assessed by western blotting and immunofluorescence. Enzymes regulating tubulin acetylation were identified via siRNA-mediated knockdowns of ATAT1, HDAC6, and SIRT2. Ac-TUBA4 levels were compared between glaucomatous (GTM) and normal (NTM) TM cells and in frozen sections of human cadaver eyes. The effect of tubulin acetylation on substrate stiffness and cell contractility was evaluated by culturing cells on substrates with varying stiffness, and by collagen gel contraction assays, respectively. Microtubule stability was examined by monitoring resistance to nocodazole-induced depolymerization. The in vivo effect on intraocular pressure (IOP) was evaluated following intracameral injections of tubacin in mice.

Results: CMS induces tubulin acetylation in human TM cells by downregulating the deacetylase HDAC6. Elevated Ac-TUBA4 levels were observed in GTM compared NTM cells and tissues. Tubulin acetylation was not affected by substrate stiffness and did not show a direct effect on TM cell contractility. Tubulin acetylation was found to provide protection against microtubule destabilization induced by nocodazole. Importantly, intracameral injection of tubacin, an HDAC6 inhibitor, significantly lowered IOP in mice.

Conclusions: Our study highlights a critical role of tubulin acetylation in TM cell response to mechanical stress and its potential impact on IOP regulation. Tubulin acetylation could represent a therapeutic target for glaucoma.

Funding: This work was supported by National Institute of Health, Eye Institute (EY026885, EY033600, EY005722 and Unrestricted Research to Prevent Blindness Grant.

Commercial relationship disclosure: None

32. MATRINE REDUCES INTRAOCULAR PRESSURE IN CORTICOSTEROID-INDUCED OCULAR HYPERTENSIVE MOUSE EYES

Yang Sun

Stanford University, Los Angeles, CA,USA

Purpose: Ocular hypertension (OHT) is a major risk factor for the development and progression of glaucoma. Previously matrine has been identified as an alkaloid with opioid mu-receptor agonistic activity. Here we investigated the role of matrine in regulating intraocular pressure (IOP) in normal and corticosteroid-induced OHT mice.

Methods: The OHT mouse model was induced by dexamethasone treatments. IOP measurements were obtained at 0, 0.5, 1, 3, and 6 hours after matrine treatments. The outflow facility following matrine treatment was measured. Anterior segment-optical coherence tomography (AS-OCT) was used to evaluate the morphological change of the anterior chamber in the mice with matrine treatment. Immunofluorescence staining of corticosteroid-induced fibrotic proteins, the alpha-smooth muscle actin (α-SMA) and collagen I (COL I), was used to evaluate changes in the extracellular matrix in the trabecular meshwork of OHT mice.

Results: Matrine treatment decreased the IOP in wildtype C57BL/6j mice in a dose-dependent manner. Outflow facility and angle opening distance (AOD) in the anterior chamber increased upon matrine treatment. In the DEX-induced OHT mice, matrine treatment reduced the elevated IOP and increased the outflow facility and AOD. Matrine treatment reduced the expression of α-SMA and COL I in the trabecular meshwork in OHT mice.

Conclusion: Matrine lowered IOP in the DEX-induced OHT mice model, presenting a promising new therapeutic option for managing glaucoma, particularly in secondary cases associated with corticosteroid.

33. UNDERSTUDIED ASPECTS OF CELL-CELL JUNCTIONS IN THE TRABECULAR MESHWORK: IMPLICATIONS FOR AQUEOUS HUMOR OUTFLOW AND INTRAOCULAR PRESSURE

P. Vasantha Rao,[1, 2] Pallavi Gorijavolu,[1] Levi Lankford,[1] Hoi Lam Li,[3] Haiyan Gong,[3] Rupalatha Maddala[1]

[1]Department of Ophthalmology, [2]Department of pharmacology and Cancer Biology, Duke University, NC. [3]Department of Ophthalmology, Boston University, MA, USA

Purpose: Trabecular meshwork (TM) cells, which play a key role in regulating aqueous humor (AH) outflow, express various cell-cell junctional proteins. The expression of these proteins is altered in response to ocular hypertensive agents, but the precise role of TM cell-cell junctions in AH outflow regulation remains unclear. This study aims to explore how cell-cell junctions in the TM may influence tissue porosity, aqueous humor drainage, and intraocular pressure (IOP) regulation.

Methods: Primary human TM cell cultures were analyzed using proteomics and immunofluorescence to characterize the expression and distribution of various cell-cell junctional proteins. Calcium switch and chelation experiments were performed to assess junctional stability. High-resolution confocal imaging and 3D rendering were used to map cell-cell junctions within the human eye's trabecular pathway, including the TM, juxtacanalicular tissue (JCT), and Schlemm's canal. Perfusion experiments using EDTA were conducted to evaluate the outflow facility changes in bovine eyes and the impact of cell-cell junctions on AH outflow on the TM tissue integrity was examined using light and transmission electron microscopy

Results: Human TM cells express multiple cell-cell junctional and associated proteins, localized primarily at cell-cell interfaces in both cultured cells and TM tissues. Calcium-dependent stability of these junctions was confirmed via calcium switch and chelation assays. EDTA perfusion led to a significant increase in AH outflow, disruption of cell-cell junctions, and structural alterations in TM tissue architecture.

Conclusions: These preliminary findings suggest that TM cells exhibit a variety of calcium-sensitive cell-cell junctions, which play a crucial role in regulating aqueous humor outflow. The integrity of these junctions appears to influence the geometry, sponginess, and porosity of the TM, contributing to its function in IOP homeostasis.

Support: Supported by funding from the NEI/NIH, Research to Prevent Blindness, and the Bright Focus Foundation.

34. MYOCILIN^{A427T} AND THE BALANCE BETWEEN PROTEOSTASIS AND PROTEOTOXICITY

Hannah Youngblood[1], Kamisha Hill[1], Hailee Scelsi[1], Jennifer A. Faralli[2], Tatsuo Itakura[3], M. Elizabeth Fini[3], Donna M. Peters[2,4], Raquel L. Lieberman[1]

Raquel Lieberman Lab, Georgia Institute of Technology, Atlanta, GA, USA; [2]Department of Pathology & Laboratory Medicine, University of Wisconsin, Madison, WI, USA; [3]USC Institute for Genetic Medicine, Keck School of Medicine of USC, University of Southern California, Los Angeles, CA, USA; [4]Department Ophthalmology & Visual Sciences University of Wisconsin, Madison, WI, USA

Purpose: Between 2-4% cases of primary open angle glaucoma are caused by mutations in myocilin (MYOC). While many MYOC mutations cause glaucoma in a highly penetrant, early onset, autosomal dominant manner, there are many other MYOC variants for which causal pathogenicity is uncertain. Missense variant A427T (MYOC^{A427T}) is one such example. Although the variant was identified in a POAG case study, it demonstrated lower penetrance and a later age of onset than severely pathogenic mutations, thereby generating speculation as to its causality. While wild-type MYOC (MYOC^{WT}) is soluble and normally secreted by trabecular meshwork (TM) cells, severe pathogenic MYOC mutations aggregate within the intracellular space and are resistant to degradation. This study sought to characterize the pathogenicity of MYOC^{A427T} by examining changes in its protein structure, secretion, and proteostatic clearance.

Methods: Structural differences between MYOC^{WT} and its variant MYOC^{A427T} were determined by X-ray crystallography. To understand the biological impact of these structural differences, altered secretion and solubility of MYOC^{A427T} was examined in immortalized human TM (TM-1) cells stably transformed with MYOC^{WT} and MYOC^{A427T} by immunoblotting (n=3). In addition, differences in proteostatic degradation of MYOC^{WT} and MYOC^{A427T} were examined by treating stably transformed TM-1 cells (n=2) with proteosome (MG132) and autophagy (Bafilomycin A1) inhibitors. Subsequent effects of proteosome and autophagy inhibition on MYOC solubility and autophagic clearance were determined by immunoblotting and immunocytochemistry.

Results: Overall, MYOC^{A427T} largely retains a wild-type-like protein structure with only minor deviations in the loops surrounding the variant. Despite having only minor structural differences, MYOC^{A427T} demonstrates increased intracellular retention as compared to MYOC^{WT}. However, this variant does not demonstrate the aggregation propensity of more severe, early-onset mutants. Differences in intracellular retention between MYOC^{WT} and MYOC^{A427T} may be explained by differences in proteostatic clearance. While TM-1 cells are capable of shuffling MYOC^{WT} from proteosomal degradation to autophagic clearance under stress (i.e., decreased intracellular MYOC^{WT} and increased atg5 colocalization after MG132 treatment), TM-1 cells rely on proteosomal degradation alone to clear MYOC^{A427T} (i.e., increased aggregated MYOC^{A427T} and no change in atg5 colocalization after MG132 treatment).

Conclusions: Taken together, these results suggest that MYOC^{A427T} has a unique intermediate phenotype between MYOC^{WT} and severe pathogenic MYOC mutants, highlighting a more nuanced range of MYOC pathogenicity than previously considered. Even variants with mild structural changes can experience differences in cellular handling and proteostatic turnover, and as a result, can lead to disease. This range in pathogenicity provides motivation for additional genetic screening and characterization of other variants of uncertain pathogenicity.

Section 7: Secondary and Angle Closure Glaucomas

35. A COMPARISON OF PRIMARY AND SECONDARY GLAUCOMATOUS AQUEOUS HUMOR DEPOSITS

Sanjoy K. Bhattacharya, Susanna Li, Isabella Moceri, Anh Pham, Richard K. Lee

Bascom Palmer Eye Institute, Miami Integrative Metabolomics Research Center, University of Miami, Miami, FL, USA

Purpose: To identify whether there are differences in deposit formation in pseudoexfoliation glaucoma (PEXG) and primary open angle (POAG) glaucoma compared to cataract only control aqueous humor (AH).

Methods: The AH samples were obtained from human donors [control (n = 10), POAG (n = 10) and PEXG (n= 10)]. The AH samples (20 µl) were subjected to one-a brief centrifugation (500xg for 2 minutes) and subjected to incubation for 48 hours at 4ºC and at 25ºC. Separately 10 µl of AH from these donors subjected to centrifugation at 500xg for 2 minutes and incubated in 4ºC for 48 hours in concavity slides and subjected to confocal microscopy on a Leica Stellaris 5 microscope. All 20 µl samples were subjected to centrifugation at 15,000xg for 15 minutes and the liquid was pipetted out the left over deposited was subjected to proteolytic digestion using trypsin+Lys+AspN and proteins were identified using LC-MS/MS on an Easy nLC-QExactive liquid chromatograph-tandem mass spectrometer. A similar 10 µl of AH after centrifugation at 500xg for 2 minutes and each sample was added with 0.1 µl of 0.00379mg/ml GC protein incubated in 4ºC for 48 hours in concavity slides and subjected to confocal microscopy on a Leica Stellaris 5 microscope, at 10x magnification.

Results: The deposits were subject to proteomic profiling (20 µl samples) and imaging of concavity slides. We found robust deposit formation in pseudoexfoliation glaucoma (PEXG) with or without addition of GC protein in AH. The cataract control showed no deposit formation with or without GC protein addition. POAG AH showed deposit formation only in 3/10 samples. All POAG AH that showed deposit formation with (3/10) or without GC addition (1/10) was samples from donors with severe and prolonged POAG had mean defect of ≥7. The proteome of the deposits from POAG and PEXG had reproducible composition. However, some protein identities were also variably associated with different independent biological replicates. Non-reproducible identities were not included in the final list. We consistently found Myeloid differentiation primary response protein MyD88, Membrane primary amine oxidase, ASNSD1, Vascular endothelial growth factor receptor 3 (VEGFR3), Apolipoprotein E, Excitatory amino acid transporter 1, Glutamine synthase, Glutamine dehydrogenase, Zinc finger protein GLI1, Alpha-galactosidase A in POAG AH deposits. The common reproducible proteins in PEXG AH are: Fibulin-1, Apolipoprotein C2, Phospholipid transfer protein, Phosphoserine amino transferase, Apolipoprotein D, Apolipoprotein A-IV, Lipocalin-1, Insulin-like growth factor binding protein 7 and Procathepsin L.

Conclusion: Only very few POAG samples showed deposit formation on prolonged incubation at 4ºC. The individuals with severity and prolonged POAG showed differences in AH deposit formation that occurs on prolonged static incubation. PEXG on the other hand showed large and more reproducible deposit formation. The composition of AH deposits in POAG and PXEG are different. In addition to reproducibly present proteins in deposits we found some varying protein identities in both types of samples.

Support: Supported by Miami Metabolomics Research Support Group (MMRSG), NIH grants EY031392, EY14801, An unrestricted grant from Research to Prevent Blindness to University of Miami.

36. IDENTIFICATION OF A NOVEL GENETIC VARIANT ASSOCIATED WITH PRIMARY ACUTE ANGLE CLOSURE (PACG) AND GONIODYSGENESIS IN DOGS

Gillian J. McLellan[1,2], Odalys Torné[1], Kazuya Oikawa[1], Julie A Kiland[2], Ben Kragerud[1], Leandro BC Teixeira[3], Peter Muir[2]

[1]Department of Ophthalmology and Visual Sciences, [2]Department of Surgical Sciences and [3]Department of Pathobiological Sciences, University of Wisconsin-Madison, Madison, WI, USA

Purpose: To elucidate the genetic basis of PACG in the Entlebucher Mountain Dog (EMD), a numerically small canine breed with a prevalence of glaucoma estimated at >1% in the USA population. We hypothesized that in EMDs, PACG is associated with a causal mutation, or risk-conferring mutation(s) with high penetrance for PACG development.

Methods: Massively parallel whole genome sequencing (WGS; Illumina NovaSeq platform) was conducted in 14 EMDs (8 cases and 6 controls of both sexes) using genomic DNA isolated from whole blood or buccal swabs. Controls were dogs >10 years of age with no clinical evidence of glaucoma and which did not have severe grades of goniodysgenesis with pectinate ligament dysplasia (PLD) identified on gonioscopy. Structural variants and single nucleotide polymorphisms (SNPs) were called from sequencing data and screened for all variants that differentially segregated cases from controls. Concordance with PACG and / or PLD phenotype was established for the top candidate variant and examined further in an expanded population of cases and controls, comprising animals examined by veterinary ophthalmologists in the USA and Europe. All animals in both the original case-control cohort and in the second validation cohort were genotyped by PCR and by Sanger sequencing for the best candidate genetic variant and associated gene(s) of interest confirm the variant as causal. Ocular expression of the gene of interest was examined by in situ hybridization in donor eye tissues from subjects with clinically confirmed absence of PLD; subjects with PACG, as well as control aged subjects with PLD but no evidence of glaucoma reported at >10 years.

Results: A large deletion was identified in a gene which encodes a transmembrane bone morphogenic protein (BMP) regulator that is known to interact with members of the TGF β superfamily. Mutations in the gene have previously been associated with a rare syndrome of colobomatous macrophthalmos with microcornea in humans. Expression of this gene transcript was confirmed in relevant anterior segment tissues of normal dogs by RNAscope in situ hybridization, and spatial expression patterns were consistent with scRNAseq atlases of the anterior segment in humans and in mice. The pattern of inheritance observed in canine pedigrees supports a recessive mode of inheritance. All glaucomatous EMDs were homozygous for the mutation, with the exception of one heterozygous animal with a history of unilateral post-operative uveitis and secondary glaucoma following cataract surgery, and one dog in the original control group was heterozygous for the variant (carrier).

Conclusions: Identification of a genetic variant associated with glaucoma represents an opportunity to enhance understanding of disease pathobiology and provides a DNA-based screening tool to inform breeding and treatment strategies to limit disease progression and severity in dogs bearing this mutation.

Support: American Kennel Club Canine Health Foundation Oak Grant 02963; unrestricted grant to the Department of Ophthalmology and Visual Sciences from Research to Prevent Blindess, and an unrestricted award from the National Entlebucher Mountain Dog Association (NEMDA) and the Entlebucher Preservation Foundation.

Section 8: Clinical "Trabeculo" Studies

37. A NEW APPROACH TO GLAUCOMA: REGENERATING THE TRABECULAR MESHWORK WITH STEM CELLS

Joel S. Schuman[1-3] Yiqin Du[4] ,W. Daniel Stamer[5], C. Ross Ethier[6]

[1]Wills Eye Hospital, Philadelphia, PA, USA; [2]Sidney Kimmel Medical College at Thomas Jefferson University, Philadelphia, PA, USA; [3]Department of Biomedical Engineering, Drexel School of Biomedical Engineering, Science and Health Systems, Philadelphia, PA, USA; [4]Department of Ophthalmology, University of South Florida, Tampa, FL, USA; [5]Departments of Ophthalmology and Biomedical Engineering, Duke University, Durham, NC, USA; [6]Wallace H. Coulter Department of Biomedical Engineering, Georgia Institute of Technology & Emory University School of Medicine, Atlanta, GA, USA

Purpose: Stem cell therapies have opened new avenues for potentially treating glaucoma. For decades, research has focused on various stem cell types to restore aqueous humor outflow by regenerating trabecular meshwork (TM) cells. Studies show that stem cells (such as TMSCs, MSCs from adipose tissue, bone marrow MSCs, and iPSCs) can transform into TM-like cells, implant safely within the TM in live mouse models, and help restore normal intraocular pressure (IOP). These cells have proven stable over extended periods without significant adverse effects. We propose conducting a human clinical trial to advance this innovative therapeutic approach further.

Methods: Based on existing evidence, we advocate for further examination of adipose-derived mesenchymal stem cells (adMSCs) in human trials for TM regeneration. Although the eye is considered an immune-privileged environment, using autologous stem cells is optimal to minimize immune rejection risk. Adipose-derived stem cells are easily accessible through minimally invasive procedures, with a lower risk of causing tumors.

iPSCs offer clinical convenience and cost-effectiveness, being widely accessible from stem cell sources. Though not autologous and carrying associated risks, iPSCs could be produced more cheaply than adMSCs, which require extraction, purification, and expansion from each patient. This could form a second arm of a clinical study.

Additionally, a cell-free treatment might further reduce patient risks. Recent research found that secretome from human TM stem cells can decrease IOP and restore TM stability and retinal ganglion cell function in models with steroid-induced or genetic myocilin-associated glaucoma. This could serve as a third study arm.

Results

Delivery Method: To effectively target TM regeneration, intracameral delivery of stem cells is recommended, leveraging natural flow patterns and previous findings indicating chemotactic mechanisms (CXCR4/SDF1) guiding cells toward the TM. However, the segmental flow variations in glaucomatous eyes might benefit from using magnetic nanoparticles to direct cells to the TM, as shown in studies by Snider et al., though this would add procedural complexity. *Study Structure:* To mitigate risk to participants, we propose an initial TM regeneration study that includes blind eyes from open-angle glaucoma patients without light perception. Ideally, the study would involve patients whose eyes are scheduled for enucleation within 1–2 months. This setup would allow a short-term follow-up to assess SC effects on TM and ocular structure, particularly TM regeneration, outflow, and SC migration. This approach also enables long-term monitoring of effects post-injection with reduced systemic risk. However, this selective criterion could hinder enrollment rates. We recommend including such cases where feasible but not restricting to this group alone. Additionally, TM function after SC transplant can be assessed clinically through tonography.

Conclusions: Patients with glaucoma often experience TM cell loss, correlating with higher IOP. Research supports stem cell therapy's promise to regenerate damaged TM. Adipose-

derived MSCs are safe, multipotent, and readily available, with low tumorigenic risk. While iPSCs are more affordable and accessible, they lack the autologous advantage. Both types have been shown to differentiate into TM-like cells, integrate within TM tissue, and maintain IOP homeostasis. Stem cell transplantation for TM repair in glaucoma could be a groundbreaking, sight-preserving therapy, impacting countless lives.

38. SELECTIVE LASER TRABECULOPLASTY IN PATIENTS ON SYSTEMIC IMMUNOSUPPRESSIVE THERAPY

Gavin W. Roddy

Mayo Clinic, Rochester, MN, USA

Purpose: To determine whether patients taking systemic immunosuppressive medications have a different intraocular pressure (IOP)-lowering response to selective laser trabeculoplasty (SLT) compared to a control group of patients.

Method: All patients who underwent SLT at Mayo Clinic 2017-2021 were identified. Patients on systemic immunosuppressive medications at the time of SLT were compared to control patients not receiving systemic immunosuppressive medications. The primary endpoints of this study were the percentage IOP reduction at 1-2, 3-6, and 12 months. Additional analyses included percentage of patients who did not require additional therapy at each time-point.

Results: There were 108 eyes of 72 patients that underwent SLT in the immunosuppressed group and 1997 eyes of 1417 patients in the control group. There was no significant difference in age-adjusted change in IOP between groups at the first post-operative visit 1-2 months following SLT (-18.8 ± 20.7% vs -16.0 ± 16.5%, p=0.256) or 3-6 months following SLT (-15.2 ± 21.6% vs -18.3 ± 23.2%, p=0.062). However, at 12 months following SLT, the IOP reduction in the immunosuppressive therapy group was significantly less compared to the control group (-15.1 ± 21.2% vs -20.3 ± 22.9%, p=0.045). There was no difference between groups in number of additional treatments during the study intervals.

Conclusion: Patients in the systemic immunosuppressive therapy group showed equivalent early IOP-lowering after SLT compared to a control group, but the treatment response was diminished at one year. Further studies investigating IOP regulation after SLT in immunosuppressed patients are needed.

39. SUPRACHOROIDAL STENTS: ACCESSING THE OTHER OUTFLOW PATHWAY

Shan Lin

Glaucoma Center of San Francisco, San Francisco, CA, USA

Traditional outflow in the eye is through the Trabecular Meshwork into the Schlemm’s canal and collector channel system. Many of the existing minimally invasive glaucoma surgeries (MIGS) target this natural plumbing system to enhance outflow and reduce intraocular pressure (IOP).

However, an alternate egress for aqueous within the eye is towards the suprachoroidal space, which is the route for the uveoscleral outflow system. Suprachoroidal stents create an opening and pathway to this potential space.

Recently there have been several devices introduced that access the suprachoroidal space. Using an ab externo approach, the Gold Micro Shunt (SOLX Inc., Waltham, MA) created a pathway with small passageways for aqueous flow to the suprachoroidal space. However, this procedure was abandoned due to the complexity of the surgical procedure, the high incidence of complications, and limited efficacy. Other ab externo suprachoroidal stents include the STARflo (iSTAR Medical Inc, Wilmington, DE) and the Aquashunt (OPKO Health, Miami, FL). Both devices are no longer available.

The CyPass Shunt (Alcon Inc., Fort Worth, TX) was a polyimide tube that was inserted an interno from the anterior chamber into the suprachoroidal space. Unfortunately, long term follow-up showed substantial and progressive corneal endothelial cell loss. The device was withdrawn from the market in 2018 despite showing good efficacy.

More recently the AlloFlo (Iantrek Inc., White Plains, NY) has become available for clinical use. Composed of processed human sclera, the implant is inserted into the suprachoroidal space, usually in a pair to create a gap for aqueous to flow in between.

The MINIject (iSTAR Medical Inc, Wilmington, DE) is a new suprachoroidal stent that is silicone-based and possesses a porous network to allow aqueous filtration. Clinical trials show excellent IOP reduction over 2 years.

40. CKLP1 TO QLS-111: THE LONG WINDING ROAD FROM INNOVATION TO PATIENT CARE

Michael P. Fautsch[1], Uttio Roy Chowdhury[1,2], Ralph Casale[2], Lisa Brandano[2], Daniel DeWalt[2], Laura Rykard[2], Thurein Htoo[2], Barbara M. Wirostko[2,3]

[1]Department of Ophthalmology, Mayo Clinic, Rochester, MN, USA; [2]Qlaris Bio, Dedham, MA, USA; [3]John Moran Eye Center, University of Utah, Salt Lake City, UT, USA

Purpose: To provide an overview and progress update for the ATP-sensitive potassium channel opener QLS-111, an ocular hypotensive agent currently in phase 2 clinical trials.

Methods: QLS-111 was identified through a formulation screen of the active pharmaceutical ingredient of cromakalim prodrug 1 (CKLP1, an ATP-sensitive potassium channel opener; aka QLS-101). IOP lowering efficacy of QLS-111 was evaluated by treating wild-type C57BL/6J mice (n=25) with various doses (0.005 – 5 mM) once daily for five consecutive days. Aqueous humor dynamics of QLS-111 were assessed by constant flow perfusion in mice. Safety, tolerability, and pharmacokinetic properties of QLS-111 were assessed in Dutch belted pigmented rabbits treated topically with various doses of QLS-111 (1mM, n=6; 2.5 mM, n=6; 5 mM, n=10) or vehicle (n=10) in both eyes for 28 consecutive days. Ocular exams were performed, and plasma was collected at predetermined timepoints. Upon completion of the treatment regimen, complete necropsies and histologic evaluations were performed in animals from the vehicle and the highest dose group. Efficacy, safety and tolerability were also evaluated in two separate exploratory, investigator-initiated research studies at a single center, following various doses and regimens (Study 1, once daily dosing with 0.5 mM or 5.0 mM QLS-111; study 2, once daily dosing followed by twice daily dosing with 0.5 or 2.5 mM QLS-111). Safety and tolerability were determined by ocular exams, vital signs, and documentation of adverse events. IOP was determined by Goldmann applanation tonometry and iCare rebound tonometry.

Results: Optimal dose for IOP reduction in mice was determined to be 0.5 mM QLS-111, showing an IOP decrease from 16.5 ± 0.5 mmHg to 12.3 ± 0.9 mmHg ($p<0.001$). In contrast, mice treated with vehicle showed no change from baseline IOP (16.3 ± 0.3 mmHg to 16.4 ± 0.5 mmHg). Mice treated with QLS-111 showed a significant ($p=0.0002$) reduction in episcleral venous pressure (4.1 ± 0.4 mmHg) compared to vehicle-treated controls (9.8 ± 1.1 mmHg). No significant changes were found in outflow facility, uveoscleral outflow or aqueous humor flow rate. In Dutch belted rabbits, QLS-111 was well tolerated with no drug related adverse events or ocular inflammation. Pharmacokinetic data showed low levels of QLS-111 (<5 ng/ml; $T_{1/2}$ of 1.3 – 2.9 hours) in plasma with no quantifiable values detected beyond 6 hours. In human volunteers dosed in investigator-initiated research studies, QLS-111 significantly lowered IOP up to 6 mm Hg from baseline across all doses (0.5 mM, 2.5 mM, and 5.0 mM) and treatment regimens (QD/BID). No significant ocular or systemic adverse events were noted except a few clinically insignificant cases of transient mild hyperemia.

Conclusions: QLS-111 is an effective ocular hypotensive agent with a unique mechanism of action affecting episcleral venous pressure and a strong safety and tolerability profile. QLS-111 is currently being evaluated in three phase 2 clinical trials for safety, tolerability, and efficacy in POAG/OHT and NTG patients as a monotherapy agent and as an additive agent with latanoprost.

Support: NEI grant EY21727; Minnesota Partnership for Biotechnology and Medical Genomics 12.06; Department of Ophthalmology RFA; Mayo Foundation; Qlaris Bio Inc.

Conflicts of interest: MPF is a Consultant and Scientific Board Member for Qlaris Bio Inc. URC, RC, LB, DD, LR, TH, and BW are employees of Qlaris Bio Inc.

TM Society Literature Review 2024

1. Adhikari B, Barakoti P, Pantcheva MB, Krebs MD. 3D printed gelatin methacryloyl hydrogels for perfusion culture of human trabecular meshwork cells and glaucoma studies. Biotechnol Bioeng 2024. https://doi.org/10.1002/bit.28849. PMid:39291858
2. Allan KC, Zhang K, Wu SZ, et al. The Impact of Trabecular Meshwork Remnants on Goniotomy Outcomes. Ophthalmol Glaucoma 2024. https://doi.org/10.1016/j.ogla.2024.08.005. PMid:39216730
3. Alpogan O, Tekcan H, Imamoglu S, Ozturk Y, Bolac R. The effect of uneventful cataract surgery on Schlemm's canal and the trabecular meshwork in cases with pseudoexfoliation. Graefes Arch Clin Exp Ophthalmol 2024; 262(4): 1271-9. https://doi.org/10.1007/s00417-023-06349-x. PMid:38141058
4. Asrani SG, McGlumphy EJ, Al-Aswad LA, et al. The relationship between intraocular pressure and glaucoma: An evolving concept. Prog Retin Eye Res 2024; 103: 101303. https://doi.org/10.1016/j.preteyeres.2024.101303. PMid:39303763
5. Bakar ASA, Razali N, Agarwal R, Iezhitsa I, Perfilev MA, Vassiliev PM. Role of TGF-beta1/SMADs signalling pathway in resveratrol-induced reduction of extracellular matrix deposition by dexamethasone-treated human trabecular meshwork cells. Korean J Physiol Pharmacol 2024; 28(4): 345-59. https://doi.org/10.4196/kjpp.2024.28.4.345. PMid:38926842 PMCid:PMC11211753
6. Balasubramanian R, Kizhatil K, Li T, et al. Transcriptomic profiling of Schlemm's canal cells reveals a lymphatic-biased identity and three major cell states. Elife 2024; 13. https://doi.org/10.7554/eLife.96459.3
7. Barberan-Bernardos L, Ariza-Gracia MA, Pinero DP. Corneal and intraocular pressure changes associated to the circadian rhythms: a narrative review. Int J Ophthalmol 2024; 17(10): 1921-8. https://doi.org/10.18240/ijo.2024.10.20. PMid:39430020 PMCid:PMC11422371
8. Baumann JM, Yarishkin O, Lakk M, et al. TRPV4 and chloride channels mediate volume sensing in trabecular meshwork cells. Am J Physiol Cell Physiol 2024; 327(2): C403-C14. https://doi.org/10.1152/ajpcell.00295.2024. PMid:38881423
9. Beri N, Gupta A, Patil A, Dada T. Aqueous angiographic evaluation of failed trabecular MIGS reveals closure of previously functional aqueous outflow pathways. BMJ Case Rep 2024; 17(7). https://doi.org/10.1136/bcr-2024-261032. PMid:39059797
10. Bikuna-Izagirre M, Aldazabal J, Moreno-Montanes J, De-Juan-Pardo E, Carnero E, Paredes J. Artificial Trabecular Meshwork Structure Combining Melt Electrowriting and Solution Electrospinning. Polymers (Basel) 2024; 16(15). https://doi.org/10.3390/polym16152162. PMid:39125188 PMCid:PMC11314991
11. Borras T, Stepankoff M, Danias J. Genes as drugs for glaucoma: latest advances. Curr Opin Ophthalmol 2024; 35(2): 131-7. https://doi.org/10.1097/ICU.0000000000001025. PMid:38117663
12. Brown SF, Nguyen H, Mzyk P, et al. ANGPTL7 and Its Role in IOP and Glaucoma. Invest Ophthalmol Vis Sci 2024; 65(3): 22. https://doi.org/10.1167/iovs.65.3.22.PMid:38497513 PMCid:PMC10950037
13. Bu Q, Zhu H, Cao G, et al. Targeting mechanics-induced trabecular meshwork dysfunction through YAP-TGFbeta Ameliorates high myopia-induced ocular hypertension. Exp Eye Res 2024; 241: 109853. https://doi.org/10.1016/j.exer.2024.109853. PMid:38453038
14. Buffault J, Reboussin E, Blond F, et al. RNA-seq transcriptomic profiling of TGF-beta2-exposed human trabecular meshwork explants: Advancing insights beyond conventional cell culture models. Exp Cell Res 2024; 442(2): 114220. https://doi.org/10.1016/j.yexcr.2024.114220. PMid:39214330
15. Chan W, Zhang C, Mittal A, Fink A, Michalovic S, Weiner A. Effect of Preoperative Trabecular Meshwork Pigmentation and Other Eye Characteristics on Outcomes of Combined Phacoemulsification/Minimally Invasive Glaucoma Surgery. Ophthalmol Glaucoma 2024; 7(3): 271-81. https://doi.org/10.1016/j.ogla.2024.01.001. PMid:38185378
16. Chaplot I, Cruz-Wegener C, Cabrera Gonzalez MD, Bhattacharya SK. Downregulation of ATP8B2 to Assess Plasmalogen Distribution and Far1 Expression in Primary Trabecular

Meshwork Cells. Methods Mol Biol 2024; 2816: 175-91. https://doi.org/10.1007/978-1-0716-3902-3_17.PMid:38977599
17. Chen HY, Ko ML, Chan HL. Effects of hyperglycemia on the TGF-beta pathway in trabecular meshwork cells. Biochim Biophys Acta Gen Subj 2024; 1868(2): 130538. https://doi.org/10.1016/j.bbagen.2023.130538. PMid:38072209
18. Chen R, Lei J, Liao Y, et al. Predicting 24-hour intraocular pressure peaks and averages with machine learning. Front Med (Lausanne) 2024; 11: 1459629. https://doi.org/10.3389/fmed.2024.1459629. PMid:39434779 PMCid:PMC11493148
19. Chung YG, Fan S, Gulati V, et al. IOP Reduction in Nonhuman Primates by Microneedle Injection of Drug-Free Hydrogel to Expand the Suprachoroidal Space. Transl Vis Sci Technol 2024; 13(10): 14. https://doi.org/10.1167/tvst.13.10.14. PMid:39377753 PMCid:PMC11469220
20. Dada T, Beri N. Analyzing the Shortcomings of Trabecular Micro-bypass Stents for Surgical Management of Glaucoma. J Curr Glaucoma Pract 2024; 18(1): 1-3. https://doi.org/10.5005/jp-journals-10078-1439. PMid:38585166 PMCid:PMC10997962
21. De Bernardo M, Cione F, De Pascale I, Pagliarulo S, Rosa N. Intraocular Pressure Measurements in Standing, Sitting, Prone, and Supine Positions. J Pers Med 2024; 14(8). https://doi.org/10.3390/jpm14080826. PMid:39202017 PMCid:PMC11355470
22. Deng X, Zhu M, Liu Y, et al. Suppression of CDK1/Drp1-mediated mitochondrial fission attenuates dexamethasone-induced extracellular matrix deposition in the trabecular meshwork. Antioxid Redox Signal 2024. https://doi.org/10.1089/ars.2023.0502. PMid:39096204
23. Doliszny K, Quinn MP, El-Defrawy SR, et al. Evolution of first-line glaucoma therapy, 2007-2018: a population-based analysis. Can J Ophthalmol 2024; 59(2): 89-95. https://doi.org/10.1016/j.jcjo.2022.11.008. PMid:36493801
24. Doyle C, Callaghan B, Roodnat AW, et al. The TGFbeta Induced MicroRNAome of the Trabecular Meshwork. Cells 2024; 13(12). https://doi.org/10.3390/cells13121060. PMid:38920689 PMCid:PMC11201560
25. Du Y, Bammidi S, Yang E. Trabecular Meshwork Stem Cells for Glaucoma Treatment. Methods Mol Biol 2025; 2858: 143-58. https://doi.org/10.1007/978-1-0716-4140-8_13. PMid:39433674
26. Fang R, Zhang P, Kim D, et al. Robotic Visible-Light Optical Coherence Tomography Visualizes Segmental Schlemm's Canal Anatomy and Segmental Pilocarpine Response. bioRxiv 2024. https://doi.org/10.1101/2024.09.23.614542.
27. Faralli JA, Filla MS, Dunn C, Peters DM. Measurements of Phagocytosis in Trabecular Meshwork Cells. Methods Mol Biol 2025; 2858: 39-48. https://doi.org/10.1007/978-1-0716-4140-8_4.PMid:39433665
28. Faralli JA, Filla MS, Yang YF, et al. Digital spatial profiling of segmental outflow regions in trabecular meshwork reveals a role for ADAM15. PLoS One 2024; 19(2): e0298802. https://doi.org/10.1371/journal.pone.0298802. PMid:38394161 PMCid:PMC10889904
29. Fard MRB, Chan J, Read AT, et al. Magnetically Steered Cell Therapy For Functional Restoration Of Intraocular Pressure Control In Open-Angle Glaucoma. bioRxiv 2024. https://doi.org/10.1101/2024.05.13.593917.
30. Fard MRB, Protocol-Guzman NS, Chan J, et al. A Comprehensive Protocol for Microbead-Induced Ocular Hypertension in Mice. Methods Mol Biol 2025; 2858: 243-64. https://doi.org/10.1007/978-1-0716-4140-8_20. PMid:39433681
31. Feng X, Chen Z, Cheng W, Liu C, Liu Q. Role for NLRP3 inflammasome-mediated, Caspase1-dependent response in glaucomatous trabecular meshwork cell death and regulation of aqueous humor outflow. Heliyon 2024; 10(19): e38258. https://doi.org/10.1016/j.heliyon.2024.e38258. PMid:39416828 PMCid:PMC11481635
32. Ferreira NS, Costa VP, Miranda JF, et al. Psychological Stress and Intraocular Pressure in Glaucoma: A Randomized Controlled Trial. Ophthalmol Glaucoma 2024. https://doi.org/10.1016/j.ogla.2024.07.004. PMid:39019157
33. Findik H, Kanat A, Aydin MD, Guvercin AR, Ozmen S. New Evidence for Regulatory Role of Trigeminal Ganglion on the Intraocular Pressure Following Subarachnoid Hemorrhage. J Neurol Surg A Cent Eur Neurosurg 2024; 85(2): 137-41. https://doi.org/10.1055/s-0042-1760433. PMid:36878468
34. Galli C, Bastia E, Hubatsch DA, et al. NCX 470 Reduces Intraocular Pressure More Effectively Than Lumigan in Dogs and Enhances Conventional and Uveoscleral Outflow in Non-

Human Primates and Human Trabecular Meshwork/Schlemm's Canal Constructs. J Ocul Pharmacol Ther 2024; 40(6): 389-96. https://doi.org/10.1089/jop.2023.0102. PMid:38088745
35. Ghosh R, Herberg S. The role of YAP/TAZ mechanosignaling in trabecular meshwork and Schlemm's canal cell dysfunction. Vision Res 2024; 224: 108477. https://doi.org/10.1016/j.visres.2024.108477. PMid:39208753
36. Ghosh S, Herberg S. ECM biomaterials for modeling of outflow cell biology in health and disease. Biomater Biosyst 2024; 13: 100091. https://doi.org/10.1016/j.bbiosy.2024.100091. PMid:38528909 PMCid:PMC10961487
37. Gildea D, Doyle A, O'Connor J. The Effect of Exercise on Intraocular Pressure and Glaucoma. J Glaucoma 2024; 33(6): 381-6. https://doi.org/10.1097/IJG.0000000000002411. PMid:38722193
38. Gillmann K, Hornbeak DM. Rates of visual field change and functional progression in glaucoma following trabecular microbypass implantation of iStent technologies: a meta-analysis. BMJ Open Ophthalmol 2024; 9(1). https://doi.org/10.1136/bmjophth-2023-001575. PMid:38360043 PMCid:PMC10875546
39. Goldberg DF, Orlich C, Flowers BE, et al. A Randomized Controlled Trial Comparing STREAMLINE Canaloplasty to Trabecular Micro-Bypass Stent Implantation in Primary Open-Angle Glaucoma. Clin Ophthalmol 2024; 18: 2917-28. https://doi.org/10.2147/OPTH.S481945. PMid:39429442 PMCid:PMC11491083
40. Gong Q, Zhou D, Chen C, Shen H, Xu X, Qian T. Knockdown of lncRNA PVT1 protects human trabecular meshwork cells against H(2)O(2)-induced injury via the regulation of the miR-29a-3p/VEGF/MMP-2 axis. Heliyon 2024; 10(1): e23607. https://doi.org/10.1016/j.heliyon.2023.e23607. PMid:38173510 PMCid:PMC10761783
41. Gong Z, Johnstone MA, Wang RK. iStent insertion orientation and impact on trabecular meshwork motion resolved by optical coherence tomography imaging. J Biomed Opt 2024; 29(7): 076008. https://doi.org/10.1117/1.JBO.29.7.076008. PMid:39070082 PMCid:PMC11283271
42. Greatbatch CJ, Lu Q, Hung S, et al. Deep Learning-Based Identification of Intraocular Pressure-Associated Genes Influencing Trabecular Meshwork Cell Morphology. Ophthalmol Sci 2024; 4(4): 100504. https://doi.org/10.1016/j.xops.2024.100504. PMid:38682030 PMCid:PMC11046128
43. Gu X, Chen X, Zhang X, et al. Macrophage-induced integrin signaling promotes Schlemm's canal formation to prevent intraocular hypertension and glaucomatous optic neuropathy. Cell Rep 2024; 43(2): 113799. https://doi.org/10.1016/j.celrep.2024.113799. PMid:38367239
44. Gun RD, Yazicioglu T, Oklar M, Gokkaya N. Assessment of Schlemm's canal with swept-source optical coherence tomography in Graves' ophthalmopathy. Graefes Arch Clin Exp Ophthalmol 2024; 262(7): 2219-26. https://doi.org/10.1007/s00417-024-06397-x. PMid:38400857 PMCid:PMC11222225
45. Guo J, Wu Y, Sun Y, et al. Bioinformatics-Based Screening of Key LncRNAs for Modulating the Transcriptome Associated with Glaucoma in Human Trabecular Meshwork Cells. Front Biosci (Landmark Ed) 2024; 29(3): 91. https://doi.org/10.31083/j.fbl2903091. PMid:38538254
46. Guo J, Yang J, Huang H, et al. A new mouse-fixation device for IOP measurement in awake mice. Vision Res 2024; 219: 108397. https://doi.org/10.1016/j.visres.2024.108397. PMid:38579406
47. Gupta S, Zhang X, Panigrahi A, et al. Reduced Aqueous Humor Outflow Pathway Arborization in Childhood Glaucoma Eyes. Transl Vis Sci Technol 2024; 13(3): 23. https://doi.org/10.1167/tvst.13.3.23. PMid:38536170 PMCid:PMC10981159
48. Hallaj S, Halfpenny W, Chuter BG, Weinreb RN, Baxter SL, Cui QN. Response to: "Comment on: Association between Glucagon-Like Peptide 1 (GLP-1) Receptor Agonists Exposure and Intraocular Pressure Change". Am J Ophthalmol 2024. https://doi.org/10.1101/2024.05.06.24306943.
49. Hallaj S, Halfpenny W, Chuter BG, Weinreb RN, Baxter SL, Cui QN. Association Between Glucagon-Like Peptide-1 Receptor Agonists Exposure and Intraocular Pressure Change: GLP-1 Receptor Agonists and Intraocular Pressure Change. Am J Ophthalmol 2024; 269: 255-65. https://doi.org/10.1016/j.ajo.2024.08.030. PMid:39237049

50. Hallaj S, Halfpenny W, Chuter BG, Weinreb RN, Baxter SL, Cui QN. Association between Glucagon-Like Peptide 1 (GLP-1) Receptor Agonists Exposure and Intraocular Pressure Change. medRxiv 2024. https://doi.org/10.1101/2024.05.06.24306943
51. Harvey DH, Sugali CK, Mao W. Glucocorticoid-Induced Ocular Hypertension and Glaucoma. Clin Ophthalmol 2024; 18: 481-505. https://doi.org/10.2147/OPTH.S442749. PMid:38379915 PMCid:PMC10878139
52. Hengerer FH, Auffarth GU, Conrad-Hengerer I. 7-Year Efficacy and Safety of iStent inject Trabecular Micro-Bypass in Combined and Standalone Usage. Adv Ther 2024; 41(4): 1481-95. https://doi.org/10.1007/s12325-024-02788-y. PMid:38363465 PMCid:PMC10960914
53. Holmes G, Jawad S, Chen S, Cui R, Dietze J, Palko J. Risk factors for hyphema following goniotomy or trabecular bypass stent placement combined with phacoemulsification. Graefes Arch Clin Exp Ophthalmol 2024. https://doi.org/10.1007/s00417-024-06647-y. PMid:39367280
54. Hsu CC, Lin FP, Tseng HC, et al. Activation of the ROCK/MYLK Pathway Affects Complex Molecular and Morphological Changes of the Trabecular Meshwork Associated With Ocular Hypertension. Invest Ophthalmol Vis Sci 2024; 65(10): 17. https://doi.org/10.1167/iovs.65.10.17. PMid:39115865 PMCid:PMC11314630
55. Hu Y, Ge K, Du Y. Paeoniflorin alleviates TGF-beta2-mediated extracellular matrix remodeling and oxidative stress in human trabecular meshwork cells. Int Ophthalmol 2024; 44(1): 229. https://doi.org/10.1007/s10792-024-02917-0. PMid:38795168
56. Huang X, Zhou X, Zhang F, Wang X, Duan X, Liu K. DDX58 variant triggers IFN-beta-induced autophagy in trabecular meshwork and influences intraocular pressure. FASEB J 2024; 38(10): e23651. https://doi.org/10.1096/fj.202302265RR. PMid:38752537
57. Jing L, Liu K, Wang F, Su Y. Role of mechanically-sensitive cation channels Piezo1 and TRPV4 in trabecular meshwork cell mechanotransduction. Hum Cell 2024; 37(2): 394-407. https://doi.org/10.1007/s13577-024-01035-4. PMid:38316716
58. Kara S, Yang M, Yeh HH, Sen S, Hwang HH, Wang SY. Beyond PhacoTrainer: Deep Learning for Enhanced Trabecular Meshwork Detection in MIGS Videos. Transl Vis Sci Technol 2024; 13(9): 5. https://doi.org/10.1167/tvst.13.9.5. PMid:39226062 PMCid:PMC11373722
59. Karimi A, Aga M, Khan T, et al. Dynamic traction force in trabecular meshwork cells: A 2D culture model for normal and glaucomatous states. Acta Biomater 2024; 175: 138-56. https://doi.org/10.1016/j.actbio.2023.12.033. PMid:38151067
60. Karimi A, Aga M, Khan T, et al. Comparative analysis of traction forces in normal and glaucomatous trabecular meshwork cells within a 3D, active fluid-structure interaction culture environment. Acta Biomater 2024; 180: 206-29. https://doi.org/10.1016/j.actbio.2024.04.021. PMid:38641184
61. Karimi A, Khan S, Razaghi R, et al. Segmental biomechanics of the normal and glaucomatous human aqueous outflow pathway. Acta Biomater 2024; 173: 148-66. https://doi.org/10.1016/j.actbio.2023.11.003. PMid:37944773
62. Karimi A, Razaghi R, D'Costa S D, et al. Implementing new computational methods for the study of JCT and SC inner wall basement membrane biomechanics and hydrodynamics. Comput Methods Programs Biomed 2024; 243: 107909. https://doi.org/10.1016/j.cmpb.2023.107909. PMid:37976613
63. Keller KE, Kaech Petrie S. Nanotubules and Cellular Communication in Trabecular Meshwork Cells. Methods Mol Biol 2025; 2858: 49-62. https://doi.org/10.1007/978-1-0716-4140-8_5. PMid:39433666
64. Kelley MJ, Aga M, Acott TS. Segmental Aqueous Humor Outflow. Methods Mol Biol 2025; 2858: 101-11. https://doi.org/10.1007/978-1-0716-4140-8_9. PMid:39433670
65. Kennedy S, Williams C, Tsaturian E, Morgan JT. Dexamethasone Impairs ATP Production and Mitochondrial Performance in Human Trabecular Meshwork Cells. Curr Issues Mol Biol 2024; 46(9): 9867-80. https://doi.org/10.3390/cimb46090587. PMid:39329939 PMCid:PMC11430611
66. Kepez Yildiz B, Freitas R, Filippini P, et al. Relationship of posterior peripheral corneal layers and the trabecular meshwork: an immunohistological and anatomical study. Br J Ophthalmol 2024. https://doi.org/10.1136/bjo-2023-324844. PMid:38418206
67. Kim D, Fang R, Zhang P, et al. In vivo quantification of anterior and posterior chamber volumes in mice: implications for aqueous humor dynamics. bioRxiv 2024. https://doi.org/10.1101/2024.07.24.604989.

68. Kim MJ, Ibrahim MM, Jablonski MM. Corrigendum: Deepening insights into cholinergic agents for intraocular pressure reduction: systems genetics, molecular modeling, and in vivo perspectives. Front Mol Biosci 2024; 11: 1490100. https://doi.org/10.3389/fmolb.2024.1490100. PMid:39430956 PMCid:PMC11486731
69. Kim MJ, Ibrahim MM, Jablonski MM. Deepening insights into cholinergic agents for intraocular pressure reduction: systems genetics, molecular modeling, and in vivo perspectives. Front Mol Biosci 2024; 11: 1423351. https://doi.org/10.3389/fmolb.2024.1423351. PMid:39130374 PMCid:PMC11310038
70. Kumar A, Yang E, Du Y. Trabecular Meshwork Regeneration for Glaucoma Treatment Using Stem Cell-Derived Trophic Factors. Methods Mol Biol 2025; 2848: 59-71. https://doi.org/10.1007/978-1-0716-4087-6_4. PMid:39240516
71. Lamont HC, Wright AL, Devries K, et al. Trabecular meshwork cell differentiation in response to collagen and TGFbeta-2 spatial interactions. Acta Biomater 2024. https://doi.org/10.1016/j.actbio.2024.08.046. PMid:39218278
72. Langer F, Binter M, Hu X, et al. In vitro comparison of human and murine trabecular meshwork cells: implications for glaucoma research. Sci Rep 2024; 14(1): 22002. https://doi.org/10.1038/s41598-024-73057-9. PMid:39313534 PMCid:PMC11420201
73. Lankford L, Maddala R, Jablonski MM, Rao PV. Influence of the calcium voltage-gated channel auxiliary subunit (CACNA2D1) absence on intraocular pressure in mice. Exp Eye Res 2024; 241: 109835. https://doi.org/10.1016/j.exer.2024.109835. PMid:38373629 PMCid:PMC11192037
74. Laroche D, Brown A, Sinon J, Martin A, Ng C, Sakkari S. Pilot report: objective quantification of trabecular meshwork pigmentation using densitometry and the NIDEK GS-1 gonioscope in glaucoma patients. Front Ophthalmol (Lausanne) 2023; 3: 1322178. https://doi.org/10.3389/fopht.2023.1322178. PMid:38983099 PMCid:PMC11182083
75. Laroche D, Brown A, Sinon J, Martin A, Ng C, Sakkari S. Corrigendum: Pilot report: objective quantification of trabecular meshwork pigmentation using densitometry and the NIDEK GS-1 gonioscope in glaucoma patients. Front Ophthalmol (Lausanne) 2024; 4: 1382567. https://doi.org/10.3389/fopht.2024.1382567. PMid:38984122 PMCid:PMC11182224
76. Lehrer S, Morello T, Karrasch C, Rheinstein PH, Danias J. Effect of Glucosamine on Intraocular Pressure and Risk of Developing Glaucoma. J Glaucoma 2024; 33(4): 240-5. https://doi.org/10.1097/IJG.0000000000002340. PMid:38031296 PMCid:PMC10954404
77. Li G, van Batenburg-Sherwood J, Safa BN, et al. Aging and intraocular pressure homeostasis in mice. Aging Cell 2024; 23(7): e14160. https://doi.org/10.1111/acel.14160. PMid:38566432 PMCid:PMC11258442
78. Li H, Harvey DH, Dai J, et al. Characterization, enrichment, and computational modeling of cross-linked actin networks in trabecular meshwork cells. bioRxiv 2024. https://doi.org/10.1101/2024.08.21.608970.
79. Li H, Kuhn M, Kelly RA, et al. Targeting YAP/TAZ mechanosignaling to ameliorate stiffness-induced Schlemm's canal cell pathobiology. Am J Physiol Cell Physiol 2024; 326(2): C513-C28. https://doi.org/10.1152/ajpcell.00438.2023. PMid:38105758
80. Li Y, Li L, Ye Z, et al. A Novel Implantable Piezoresistive Microsensor for Intraocular Pressure Measurement. ACS Sens 2024; 9(8): 3958-66. https://doi.org/10.1021/acssensors.4c00705. PMid:39069735
81. Liu C, Tang J, Chen Y, et al. Intracellular Zn(2+) promotes extracellular matrix remodeling in dexamethasone-treated trabecular meshwork. Am J Physiol Cell Physiol 2024; 326(5): C1293-C307. https://doi.org/10.1152/ajpcell.00725.2023. PMid:38525543
82. Liu K, Xu J, Yang R, Wang F, Su Y. Ion Channel Piezo1 Induces Ferroptosis of Trabecular Meshwork Cells: A Novel Observation in the Pathogenesis in Primary Open Angle Glaucoma. Am J Physiol Cell Physiol 2024. https://doi.org/10.1152/ajpcell.00173.2024 PMid:39466179
83. Liu Y, Bu Q, Hu D, et al. NAD(+) supplementation improves mitochondrial functions and normalizes glaucomatous trabecular meshwork features. Exp Cell Res 2024; 440(1): 114137. https://doi.org/10.1016/j.yexcr.2024.114137. PMid:38897410
84. Lozano DC, Cepurna WO, Johnson EC, Morrison JC. Controlled elevation of intraocular pressure in anesthetized mice. Exp Eye Res 2024; 248: 110106. https://doi.org/10.1016/j.exer.2024.110106. PMid:39307451

85. Lozano DC, Yang YF, Cepurna WO, et al. Profiling IOP-Responsive Genes in the Trabecular Meshwork and Optic Nerve Head in a Rat Model of Controlled Elevation of Intraocular Pressure. Invest Ophthalmol Vis Sci 2024; 65(5): 41. https://doi.org/10.1167/iovs.65.5.41. PMid:38809543 PMCid:PMC1114605
86. Lozano DC, Yang YF, Cepurna WO, et al. Profiling IOP-responsive genes in anterior and posterior ocular tissues in the rat CEI glaucoma model. bioRxiv 2024. https://doi.org/10.1101/2024.02.11.579818.
87. Luo J, Fajardo-Sanchez J, Qin M, et al. Preliminary antifibrotic and vasoconstrictor effects of adrenaline in Schlemm's canal and suprachoroidal minimally invasive glaucoma surgery in primary open-angle glaucoma. Graefes Arch Clin Exp Ophthalmol 2024. https://doi.org/10.1007/s00417-024-06642-3. PMid:39347799
88. Maddala R, Eldawy C, Ho LTY, Challa P, Rao PV. Influence of Growth Differentiation Factor 15 on Intraocular Pressure in Mice. Lab Invest 2024; 104(4): 102025. https://doi.org/10.1016/j.labinv.2024.102025. PMid:38290601
89. Maddala R, Rao PV. Protocol for the Extraction and Characterization of Trabecular Meshwork Cell Cytoskeleton Fraction. Methods Mol Biol 2025; 2858: 31-7. https://doi.org/10.1007/978-1-0716-4140-8_3. PMid:39433664
90. Masdipa A, Kaidzu S, Tanito M. Assessing the Impact of PRESERFLO MicroShunt on Intraocular Pressure in Porcine Eyes Ex Vivo Using Infusion Pump System. Bioengineering (Basel) 2024; 11(7). https://doi.org/10.3390/bioengineering11070669 PMid:39061751 PMCid:PMC11274192
91. McDowell CM. The Inducible TGFbeta2 Ocular Hypertension Mouse Model. Methods Mol Biol 2025; 2858: 123-9. https://doi.org/10.1007/978-1-0716-4140-8_11. PMid:39433672
92. Mohanty S, Batabyal S, Idigo C, et al. Engineered sensor actuator modulator as aqueous humor outflow actuator for gene therapy of primary open-angle glaucoma. J Transl Med 2024; 22(1): 791. https://doi.org/10.1186/s12967-024-05581-1. PMid:39198903 PMCid:PMC11350963
93. Ndou R, Perry V, Dlamini GF. Diabetes disrupts osteometric and trabecular morphometric parameters in the Zucker Diabetic Sprague-Dawley rat femur. Anat Cell Biol 2024; 57(2): 294-304. https://doi.org/10.5115/acb.24.008. PMid:38650480 PMCid:PMC11184436
94. Neuhann TH, Neuhann RT, Hornbeak DM. Ten-Year Effectiveness and Safety of Trabecular Micro-Bypass Stent Implantation with Cataract Surgery in Patients with Glaucoma or Ocular Hypertension. Ophthalmol Ther 2024; 13(8): 2243-54. https://doi.org/10.1007/s40123-024-00984-1. PMid:38907091 PMCid:PMC11246400
95. Oikawa K, Kiland JA, Mathu V, et al. Effects of Telmisartan on Intraocular Pressure, Blood Pressure, and Ocular Perfusion Pressure in Normal and Glaucomatous Cats. Transl Vis Sci Technol 2024; 13(9): 15. https://doi.org/10.1167/tvst.13.9.15. PMid:39264603 PMCid:PMC11407481
96. Overby DR, Ethier CR, Miao C, Kelly RA, Reina-Torres E, Stamer WD. The Factors Affecting the Stability of IOP Homeostasis. Invest Ophthalmol Vis Sci 2024; 65(6): 4. https://doi.org/10.1167/iovs.65.6.4. PMid:38833261 PMCid:PMC11157970
97. Park S, Raghunathan VK, Ramarapu R, et al. Biomechanic, proteomic and miRNA transcriptional changes in the trabecular meshwork of primates injected with intravitreal triamcinolone. Vision Res 2024; 222: 108456. https://doi.org/10.1016/j.visres.2024.108456. PMid:38991466
98. Parrilla Vallejo M, Aguiar Caro JA, Giron Ortega M, et al. Three-year analysis of results, safety and progression in patients with open-angle glaucoma or ocular hypertension, undertaking trabecular microsurgery. Arch Soc Esp Oftalmol (Engl Ed) 2024; 99(11): 485-92. https://doi.org/10.1016/j.oftal.2024.06.002. PMid:39025229
99. Patel PD, Clark AF. Evaluation of Cross-Linked Actin Networks (CLANs) in Human Trabecular Meshwork Cells and Tissues. Methods Mol Biol 2025; 2858: 1-15. https://doi.org/10.1007/978-1-0716-4140-8_1. PMid:39433662
100. Patil SV, Kaipa BR, Ranshing S, et al. Lentiviral mediated delivery of CRISPR/Cas9 reduces intraocular pressure in a mouse model of myocilin glaucoma. Sci Rep 2024; 14(1): 6958. https://doi.org/10.1038/s41598-024-57286-6 PMid:38521856 PMCid:PMC10960846

101. Peters KS, Brambilla E, Ferguson T, Kramer B, Terveen D, Berdahl J. Manometric Intraocular Pressure Reduction with Negative Pressure Using Ocular Pressure Adjusting Pump Goggles. Ophthalmol Glaucoma. 2024. https://doi.org/10.1016/j.ogla.2024.09.005.
102. Porto de Souza V, Kanadani FN, Paranhos A, Prata TS. Re: Chan et al.: Effect of preoperative trabecular meshwork pigmentation and other eye characteristics on outcomes of combined phacoemulsification/minimally invasive glaucoma surgery (Ophthalmol Glaucoma. 2024; 7:271-281). Ophthalmol Glaucoma. 2024. https://doi.org/10.1016/j.ogla.2024.08.006. PMid:39373682
103. Prokosch V, Zwingelberg SB, Efremova DV, Buonfiglio F, Pfeiffer N, Gericke A. The Effect of Trabecular Aspiration on Intraocular Pressure, Medication and the Need for Further Glaucoma Surgery in Eyes with Pseudoexfoliation Glaucoma. Diseases. 2024;12(5). https://doi.org/10.3390/diseases12050092. PMid:38785747 PMCid:PMC11119255
104. Qin B, Hu C, Zhang Y, Chen Y, Lei Y. ABCA1 Deletion Does Not Affect Aqueous Humor Outflow Function in Mice. J Ophthalmol. 2024;2024:7195550. https://doi.org/10.1155/2024/7195550. PMid:39049847 PMCid:PMC11268963
105. Queiruga-Pineiro J, Lozano-Sanroma J, Barros A, Rodriguez-Una I, Fernandez-Vega Cueto-Felgueroso L, Merayo-Lloves J. Short-term changes in the trabecular iris angle and anterior chamber during wear of scleral lenses with different diameters. Clin Exp Optom. 2024:1-7. https://doi.org/10.1080/08164622.2024.2418822. PMid:39462799
106. Rao A. Histopathologic correlates of trabecular meshwork in microincisional trabeculectomy. Indian J Ophthalmol. 2024;72(3):335-8. https://doi.org/10.4103/IJO.IJO_1390_23. PMid:38099375 PMCid:PMC11001220
107. Razavi SMS, Daneshvar R. Authors' Response: Possible dose-dependent effect of eplerenone on intraocular pressure. Indian J Ophthalmol. 2024;72(8):1227. https://doi.org/10.4103/IJO.IJO_487_24. PMid:39078974 PMCid:PMC11451772
108. Redmon SN, Lakk M, Tseng YT, et al. TRPV4 subserves physiological and pathological elevations in intraocular pressure. Res Sq. 2024. https://doi.org/10.21203/rs.3.rs-4714050/v1.
109. Ricci CL, Passareli J, Nascimento FF, et al. Comparison of three methodologies for measuring intraocular pressure in healthy cats. Vet World. 2024;17(8):1803-9. https://doi.org/10.14202/vetworld.2024.1803-1809. PMid:39328448 PMCid:PMC11422646
110. Richter GM, Takusagawa HL, Sit AJ, et al. Trabecular Procedures Combined with Cataract Surgery for Open-Angle Glaucoma: A Report by the American Academy of Ophthalmology. Ophthalmology. 2024;131(3):370-82. https://doi.org/10.1016/j.ophtha.2023.10.009. PMid:38054909
111. Riesterer J, Warchock A, Krawczyk E, et al. Effects of Genipin Crosslinking of Porcine Perilimbal Sclera on Mechanical Properties and Intraocular Pressure. Bioengineering (Basel). 2024;11(10). https://doi.org/10.3390/bioengineering11100996. PMid:39451372 PMCid:PMC11504492
112. Roddy GW, Kohli D, Niknam P, et al. Subconjunctival Administration of an Adeno-Associated Virus Expressing Stanniocalcin-1 Provides Sustained Intraocular Pressure Reduction in Mice. Ophthalmol Sci. 2025;5(1):100590. https://doi.org/10.1016/j.xops.2024.100590. PMid:39328825 PMCid:PMC11426120
113. Rong H, Luo Z, Tang M, et al. Establishment of a Disease Model Using Patient-Specific Induced Pluripotent Stem Cells-Derived Trabecular Meshwork Cells in a Chinese Primary Open-Angle Glaucoma Mega-Pedigree. Discov Med. 2024;36(189):2013-25. https://doi.org/10.24976/Discov.Med.202436189.185. PMid:39463221
114. Roodnat AW, Callaghan B, Doyle C, Vallabh NA, Atkinson SD, Willoughby CE. Genome-wide RNA sequencing of ocular fibroblasts from glaucomatous and normal eyes: Implications for glaucoma management. PLoS One. 2024;19(7). https://doi.org/10.1371/journal.pone.0307227. PMid:38990974 PMCid:PMC11239048
115. Safa BN, Fraticelli Guzman NS, Li G, Stamer WD, Feola AJ, Ethier CR. A Histomorphometric and Computational Investigation of the Stabilizing Role of Pectinate Ligaments in the Aqueous Outflow Pathway. J Biomech Eng. 2024;146(8). https://doi.org/10.1115/1.4065164. PMid:38529724
116. Sagdic Ozcelik S, Alagoz N, Yasar T. Changes in Schlemm's canal morphology after trabeculectomy in open angle glaucoma assessed using anterior segment optical coherence

tomography. Clin Exp Optom. 2024:1-6. https://doi.org/10.1080/08164622.2024.2400319. PMid:39397493
117. Saleem MA, Kennedy M, Badla O, Neag EJ, Bhattacharya SK. Analysis of Sphingosine and Sphinganine from the Aqueous Humor for Signaling Studies Using Ultrahigh-Performance Liquid Chromatography-Mass Spectrometry. Methods Mol Biol. 2024;2816:35-40. https://doi.org/10.1007/978-1-0716-3902-3_4. PMid:38977586
118. Sarr IL, Sakho B, Guisse E, Fall R. Effects of Hemodialysis on Intraocular Pressure and Ocular Perfusion Pressure. Cureus. 2024;16(4). https://doi.org/10.7759/cureus.59138. PMid:38803770 PMCid:PMC11129607
119. Schwakopf J, Romero CO, Lopez NN, Millar JC, Vetter ML, Bosco A. Schlemm's canal-selective Tie2/TEK knockdown induces sustained ocular hypertension in adult mice. Exp Eye Res. 2024;248:110114.https://doi.org/10.1016/j.exer.2024.110114. PMid:39368692
120. Sharif NA, Millar JC, Zode G, Ota T. Steroid-Induced Ocular Hypertension in Mice Is Differentially Reduced by Selective EP2, EP3, EP4, and IP Prostanoid Receptor Agonists. Int J Mol Sci. 2024;25(6). https://doi.org/10.3390/ijms25063328. PMid:38542305 PMCid:PMC10970031
121. Shim MS, Liton PB. Time-Lapse Live-Cell Imaging Using Fluorescent Protein Sensors in Outflow Pathway Cells Under Fluid Flow Conditions. Methods Mol Biol 2025; 2858: 77-86. https://doi.org/10.1007/978-1-0716-4140-8_7. PMid:39433668
122. Shui YB, Liu Y, Huang AJW, Siegfried CJ. SDPR expression in human trabecular meshwork and its potential role in racial disparities of glaucoma. Sci Rep 2024; 14(1): 10258. https://doi.org/10.1038/s41598-024-61071-w. PMid:38704467 PMCid:PMC11069504
123. Singh A, Ghosh R, Li H, et al. Three-Dimensional Extracellular Matrix Protein Hydrogels for Human Trabecular Meshwork Cell Studies. Methods Mol Biol 2025; 2858: 17-29. https://doi.org/10.1007/978-1-0716-4140-8_2. PMid:39433663
124. Soundappan K, Cai J, Yu H, et al. Influence of dexamethasone-induced matrices on the TM transcriptome. Exp Eye Res 2024; 248: 110069. https://doi.org/10.1016/j.exer.2024.110069. PMid:39233306
125. Soundararajan A, Pattabiraman PP. Method to Assess the Intracellular Fate and Bioavailability of Clusterin Using Live Cell Confocal Microscopy Imaging. Methods Mol Biol 2024; 2816: 145-9. https://doi.org/10.1007/978-1-0716-3902-3_14. PMid:38977596
126. Soundararajan A, Wang T, Pattabiraman PP. Proteomic analysis uncovers clusterin-mediated disruption of actin-based contractile machinery in the trabecular meshwork to lower intraocular pressure. bioRxiv 2024. https://doi.org/10.1101/2024.02.16.580757
127. Strohmaier CA, McDonnell F, Huang AS. Aqueous Humor Angiography. Methods Mol Biol 2025; 2858: 159-72. https://doi.org/10.1007/978-1-0716-4140-8_14. PMid:39433675
128. Strohmaier CA, Wanderer D, Zhang X, et al. Lack of Correlation Between Segmental Trabecular Meshwork Pigmentation and Angiographically Determined Outflow in Ex Vivo Human Eyes. J Glaucoma 2024; 33(5): 355-60. https://doi.org/10.1097/IJG.0000000000002318. PMid:37851964
129. Stubbs EB, Jr. Determining Isoprenoid-Facilitated Monomeric GTPase Turnover in Primary Human Trabecular Meshwork Cultures. Methods Mol Biol 2024; 2816: 101-15. https://doi.org/10.1007/978-1-0716-3902-3_10. PMid:38977592
130. Sugali CK, Rayana NP, Dai J, Harvey DH, Dhamodaran K, Mao W. GSK3beta Inhibitors Inhibit TGFbeta Signaling in the Human Trabecular Meshwork. Invest Ophthalmol Vis Sci 2024; 65(10): 3. https://doi.org/10.1167/iovs.65.10.3. PMid:39087933 PMCid:PMC11305430
131. Tan J, Cai S, Luo X, et al. Stop codon variant in EFEMP1 is associated with primary open-angle glaucoma due to impaired regulation of aqueous humor outflow. Exp Eye Res 2024; 241: 109859. https://doi.org/10.1016/j.exer.2024.109859. PMid:38467175
132. Tan SS, Tun TA, Aung T, Nongpiur ME. Comparison of intraocular pressure and anterior segment parameters in subjects with asymmetrical primary angle closure disease. Clin Exp Ophthalmol 2024; 52(7): 724-31. https://doi.org/10.1111/ceo.14402. PMid:38803136
133. Tang WZ, Chen HW, Liu TH. Comment on: Association between Glucagon-Like Peptide 1 (GLP-1) Receptor Agonists Exposure and Intraocular Pressure Change. Am J Ophthalmol 2024. https://doi.org/10.1016/j.ajo.2024.09.038.
134. Tian A, Baidouri H, Kim S, et al. To be or not to be - Decoding the Trabecular Meshwork Cell Identity. bioRxiv 2024. https://doi.org/10.1101/2024.04.26.591346

135. Torne O, Oikawa K, Teixeira LBC, Kiland JA, McLellan GJ. Trabecular Meshwork Abnormalities in a Model of Congenital Glaucoma Due to LTBP2 Mutation. Invest Ophthalmol Vis Sci 2024; 65(12): 28. https://doi.org/10.1167/iovs.65.12.28. PMid:39432401 PMCid:PMC11500042
136. Tsutsui A, Hamanaka T, Kaidzu S, et al. Comparison of Schlemm's Canal Morphology Parameters Between Propensity Score-Matched Primary Open-Angle Glaucoma and Exfoliation Glaucoma. Invest Ophthalmol Vis Sci 2024; 65(2): 15. https://doi.org/10.1167/iovs.65.2.15. PMid:38324302 PMCid:PMC10854412
137. Tundo GR, Cavaterra D, Pandino I, et al. The Delayed Turnover of Proteasome Processing of Myocilin upon Dexamethasone Stimulation Introduces the Profiling of Trabecular Meshwork Cells' Ubiquitylome. Int J Mol Sci 2024; 25(18). https://doi.org/10.3390/ijms251810017. PMid:39337505 PMCid:PMC11432723
138. Vallabh NA, Lane B, Simpson D, et al. Massively parallel sequencing of mitochondrial genome in primary open angle glaucoma identifies somatically acquired mitochondrial mutations in ocular tissue. Sci Rep 2024; 14(1): 26324. https://doi.org/10.1038/s41598-024-72684-6. PMid:39487142 PMCid:PMC11530638
139. Vallee R, Meduri E, Vallee JN, et al. Predictive biomarkers of intra-ocular pressure decrease after cataract surgery associated with trabecular washout in patients with pseudo exfoliative glaucoma. Sci Rep 2024; 14(1): 13567. https://doi.org/10.1038/s41598-024-53893-5 PMid:38866840 PMCid:PMC11169244
140. Wang B, Naithani R, Alvarez S, Glaser T, Freedman SF. In Vivo Assessment of the Pediatric Trabecular Meshwork, Schlemm Canal, and Iridocorneal Angle Using Overhead-Mounted Optical Coherence Tomography. Am J Ophthalmol 2024; 269: 402-8. https://doi.org/10.1016/j.ajo.2024.09.001. PMid:39265692
141. Wang G, Zhao R, Guo Z, et al. Autophagy activation ameliorates the fibrosis of trabecular meshwork cells induced by TGFbeta2 through the promotion of fibrotic proteins degradation. Hum Cell 2024; 38(1): 4. https://doi.org/10.1007/s13577-024-01141-3. PMid:39436499
142. Wang R, Wang Y, Qin Y, Wei H. Antioxidative effects of ghrelin on human trabecular meshwork cells. J Fr Ophtalmol 2024; 47(1): 103746. https://doi.org/10.1016/j.jfo.2022.11.023. PMid:37806937
143. Wang R, Wei H, Shi Y, et al. Self-generating electricity system driven by aqueous humor flow and trabecular meshwork contraction motion activated BCKa for glaucoma intraocular pressure treatment. Mater Horiz 2024. https://doi.org/10.1039/D4MH01004C.
144. Wang T, Kimmel HRC, Park C, et al. Regulatory role of cholesterol in modulating actin dynamics and cell adhesive interactions in the trabecular meshwork. bioRxiv 2024. https://doi.org/10.1101/2024.02.02.578717.
145. Wasilewicz R, Wasilewicz J, Pruszynska-Oszmalek E, Stuper-Szablewska K, Leciejewska N, Kolodziejski PA. Genistein stimulates the viability and prevents myofibroblastic transformation in human trabecular meshwork cells stimulated by TGF-beta. Exp Eye Res 2024; 240: 109806. https://doi.org/10.1016/j.exer.2024.109806. PMid:38272381
146. Watanabe M, Sato T, Umetsu A, et al. Differential Effects of Benzalkonium Chloride on Human Trabecular Meshwork Cells Not Treated or Treated with Transforming Growth Factor-beta2 or Dexamethasone. J Ocul Pharmacol Ther 2024; 40(3): 189-96. https://doi.org/10.1089/jop.2023.0136. PMid:38502813
147. Watanabe M, Sato T, Umetsu A, et al. The Specific ROCK2 Inhibitor KD025 Alleviates Glycolysis through Modulating STAT3-, CSTA- and S1PR3-Linked Signaling in Human Trabecular Meshwork Cells. Biomedicines 2024; 12(6). https://doi.org/10.3390/biomedicines12061165. PMid:38927372 PMCid:PMC11200618
148. Wong CA, Fraticelli Guzman NS, Read AT, et al. A method for analyzing AFM force mapping data obtained from soft tissue cryosections. J Biomech 2024; 168: 112113. https://doi.org/10.1016/j.jbiomech.2024.112113. PMid:38648717
149. Wu X, Liang J, Liu J, et al. Silibinin attenuates TGF-beta2-induced fibrogenic changes in human trabecular meshwork cells by targeting JAK2/STAT3 and PI3K/AKT signaling pathways. Exp Eye Res 2024; 244: 109939. https://doi.org/10.1016/j.exer.2024.109939. PMid:38789021
150. Xi G, Feng P, Zhang X, et al. iPSC-derived cells stimulate ABCG2(+)/NES(+) endogenous trabecular meshwork cell proliferation and tissue regeneration. Cell Prolif 2024; 57(7): e13611.

151. Xie ZJ, Wu QY, Qu JH, Lin JY, Hong J. Impact of postoperative intraocular pressure elevation on graft endothelial cells in non-preexisting glaucoma eyes undergoing descemet membrane endothelial keratoplasty: a cohort study. BMC Ophthalmol 2024; 24(1): 460. https://doi.org/10.1186/s12886-024-03728-8. PMid:39434062 PMCid:PMC11492462
152. Xu C, Wei J, Song D, et al. Effects of SIPA1L1 on trabecular meshwork extracellular matrix protein accumulation and cellular phagocytosis in POAG. JCI Insight 2024.
153. Xu L, Zhao Y, Zhang X, et al. Low Intraocular Pressure Induces Fibrotic Changes in the Trabecular Meshwork and Schlemm's Canal of Sprague Dawley Rats. Transl Vis Sci Technol 2024; 13(10): 10. https://doi.org/10.1167/tvst.13.10.10. PMid:39374003 PMCid:PMC11463712
154. Xu Y, Ye Y, Chen Z, et al. The Impact of Intraocular Pressure Changes on Corneal Biomechanics in Primary Open-angle Glaucoma. Am J Ophthalmol 2024; 269: 216-25. https://doi.org/10.1016/j.ajo.2024.08.027. PMid:39218382
155. Yan X, Wu S, Liu Q, et al. Serine to proline mutation at position 341 of MYOC impairs trabecular meshwork function by causing autophagy deregulation. Cell Death Discov 2024; 10(1): 21. https://doi.org/10.1038/s41420-024-01801-1. PMid:38212635 PMCid:PMC10784477
156. Yan X, Wu S, Liu Q, Teng Y, Wang N, Zhang J. The S341P mutant MYOC renders the trabecular meshwork sensitive to cyclic mechanical stretch. Heliyon 2024; 10(17): e37137. https://doi.org/10.1016/j.heliyon.2024.e37137. PMid:39286096 PMCid:PMC11402775
157. Yang Y, Qin B, Ng TK, Sun X, Cao W, Chen Y. Serum lipid and lipoprotein profiles and their association with intraocular pressure in primary open-angle glaucoma: an observational cross-sectional study in the Chinese population. Lipids Health Dis 2024; 23(1): 323. https://doi.org/10.1186/s12944-024-02316-5. PMid:39350087 PMCid:PMC11441088
158. Yarishkin O, Lakk M, Rudzitis CN, Kirdajova D, Krizaj D. Resting human trabecular meshwork cells experience tonic cation influx. Res Sq 2024. https://doi.org/10.21203/rs.3.rs-4980372/v1
159. Yarishkin O, Lakk M, Rudzitis CN, Searle JE, Kirdajova D, Krizaj D. Resting trabecular meshwork cells experience constitutive cation influx. Vision Res 2024; 224: 108487. https://doi.org/10.1016/j.visres.2024.108487. PMid:39303640
160. Youn KI, Lee JW, Song Y, Lee SY, Song KH. Development of Cell Culture Platforms for Study of Trabecular Meshwork Cells and Glaucoma Development. Tissue Eng Regen Med 2024; 21(5): 695-710. https://doi.org/10.1007/s13770-024-00640-6. PMid:38642251
161. Zeng Y, Lin Y, Yang J, Wang X, Zhu Y, Zhou B. The Role and Mechanism of Nicotinamide Riboside in Oxidative Damage and a Fibrosis Model of Trabecular Meshwork Cells. Transl Vis Sci Technol 2024; 13(3): 24. https://doi.org/10.1167/tvst.13.3.24
162. Zhang H, Wang JM. [To discuss the minimally invasive glaucoma surgery related to trabeculotomy from the perspective of physiological function of trabecular meshwork drainage pathway]. Zhonghua Yan Ke Za Zhi 2024; 60(5): 399-402.
163. Zhang J, Yang X, Zong Y, Yu T, Yang X. miR-196b-5p regulates inflammatory process and migration via targeting Nras in trabecular meshwork cells. Int Immunopharmacol 2024; 129: 111646. https://doi.org/10.1016/j.intimp.2024.111646. PMid:38325046
164. Zhang Q, Feng H, Zhang Y, et al. Comparing 24-hour IOP fluctuation slope curve between newly diagnosed ocular hypertension and primary open-angle glaucoma. BMJ Open Ophthalmol 2024; 9(1). https://doi.org/10.1136/bmjophth-2024-001821. PMid:39313295 PMCid:PMC11418482
165. Zhang X, Xi G, Feng P, Li C, Kuehn MH, Zhu W. Intraocular pressure across the lifespan of Tg-MYOC(Y437H) mice. Exp Eye Res 2024; 241: 109855. https://doi.org/10.1016/j.exer.2024.109855. PMid:38453040
166. Zhang Y, Han R, Xu S, et al. TMCO1 promotes ferroptosis and ECM deposition in glaucomatous trabecular meshwork via ERK1/2 signaling. Biochim Biophys Acta Mol Basis Dis 2024; 1871(1): 167530. https://doi.org/10.1016/j.bbadis.2024.167530. PMid:39343416
167. Zhou Y, Liu Z, Gao W, Yang Y, Peng Q, Tan H. Pathological Mechanism and Clinical Therapy Progress of Schlemm's Canal. J Ophthalmol 2024; 2024: 9978312. https://doi.org/10.1155/2024/9978312. PMid:39492954 PMCid:PMC11531356
168. Zhu M, Deng X, Zhang N, et al. Dexamethasone induces trabecular meshwork cell myofibroblast transdifferentiation through ARHGEF26. FASEB J 2024; 38(15): e23848. https://doi.org/10.1096/fj.202400400RR. PMid:39092889

Participants

Inas Aboobakar, MD Instructor in Ophthalmology Mass Eye and Ear/Harvard Medical School 243 Charles St. Room 501B Boston, MA 02114 USA	inas_aboobakar@meei.harvard.edu Tel: (310) 621-7261
Ted Acott, PhD Professor of Ophthalmology and Biochemistry & Molecular Biology Oregon Health & Science University Portland, OR 97239 USA	acott@ohsu.edu
Simon Bakker, MSc Managing Director Kugler Publications Nieuwe Hemweg 7P 1013 BG Amsterdam, The Netherlands	simonbakker@kuglerpublications.com Tel: +31 20 68 45 700, office Tel: +31 61 48 11 488, mobile
Revathi Balasubramanian, PhD Asstistant Professor Dept. of Ophthalmology Columbia University Irving Medical Center 701 W 168th Street Floor 2, 201E New York NY 10032 USA	rb3132@cumc.columbia.edu Tel: 212-342-3516, office Tel: 585-775-7342, mobile
Sanjoy K. Bhattacharya, M. Tech., PhD, FARVO Professor of Ophthalmology Graduate Program Director (MVSIO and Translational Focus of medical school PhD Programs) Founding Director, Miami Integrative Metabolomics Research Center Speaker, Medical School Faculty Council Bascom Palmer Eye Institute (McKnight Bldg.) 1638 NW 10th Avenue, Suite 707A University of Miami Miami, FL, 33136 USA	sbhattacharya@med.miami.edu Tel: 305-482-4103, Office Tel: 305-482-4109, Lab Tel: 305-482-4987, Mass spec lab Fax: 305-326-6547
Terete Borras, PhD Emeritus Professor University of North Carolina at Chapel Hill USA	tborras@med.unc.edu

Abe Clark Regents Professor Dept. Pharmacology & Neuroscience North Texas Eye Research Institute 3500 Camp Bowie Blvd, Fort Worth, TX 76107 USA	abe.clark@unthsc.edu Tel: 817-735-2094
John Danias, MD, PhD Chair of Ophthal/SUNY Downstate Medical Center Director of Research Professor of Ophthalmology and Cell Biology	john.danias@downstate.edu
Yiqin Du, MD, PhD Professor Department of Ophthalmology Morsani College of Medicine, University of South Florida 12901 Bruce B. Downs Blvd., MDC 2041 Tampa, FL 33612 USA	yiqindu@usf.edu Tel: 412-482-0615, mobile
Michael H. Elliott, PhD, FARVO Presbyterian Health Fdn. Presidential Professor Professor of Ophthalmology, College of Medicine Professor of Physiology, College of Medicine Member, Harold Hamm Diabetes Center U. of Oklahoma Health Sciences Center Dean A. McGee Eye Institute 608 Stanton L. Young Blvd. DMEI PA-405 Oklahoma City, OK 73104 USA	michael-elliott@ouhsc.edu Tel: 405-271-4019 Fax: 405-271-8128
C. Ross Ethier, PhD Lawrence L. Gellerstedt, Jr. and Mary Duckworth Gellerstedt Chair in Bioengineering Georgia Research Alliance Eminent Scholar in Biomechanics and Mechanobiology Professor of Biomedical Engineering Wallace H. Coulter Department of Biomedical Engineering at Georgia Institute of Technology & Emory University School of Medicine IBB, 315 Ferst Drive, Room 2306 Atlanta, GA 30332-0363 USA	ross.ethier@bme.gatech.edu Tel: 404.385.0100 Fax: 404.385.1397

Mike Fautsch, PhD Joseph E. and Rose Marie Green Professor of Ophthalmology Department of Ophthalmology Mayo Clinic 200 1st St SW Rochester, MN USA	fautsch.michael@mayo.edu Tel: 507-284-2244
Haiyan Gong, MD, PhD Professor of Ophthalmology, Anatomy and Neurobiology Boston University Chobanian & Avedisian School of Medicine 72 East Concord St., Rm L905 Boston, MA 02118 USA	haiyan.gong@gmail.com Tel: 617-358-2213
Samuel Herberg, PhD Assistant Professor Dept. of Ophthalmology and Visual Sciences SUNY Upstate Medical University Center for Vision Research 505 Irving Ave., NRB 4609 Syracuse, NY 13210 USA	herbergs@upstate.edu Tel: 315-464-7773
Murray Johnstone, MD Clinical Professor Dept. of Ophthalmology University of Washington-Eye Institute Seattle, WA USA	johnstone.murray@gmail.com
Alireza Karimi, PhD Assistant Professor Department of Ophthalmology Casey Eye Institute Oregon Health and Science University 3215 SW Pavilion Loop Portland, OR, 97239 USA	karimi@ohsu.edu Tel: 503-494-8455, office Tel: 402-810-1305, mobile
Paul Kaufman, MD Ernst H. Barany Professor of Ocular Pharmacology Dept. of Ophthalmology & Visual Sciences School of Medicine & Public Health University of Wisconsin-Madison 600 Highland Ave., CSC K4/430 Madison, WI 53792-4673 USA	kaufmanp@mhub.ophth.wisc.edu Tel: 608-263-6074 Fax: 608-263-0543

Kate Keller, PhD Prof. of Ophthalmology School of Medicine Graduate Faculty Program in Molecular and Cellular Biosciences Oregon Health & Science University Portland, OR 97239 USA	gregorka@ohsu.edu Tel: 503-494-2366
Mary Kelley, PhD Casey Eye Institute Oregon Health & Science University 3181 SW Sam Jackson Park Rd. Portland, OR 97239 USA	kelleyma@ohsu.edu Tel: 503-494-3593, office Tel: 503-312-5753, mobile
Krish Kizhatil, PhD The Ohio State University The Ohio State University Medical Center Department of Ophthalmology and Visual Sciences 368 Bevis Hall 1080 Carmack Road, Columbus, OH 43210 USA	kizha01@osumc.edu
David Krizaj, PhD John Frederick Carter Endowed Professor in Ophthalmology University of Utah 65 Mario Capecchi Dr. Salt Lake City, UT 84132 USA	david.krizaj@hsc.utah.edu Tel: 801-213-2777, office Tel: 801-213-2775, lab Fax:801-587-8314
Markus H. Kuehn, PhD Prof, Dept. Ophthalmology and Visual Sciences Assoc. Director, Iowa City VA Center for Prevention and Treatment of Visual Loss The University of Iowa 3135 MERF 375 Newton Rd. Iowa City, IA 52242 USA	markus-kuehn@uiowa.edu Tel: 319-335-9565, office Tel: 319-335-7537, lab Fax: 319-335-6641 https://myweb.uiowa.edu/kuehnm
Shan Lin, MD Glaucoma Center of San Francisco 55 Stevenson Street San Francisco, CA 94105 USA	sl@glaucomasf.com
Paloma Liton, PhD Professor Dept. of Ophthalmology Duke University 2352 Erwin Rd. Durham, NC 27705 USA	paloma.liton@duke.edu

Katy Liu, MD, Ph.D. Medical Instructor Glaucoma Division, Duke Eye Center USA	katy.liu@duke.edu Tel: 919-681-0472
Yutao Liu, PhD Associate Professor Dept. of Cellular Biology and Anatomy Medical College of Georgia Augusta University Augusta, GA 30912 USA	yutliu@augusta.edu Tel: 706-721-2015
Weiming Mao, PhD Associate Professor Jay C. and Lucile L. Kahn Scholar in Glaucoma Research and Education, Showalter Scholar Eugene and Marilyn Glick Eye Institute Dept. of Ophthalmology Dept. of Biochemistry & Molecular Biology Dept. of Pharmacology and Toxicology Indiana University School of Medicine RM305V, 1160 W. Michigan St, Indianapolis, IN, 46202 USA	weimmao@iu.edu Tel: 317-278-0801
Gillian McLellan, PhD Professor Dept. of Surgical Sciences and Dept. of Ophthalmology and Visual Sciences University of Wisconsin-Madison Madison, WI, 53706 USA	gillian.mclellan@wisc.edu
Fiona McDonnell, PhD Assistant Professor John A. Moran Eye Center Room S6871 University of Utah Salt Lake City, UT 84132 USA	fiona.mcdonnell@utah.edu Tel: 801-585-7934
Colleen McDowell, PhD Associate Professor Dept. of Ophthalmology and Visual Sciences University of Wisconsin-Madison 3375A Medical Sciences Center 1300 University Ave Madison, WI 53706 USA	cmmcdowell@wisc.edu Tel: 608-265-3996

Sai Nair, PhD Associate Professor Department of Ophthalmology University of CA-San Francisco School of Medicine 10 Koret Way San Francisco, CA 94143 USA	saidas.nair@ucsf.edu Tel: 415-476-0461
Darryl Overby, PhD, FARVO Professor of Mechanobiology Dept. of Bioengineering Imperial College London London UK	d.overby@imperial.ac.uk
Donna M. Peters, PhD Professor Department of Pathology & Laboratory Medicine Univeristy of Wisconsin-Madison Madison, WI USA	dmpeter2@wisc.edu Tel: 608-262-4626
Vasanth Rao, PhD Richard and Kit Barkhouser Distinguished Professor Professor in Pharmacology and Cancer Biology, and Ophthalmology and Visual Sciences (OVS) Box 3802 Medical Center Durham, NC 27710 USA	p.rao@duke.edu Tel: 919-681-5883
Ester Reina-Torres, PhD Department of Bioengineering Imperial College London London UK	e.reina-torres12@imperial.ac.uk
Gavin W. Roddy, MD, PhD Assistant Professor of Ophthalmology Glaucoma Service Mayo Clinic, Rochester, MN USA	roddy.gavin@mayo.edu Tel: 817-613-6206, mobile
John R. Samples, MD Western Glaucoma Foundation 1910 4th Ave., E., PMB 264 Olympia, WA 98506-4632 USA	glaucoma@gmail.com Tel: 303-505-0776, mobile

Joel Schuman, MD, FACS Kenneth L. Roper, MD Endowed Chair Professor of Ophthalmology and Biomedical Engineering Vice Chair for Research Innovation Co-Director, Glaucoma Service Wills Eye Hospital 840 Walnut Street, Suite 1110 Philadelphia, PA 19107 USA	jschuman@willseye.org
W. Daniel Stamer, PhD, FARVO Joseph A. C. Wadsworth Professor of Ophthalmology Professor of Biomedical Engineering Duke University Durham, NC 27705 USA	dan.stamer@duke.edu Tel: 919-684-3745, office Tel: 919-681-1566, lab
David Swain M.D./Ph.D. Candidate Boston University Chobanian & Avedisian School of Medicine USA	dlswain@bu.edu
Yang Sun, MD, PhD Professor Vice Chair Academic Affairs Ophthalmology Stanford University USA	yangsun@stanford.edu
Ernst Tamm, PhD Professor and Chairman Institute fur Human Anatomy and Embryology University of Regensburg Regensburg Germany	ernst.tamm@vkl.uni-regensburg.de
Benjamin Thomson, PhD Assistant Professor of Ophthalmology Northwestern University Feinstein School of Medicine 259 E. Erie St., Suite 1520 Chicago, IL, 60611 USA	benjamin.thomson@northwestern.edu Tel: 312-292-8691

Carol B. Toris, PhD Professor, Havener Eye Institute Dept. of Ophthalmology and Visual Sciences The Ohio State University Wexner Medical Center 915 Olentangy River Rd, Suite 3010B Columbus, OH 43212 USA	carol.toris@osumc.edu
Amir Vahabikashi, PhD Assistant Professor Bioengineering Department Northeastern University USA	a.vahabikashi@northeastern.edu
Hannah Youngblood, PhD Postdoctoral Fellow Raquel Lieberman Lab (IBB 1220) Georgia Institute of Technology USA	hyoungblood6@gatech.edu
Hao Zhang, PhD Professor of Biomedical Engineering McCormick School of Engineering Northwestern University Tech M335 2145 Sheridan Rd. Chicago, IL 60208-3107 USA	hzhang@northwestern.edu Tel: 847-491-2946, Office Tel: 847-491-7167, Lab Fax: 847-491-4928 Twitter: @visibleOCT
Gulab Zode, PhD Professor of Ophthalmology Center for Translational Vision Research Gavin Herbert Eye Institute Plumwood house, lab 315 University of California, Irvine, CA USA	gzode@hs.uci.edu Tel: 949-824-4366